




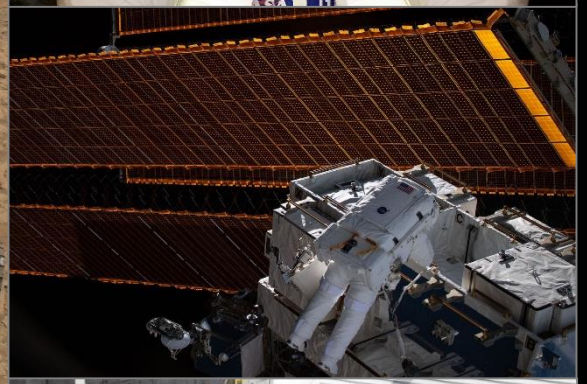

SHORT COURSE ON LITHIUM-ION BATTERIES:

FUNDAMENTAL CONCEPTS, BATTERY SAFETY, AND MODELING TECHNIQUES

William Walker, Ph.D.
william.walker@nasa.gov

NASA Johnson Space Center (JSC)
Engineering Directorate (EA)
Structural Engineering Division (ES)
Thermal Design Branch (ES3)

ABOUT THE INSTRUCTOR

- **B.S. Mechanical Engineering from West Texas A&M University**
- **Ph.D. Materials Science and Engineering from the University of Houston where my research was primarily focused on the following:**
  - Simulating the heat generated during lithium-ion (Li-ion) battery charge and discharge operations
  - Characterizing the energy released during Li-ion battery thermal runaway events
- **Civil Servant at the National Aeronautics and Space Administration (NASA) Johnson Space Center (JSC)**
  - Employed by NASA JSC for ~10 years
  - Specialized in Lithium-ion (Li-ion) batteries for ~6 years
  - Supported battery safety related tasks for the Orion Multi-Purpose Crew Vehicle (MPCV), the International Space Station (ISS), Commercial Crew Program (CCP), space suits, robotics, and other various applications that utilize Li-ion technology
  - Recent focus has been on the development of fractional thermal runaway calorimetry techniques (more on that later…)

NASA

West Texas A&M University™

UNIVERSITY of HOUSTON

ABOUT THIS COURSE

- **This short course is designed to educate participants in the following areas:**
  - Fundamental concepts regarding Lithium-ion (Li-ion) batteries and how they work
  - Heat generation mechanisms for nominal operations (charge and discharge) and during thermal runaway
  - Battery safety, best handling practices, abuse testing, and lessons learned
  - Practical model construction techniques and example simulation results for both nominal operations and for thermal runaway
- **In general, this short course focuses on Li-ion batteries from a thermo-electrochemical perspective**
- **Although extensive, this short course is not comprehensive and should not be used as a replacement for consulting with your resident battery experts for specific advice and design guidelines**

COURSE OVERVIEW

Module 1: Fundamental Concepts	**Section 1: Introduction to Lithium-ion Batteries** **Section 2: Heat Generation from Electrochemical Processes**
Module 2: Battery Safety	**Section 1: Fundamentals of Thermal Runaway** **Section 2: Thermal Runaway Testing Techniques** **Section 3: Addressing the Variance of Thermal Runaway** **Section 4: NASA's Response to Thermal Runaway**
Module 3: Modeling Techniques	**Section 1: Practical Thermal Model Construction Techniques** **Section 2: Example Thermal Simulations Part 1, Nominal Operations** **Section 3: Example Thermal Simulations Part 2, Thermal Runaway**
Module 4: Handling	**Section 2: Safe Handling Practices**
	Wrap-Up and Questions **Acknowledgements**








MODULE 1 SECTION 1:

INTRODUCTION TO LITHIUM-ION BATTERIES

GLOBAL DEMAND FOR LITHIUM-ION BATTERIES

- **Lithium-ion batteries provide energy dense and low mass energy storage solutions for a wide array of applications including the following:**
  - Automobile, aerospace, industrial, medical, military, small portable electronics, railway, and space exploration:
  - Growing demand for advanced energy storage systems drives the Li-ion battery market which is expected to reach $43 billion USD by 2020 [1, 11-13]

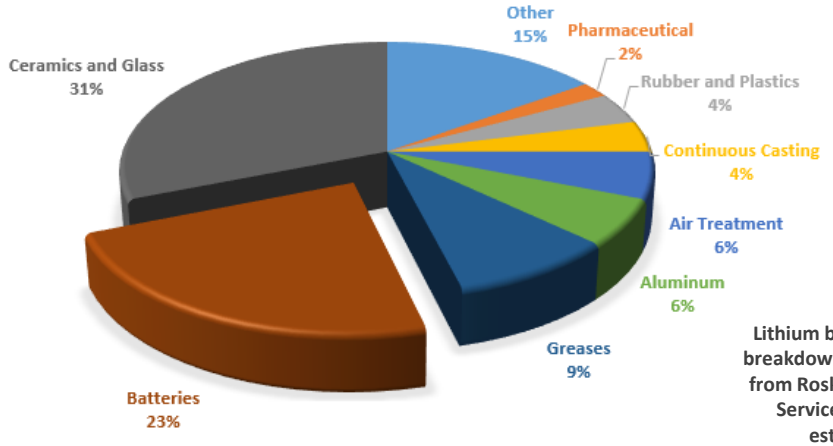

Lithium battery end use breakdown based on data from Roskill Information Services LTD. 2009 estimates [1]

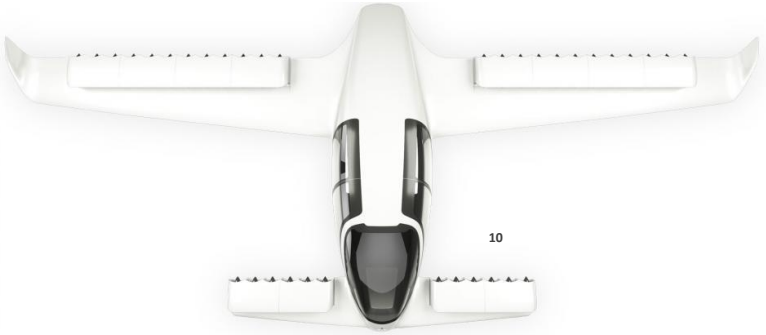
10


4


2


5


6


7


8

9


3

1 Energy and Capital, "Energy storage companies: investing in lithium batteries," 2012. [Online]. Available: https://www.energyandcapital.com/resources/energy-storage-companies.
2 Apple, "Why Lithium-ion?," Apple, [Online]. Available: https://www.apple.com/batteries/why-lithium-ion/. [Accessed 5 June 2015].
3 Tesla Motors, "Tesla Motors," Tesla Motors, [Online]. Available: http://www.teslamotors.com/en_GB/support. [Accessed 5 June 2015].
4 Milwaukee, "M18 Cordless 1/2" Hammer Drill/Driver (Bare Tool)," Milwaukee, [Online]. Available: http://www.milwaukeetool.com/power-tools/cordless/2602-20. [Accessed 5 June 2015].
5 Varta, "Li-ion battery cell / energy storage / flat CP series," Varta, [Online]. Available: http://www.directindustry.com/prod/varta-microbattery-gmbh/product-88149-1349927.html. [Accessed 15 June 2015].
6 C. Macmanus, "New Sony Rechargeable battery has 4x the lifespan of current lithium ion batteries," Sony, [Online]. Available: http://www.sonyinsider.com/2009/08/11/new-sony-rechargeable-battery-has-4x-the-lifespan-of-current-lithium-ion-batteries/. [Accessed 5 June 2015].
7 All-Battery, "Li-polymer 3.7V 3000mAh (506090) Battery," All-Battery, [Online]. Available: http://www.all-battery.com/polymerli-ionbattery37v3000mah506090.aspx. [Accessed 5 June 2015].
8 "Tenergy Li-ion prismatic (103450) 3.7V 1800mAh rechargeable battery," Tenergy, [Online]. Available: http://www.tenergy.com/30052. [Accessed 1 July 2015].
9 Smart Battery, "12V 50Ah Lithium ion battery SB50," Smart Battery, [Online]. Available: http://www.lithiumion-batteries.com/products/product/12v-50ah-lithium-ion-battery.php. [Accessed 15 June 2015].
10 Huber, M., "It's a bird, it's a plane, it's... an uber?", https://www.bjtonline.com/business-jet-news/its-a-bird-its-a-plane-itsan-uber. [Accessed 13 August 2018].
11 A. Franco, Rechargeable lithium batteries: from fundamentals to applications, London: Woodhead Publishing, 2015.
12 EnerSys, "EnerSys power/full solutions investors presentation," 2014.
13 C. Carella, "Frost & Sullivan, global lithium-ion market to double despite recent issues," 21 February 2013. [Online]. Available: http://www.frost.com/prod/servlet/press-release.pag?docid=274194514.

HOW LITHIUM-ION BATTERIES WORK

- **The primary components of Li-ion batteries are the anode, cathode, electrolyte, and separator (collectively, these materials are referred to as the electrode winding or stack-up):**
  - Li ions intercalate/de-intercalate between the anode and cathode (i.e. electrodes) during discharge/charge respectively; intercalation refers to the insertion and extraction of ions between the layers of cathode/anode materials
  - Ions flow through an ionically-conductive and electrically insulating separator to prevent internal short circuiting (i.e. the touching of electrodes)
  - Electrons flow through an external circuit

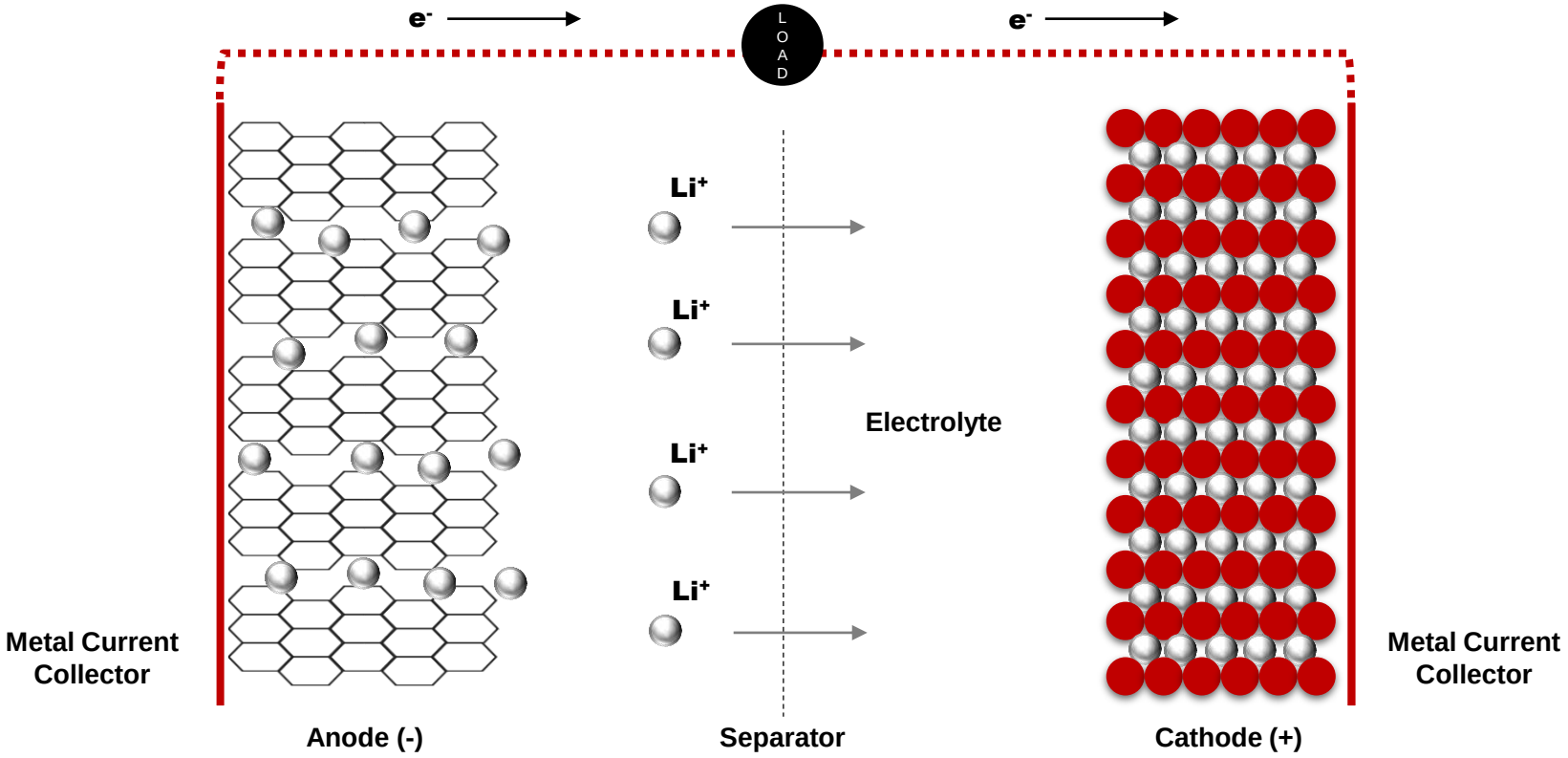

Schematic applies to discharge: reverse ion-electron flow for charge

RAGONE PLOT COMPARISON OF ENERGY STORAGE DEVICES

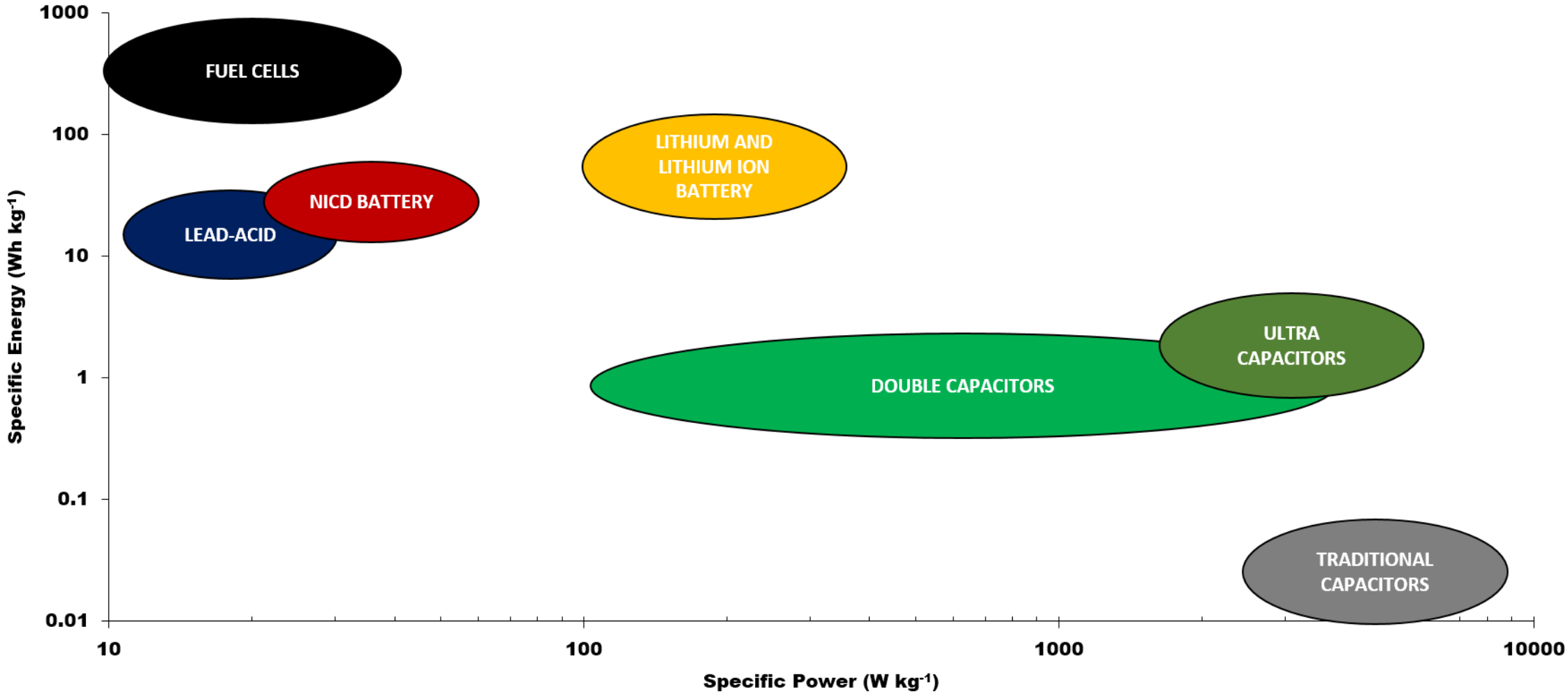

14 Ragone plot of energy storage device specific energy density vs. specific power density. Data adapted from the United States Defense Logistics Agency.

PRIMARY DISADVANTAGES OF LITHIUM-ION BATTERIES

- **More expensive than alkaline counterparts**
- **Losses in capacity through cycling**
- **Poor cold temperature performance, and a generally limited optimal operating range (between 15°C and 40°C)**
- **Solid Electrolyte Interphase (SEI) formation at the interface:**
  - A passive layer consisting of organic and inorganic electrolyte decomposition products that occurs at the interface of the electrolyte and the negative electrode (anode); forms during the first charge cycle
  - While the SEI provides some benefits (ionic conductivity and electrical isolation), there can also be negative effects with respect to, overall cell stability, cyclability, and the C-rate capability of the cell
  - SEI formation will always be a limiting factor for cell capacity and can also lead to long-term and irreversible capacity losses as the SEI grows
- **Volumetric expansion**
  - Too much volumetric change during insertion and de-insertion of Li-ions can damage electrodes and detrimentally affect battery life and performance [15-16]
- **Other disadvantages center around safety concerns:**
  - Thermal runaway, which can occur due to mechanical failure, electrochemical failure or thermal failure (detailed discussion later)
  - Single cell thermal runaway energy can propagate to surrounding Li-ion cells causing a chain-reaction event
  - Ejected materials and gases during runaway events are toxic, acidic and highly dangerous (e.g. toxic organic electrolytes)
- **Due to the safety concerns, there are significant, and costly, transportation restrictions**

15 Zhang, H., & Braun, P. V. (2012). Three-Dimensional Metal Scaffold Supported Bicontinuous Silicon Battery Anodes. *Nano Letters*, *12*, 2778-2783.
16 NASA Ares Laboratories, "Scanning Electron Microscopes Laboratory," NASA ARES, [Online]. Available: http://ares.jsc.nasa.gov/Laboratories/kr_laboratories/SEM.cfm. [Accessed 15 July 2015].

KEY TERMINOLOGY

- **Cell** refers to a single assembly of the electrode winding materials placed inside of a cell casing
- **Cell casing** refers to the encapsulation material used to encase the electrode winding (e.g. the steel can for cylindrical cells)
- **Jellyroll** and **electrode winding** are common terms used to describe the lay-up of cathode, anode, separator, and electrolyte

- **Battery** can refer to an assembly of Li-ion cells or, depending on who you talk to, can also refer to a single Li-ion cell
- **Banks**, **packs, and assemblies** refer to small collections of multiple cells; assemblies can also refer to an arrangement of multiple banks and packs

What

KEY TERMINOLOGY

- **Open circuit voltage (OCV or V_{OC})** refers to the voltage difference between the electrode terminals when no current is applied; OCV is state-of-charge dependent
- **Working voltage (V_W)** refers to the actual voltage during charge and discharge
- **Nominal voltage** is a mid-point voltage (or average voltage) representative of the overall voltage to expect between a battery being completely charged and completely discharged
- **State-of-charge (SOC)** refers to the percent state of charge that the battery is at for any given point in time
- **Depth-of-discharge (DOD)** refers to how deeply the battery is discharged (also described in percent)
- **Capacity** defines how much energy the cell can store and is typically rated based on 1-Coulomb discharge rate (i.e. how many Amps can be pulled from the cell constantly for 1 hour when starting at 100% state-of-charge):
  - 1 Ah cell can support a 1 A discharge for 1 hour
  - 3.5 Ah cell can support a 3.5 A discharge for 1 hour
- **Coulomb** refers to the rate of charge or discharge in relationship to how quickly or slowly a full charge is reached (on charging) or a full charge is depleted (on discharge) – example for a 1 Ah cell provided below:
  - 0.2 C-rate (or C/5) allows 0.2 A to be drawn for 5 hours
  - 0.5 C-rate (or C/2) allows 0.5 A to be drawn for 2 hours
  - 1 C-rate allows 1 A to be drawn for 1 hour
  - 2 C-rate allows 2 A to be drawn for 0.5 hours (30 minutes)
  - 5 C-rate allows 5 A to be drawn for 0.2 hours (12 minutes)






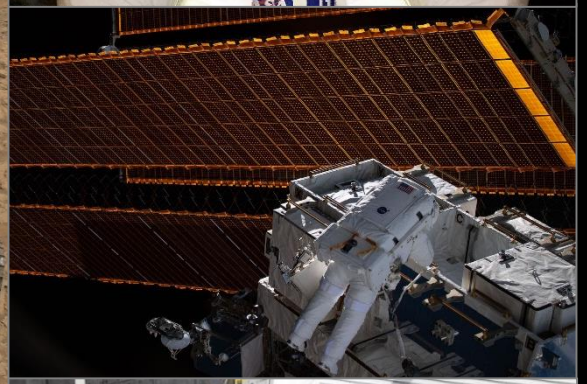

MODULE 1 SECTION 2:

HEAT GENERATION FROM ELECTROCHEMICAL PROCESSES

HEAT GENERATION FROM ELECTROCHEMICAL PROCESSES

- **Battery designers should understand that heat is generated when a Li-ion battery is operated; this heat generation is due to certain reversible and irreversible processes that are associated with the electrochemical reactions that drive battery charge and discharge**

- **Sherfey and Brenner (1958) first associated the heat generation during electrochemical processes as a function of the over-potential (irreversible processes) and entropy change (reversible process) [17-20]:**
  - Over-potential refers to the difference between the open circuit voltage (V_{OC}) and the working voltage (V_W), and exists primarily due to charge transfer resistance (i.e. resistance to ion movement at the electrolyte to electrode interface – also referred to as electrode over-potential), transport resistance in phase (i.e. Joule/Ohmic heating due to resistance in the electrode and electrolyte materials), and mass transfer limitations
  - "Entropic" heat is generated from the reversible entropy change associated with the electrochemical reactions; i.e. we have "exothermic and endothermic reactions within the cell due to the transfer of ions and electrons"

- **Bernardi et. al. (1985) developed an energy balance that expanded from the Sherfey and Brenner definition to represent the temperature change of a Li-ion cell as a function of the following [17-20]:**
  - Enthalpy of reactions and the associated entropic heating
  - Enthalpy of mixing (i.e. heat generation due to the inhomogeneous distribution of ions during charge/discharge)
  - Phase change due to diffusion of ions
  - Change in heat capacity
  - Heat associated with electrical work and over-potential
  - Heat transfer to the surroundings

- **<u>Simplified</u> derivation provided on the following two slides**

17 J. M. Sherfey and A. Brenner, "Electrochemical Calorimetry," Journal of the Electrochemical Society, vol. 105, no. 11, 1958.
18 D. Bernardi, E. Pawlikowski and J. Newman, "A General Energy Balance for Battery Systems," Journal of the Electrochemical Society, vol. 132, no. 4, 1985.
19 T. Bandhauer et. al., "A critical review of thermal issues in lithium-ion batteries," Journal of the Electrochemical Society, vol. 158, no. 3, 2011
20 M. Keyser et. al., "Battery Thermal Characterization," NREL Report, 2015.

HEAT GENERATION FROM ELECTROCHEMICAL PROCESSES

- The derivation by Bernardi et. al. (1985), assuming discharge, begins with the First Law of Thermodynamics:

$$\frac{dH_{Tot}}{dt} = q - IV \quad (1)$$

Sum of the enthalpies

Heat transfer with the environment

Electrical work term

- Expand the sum of the enthalpies to include each phase:

$$H_{Reaction} - H_{Mixing} - H_{Phase\ Change} + H_{Heat\ Capcity} = q - IV \quad (2)$$

- Assume that mixing and phase change can be neglected, and also assume that heat capacity can be represented with an average value (fine for most practical applications):

$$q = IV + H_{Reaction} + MC_p \frac{dT}{dt} \quad (3)$$

Heat capacity term

- Write-out the full representation of enthalpy of reaction:

$$q = IV + \sum_1 I_1 \left(T^2 d \frac{\frac{U_{1,Avg}}{T}}{\partial T} \right) + MC_p \frac{dT}{dt} \quad (4)$$

Enthalpy of reaction term

17 J. M. Sherfey and A. Brenner, "Electrochemical Calorimetry," Journal of the Electrochemical Society, vol. 105, no. 11, 1958.
18 D. Bernardi, E. Pawlikowski and J. Newman, "A General Energy Balance for Battery Systems," Journal of the Electrochemical Society, vol. 132, no. 4, 1985.
19 T. Bandhauer et. al., "A critical review of thermal issues in lithium-ion batteries," Journal of the Electrochemical Society, vol. 158, no. 3, 2011
20 M. Keyser et. al., "Battery Thermal Characterization," NREL Report, 2015.

HEAT GENERATION FROM ELECTROCHEMICAL PROCESSES

- Account for the irreversibilities associated with electrical work (i.e. over-potential) and simplify the enthalpy of reaction term to reflect entropic heat:

$$q = \left[IV - \sum_1 I_1 U_{1,Avg}\right] + \sum_1 I_1 \left(Td\frac{U_{1,Avg}}{\partial T}\right) + MC_p\frac{dT}{dt} \quad (5)$$

- Account for the irreversibilities associated with electrical work (i.e. over-potential):

$$MC_p\frac{dT}{dt} = -q + I\left(U_{1,Avg} - V - T\frac{dU_{1,Avg}}{\partial T}\right) \quad (6)$$

- Extracting only the heat generated due to over-potential and entropic heating (Q_{Cell}) from Equation (6), and with the nomenclature adjusted to match this presentation, we have the following:

$$Q_{Cell} = I\left(V_{OC} - V_W - T\frac{dV_{OC}}{\partial T}\right) \quad (7a)$$

- For charging, current (I) is reversed and the equation becomes the following:

$$Q_{Cell} = I\left(V_W - V_{OC} + T\frac{dV_{OC}}{\partial T}\right) \quad (7b)$$

These are the heat load functions you put in your thermal model

"Overpotential heat"
"Polarization heat"
"Joule heat"
"Ohmic heat"

"Entropic heat"

17 J. M. Sherfey and A. Brenner, "Electrochemical Calorimetry," Journal of the Electrochemical Society, vol. 105, no. 11, 1958.
18 D. Bernardi, E. Pawlikowski and J. Newman, "A General Energy Balance for Battery Systems," Journal of the Electrochemical Society, vol. 132, no. 4, 1985.
19 T. Bandhauer et. al., "A critical review of thermal issues in lithium-ion batteries," Journal of the Electrochemical Society, vol. 158, no. 3, 2011
20 M. Keyser et. al., "Battery Thermal Characterization," NREL Report, 2015.

EXAMPLE OF HEAT GENERATION WHEN DISCHARGING

- **Discharge example for a large format 185 Ah $LiCoO_2$ electric vehicle battery based on Chen et. al. [19] and Walker et. al. [20] which compared test and analysis for various discharge rates and convective cooling environment combinations:**
  - The stack of Li-ion cells was treated as a lump mass surrounded in electrolyte
  - The data presented in this section are based on Walker et. al. Case study 1 which considered 1-C, 2-C, and 3-C discharge rates in a 27 °C natural convection environment; only the test data is shown in this section – the comparison of test data to analysis is provided in Module 3

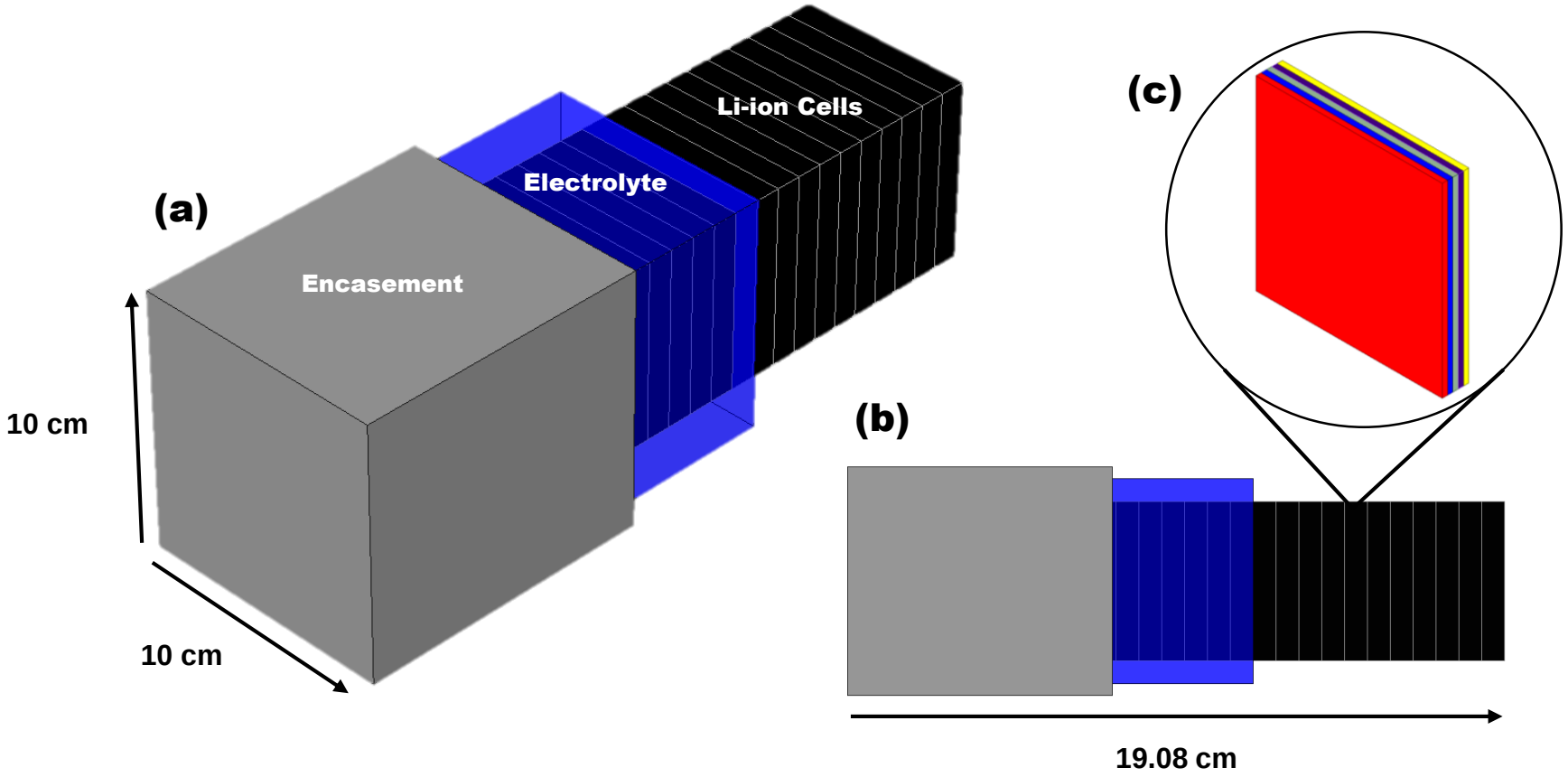

Image courtesy of Walker and Ardebili [20]

19 S. Chen, C. Wan and Y. Wang, "Thermal Analysis of Lithium-Ion Batteries," Journal of Power Sources, vol. 140, pp. 111-124, September 2005.
20 W. Walker and H. Ardebili, "Thermo-electrochemical analysis of lithium ion batteries for space applications using Thermal Desktop," Journal of Power Sources, vol. 269, pp. 486-497, 2014.

EXAMPLE OF HEAT GENERATION WHEN DISCHARGING

- **Discharge example for a large format 185 Ah $LiCoO_2$ electric vehicle battery based on Chen et. al. [19] and Walker et. al. [20] which compared test and analysis for various discharge rates and convective cooling environment combinations:**
  - Image below compares the voltage profiles to the corresponding temperature profiles, at three different C-rates, for operation in a room temperature environment under natural convection conditions
  - Less heat is generated when operating at lower C-rates which results in lower overall temperatures; note that smaller amounts of heat is generated at lower C-rates because the battery is operating more efficiently (i.e. less heat due to over-potential)

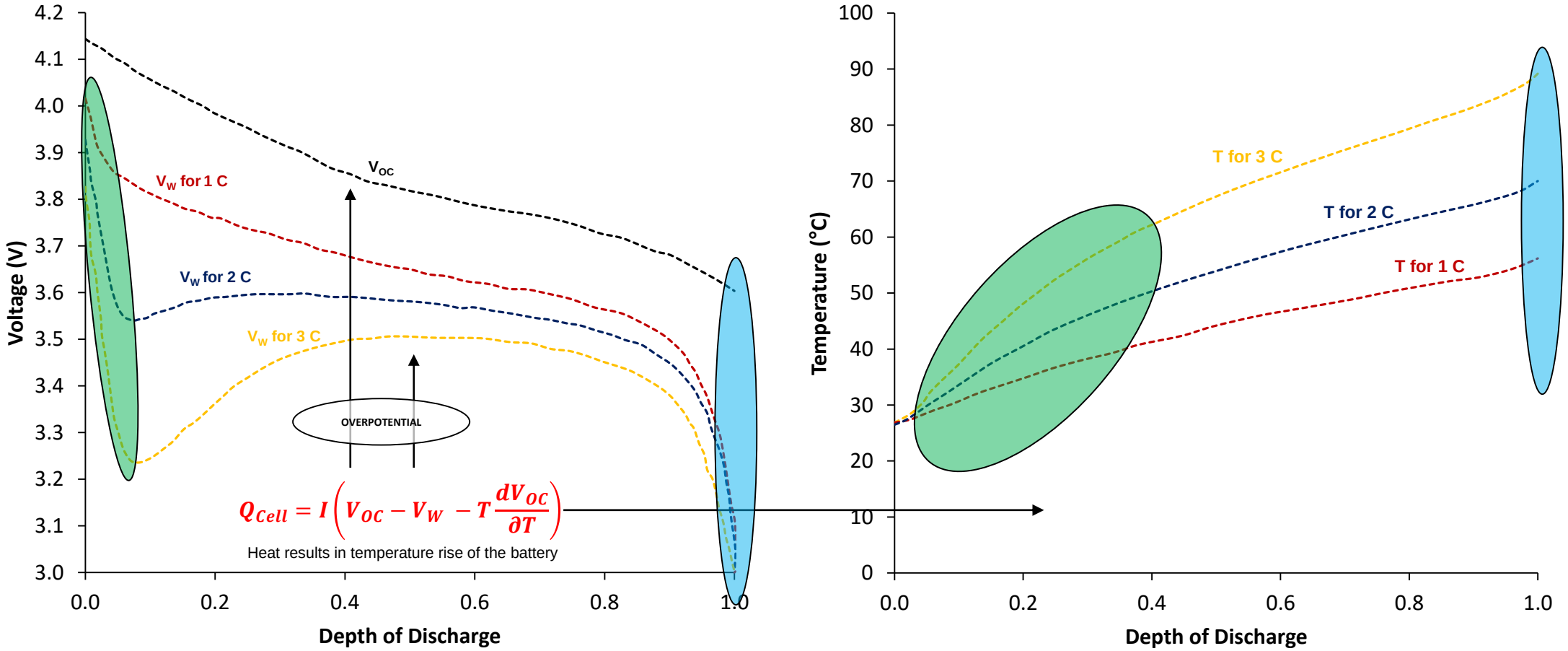

Image courtesy of Walker and Ardebili [20]

19 S. Chen, C. Wan and Y. Wang, "Thermal Analysis of Lithium-Ion Batteries," Journal of Power Sources, vol. 140, pp. 111-124, September 2005.
20 W. Walker and H. Ardebili, "Thermo-electrochemical analysis of lithium ion batteries for space applications using Thermal Desktop," Journal of Power Sources, vol. 269, pp. 486-497, 2014.

EXAMPLE OF HEAT GENERATION WHEN CHARGING

- **Charge example based on various charging rates of a Boston Power Swing® 5300 Li-ion cell [21] and Walker et. al. [22] :**
  - The Boston Power 5300 cell was charged at the following three rates for this example: 0.7-C, 1-C, and 2-C
  - This example does not employ constant current like the discharge example; current (I) starts tapering when the cell reaches 80% SOC (for safety purposes to prevent overcharge)
  - Image Credit: Walker et. al. [22]

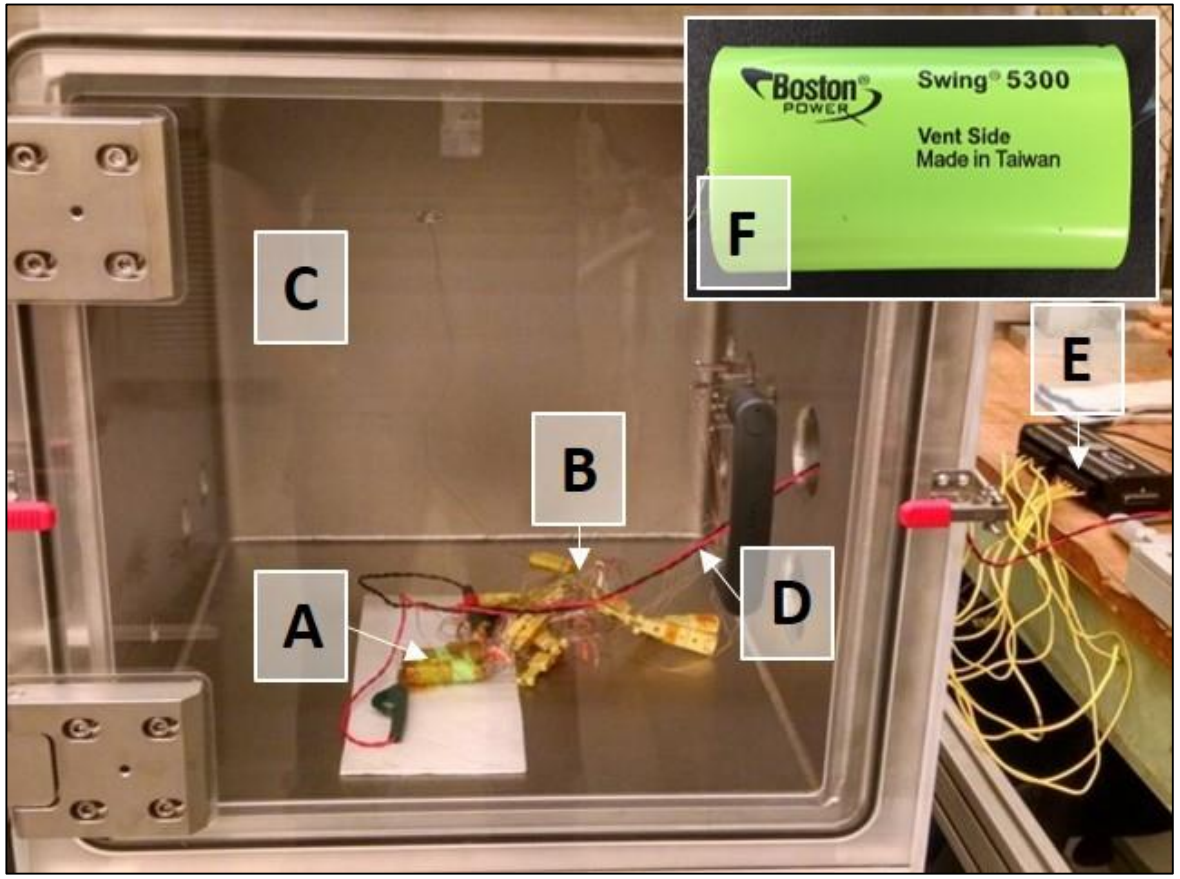

21 Boston Power, *Swing 5300 Rechargeable Lithium-ion Cell*, Westborough: Boston-Power, Incorporated, 2013.
22 W. Walker, S. Yayathi, J. Shaw and H. Ardebili, "Thermo-electrochemical evaluation of lithium-ion batteries for space applications." Submitted to Journal of Power Sources June 27th, 2015.

EXAMPLE OF HEAT GENERATION WHEN CHARGING

- **Charge example based on various charging rates of a Boston Power Swing 5300 Li-ion cell [21] and Walker et. al. [22]:**
  - The transient temperature profile observed for each of the curves is in direct relationship with the over-potential and the current taper
  - Unlike with discharge, there is not a temperature spike at the end of charging because the over-potential is nearly zero and the cell is operating under nearly entirely reversible conditions (i.e. it is operating as efficiently as possible)
  - Image Credit: Walker et. al. [22]

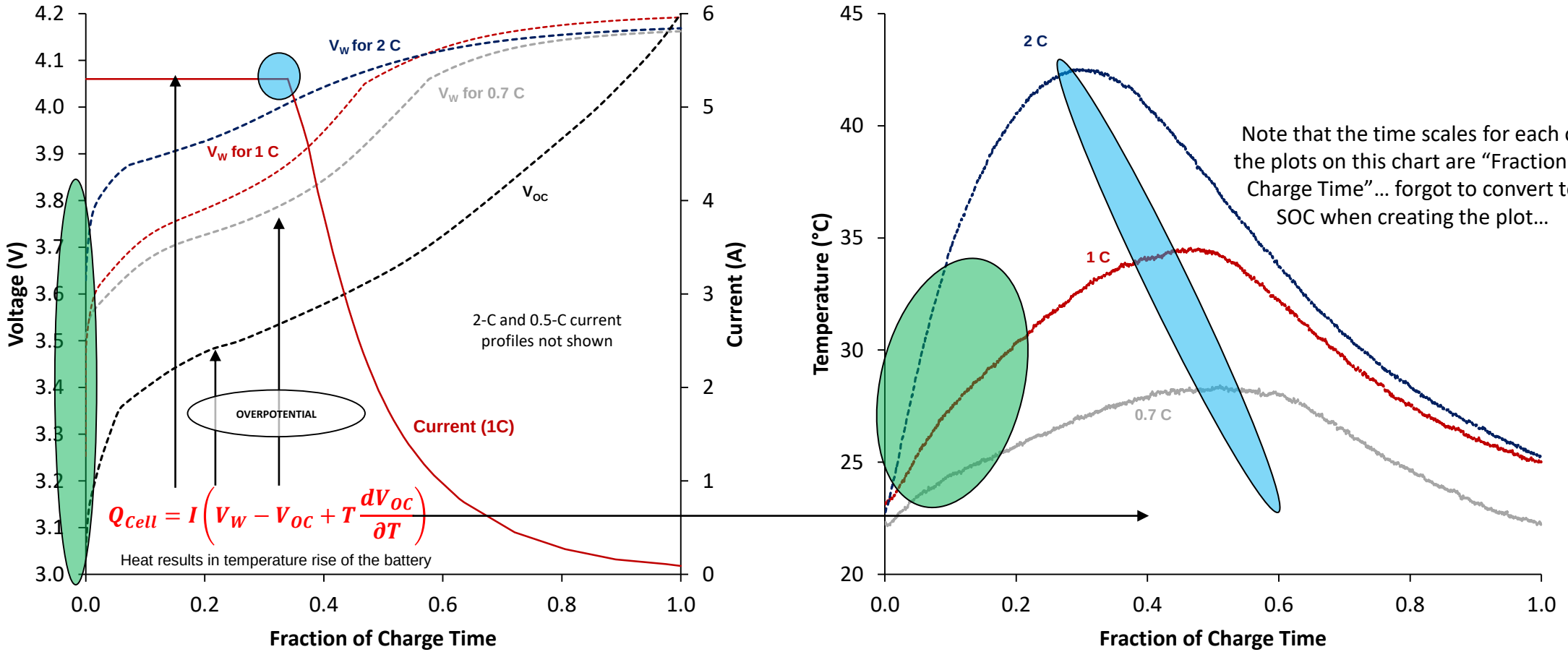

21 Boston Power, *Swing 5300 Rechargeable Lithium-ion Cell*, Westborough: Boston-Power, Incorporated, 2013.
22 W. Walker, S. Yayathi, J. Shaw and H. Ardebili, "Thermo-electrochemical evaluation of lithium-ion batteries for space applications." Submitted to Journal of Power Sources June 27th, 2015.

Image courtesy of Walker et. al. [22]

LESSONS LEARNED FROM HEAT GENERATION EXAMPLES

- **The heat generation rate during electrochemical processes are primarily a function of over-potential and entropy change, but can also include the effects of:**
  - Enthalpy of mixing
  - Phase change due to diffusion of ions
  - Changes in heat capacity
- **Heat generation should not be considered as a single value (i.e. I^2R), but rather a transient value that is a function of state-of-charge (for charging) or depth-of-discharge (for discharging)**
- **When $V_{OC} \approx V_W$, the cell is said to be operating reversibly and is delivering the maximum amount of electrical work:**
  - In this case there is little to know heat generation due to over-potential, and the temperature change of the cell is primarily a function of the entropic heat (whether endothermic or exothermic for charge and discharge, respectively)
  - The effects of entropic heat can often be masked by the over-potential heat, and thus become most apparent when over-potential is minimized
  - In general, the examples demonstrate that higher discharge rates lead to greater over-potential

17 J. M. Sherfey and A. Brenner, "Electrochemical Calorimetry," Journal of the Electrochemical Society, vol. 105, no. 11, 1958.
18 D. Bernardi, E. Pawlikowski and J. Newman, "A General Energy Balance for Battery Systems," Journal of the Electrochemical Society, vol. 132, no. 4, 1985.
19 T. Bandhauer et. al., "A critical review of thermal issues in lithium-ion batteries," Journal of the Electrochemical Society, vol. 158, no. 3, 2011
20 M. Keyser et. al., "Battery Thermal Characterization," NREL Report, 2015.

TEMPERATURE DEPENDENCY OF HEAT GENERATION RATES

- **Li-ion battery designers should understand that both performance and safety are temperature dependent:**
  - From a performance perspective, V_{OC}, V_W, and the entropy term from the Bernardi et. al. (1985) equation are all temperature dependent; i.e. the respective voltage profiles will look completely different at different temperature increments (…-20 °C, -10 °C, 0 °C, +10 °C, +20 °C…)
  - The previous two examples were for charge and discharge at room temperature; i.e. only representative of performance based on one set of voltage profiles defined at ~20 °C
  - The temperature dependencies of voltage also translates to capacity being temperature dependent
  - Also from a performance perspective, operating the cells beyond the certified temperature ranges can permanently damage the cell
  - From a safety perspective, over-heating is one abuse type that can lead to thermal runaway (more discussion on this in Module 2)
  - Therefore, design consideration must be given to any mechanism that can change the internal temperature of the Li-ion battery
- **Additional thoughts from the instructor:**
  - From an analysis perspective, some analysts simplify nominal internal heat generation to be a function of the current multiplied by the internal resistance of the cell, which, per Ohm's law, also yields the heat generated from operating the cell
  - Unfortunately, this method yields a constant value, and as shown on the next few slides, will fail to adequately characterize the thermal profile of a given cell during charge and discharge operations – including peak temperatures
  - This instructor recommends always considering the effects of temperature and voltage change on charge and discharge heat generation rates
- **More on how to apply use principles for battery thermal analysis with Module 3**






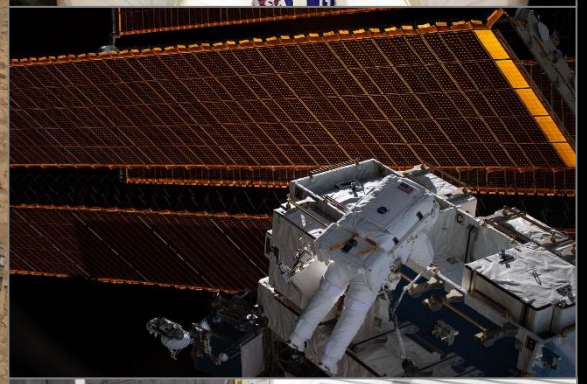

MODULE 2 SECTION 1:

FUNDAMENTALS OF THERMAL RUNAWAY

DEFINING THERMAL RUNAWAY

- **Safety concerns exist for Li-ion battery utilization due to the possibility of thermal runaway (TR); see example to the right which depicts an 18650 cell experiencing thermal runaway (Image Credit: Walker et. al., 2019, J. Power Sources)**

- **Thermal runaway can occur when a Li-ion cell achieves elevated temperatures due to:**
  - Thermal failure (e.g. over-temp)
  - Mechanical failure (e.g. nail penetration)
  - Internal short circuiting (hard and soft variations)
  - External short circuiting
  - Electrochemical abuse (e.g. overcharge and over-discharge)

- **At elevated temperatures, exothermic decomposition reactions begin:**
  - Self-heating begins when heat generation rates exceed the heat dissipation capability
  - The rate of the exothermic reactions increase with temperature in Arrhenius form
  - Eventually, stability is lost and cell rupture and fire occurs; all remaining electrochemical energy is released
  - The models describing the decomposition reaction rates and self heating rates (i.e. kinetic relationships) are provided with the following charts

- **The severity of the event can increase if combustion between the gases released from the cell and the surrounding atmosphere is not prevented**

- **Propagation is a chain reaction event that occurs when the thermal runaway energy from an initial cell causes neighboring cells to overheat and also suffer thermal runaway failures**

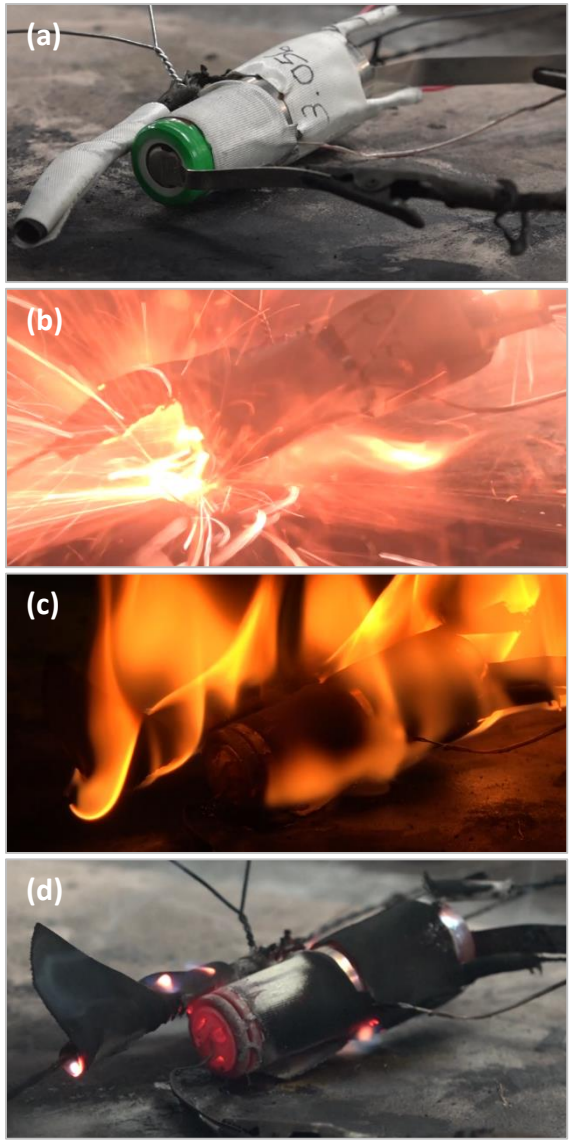

THERMAL RUNAWAY EXAMPLE 1

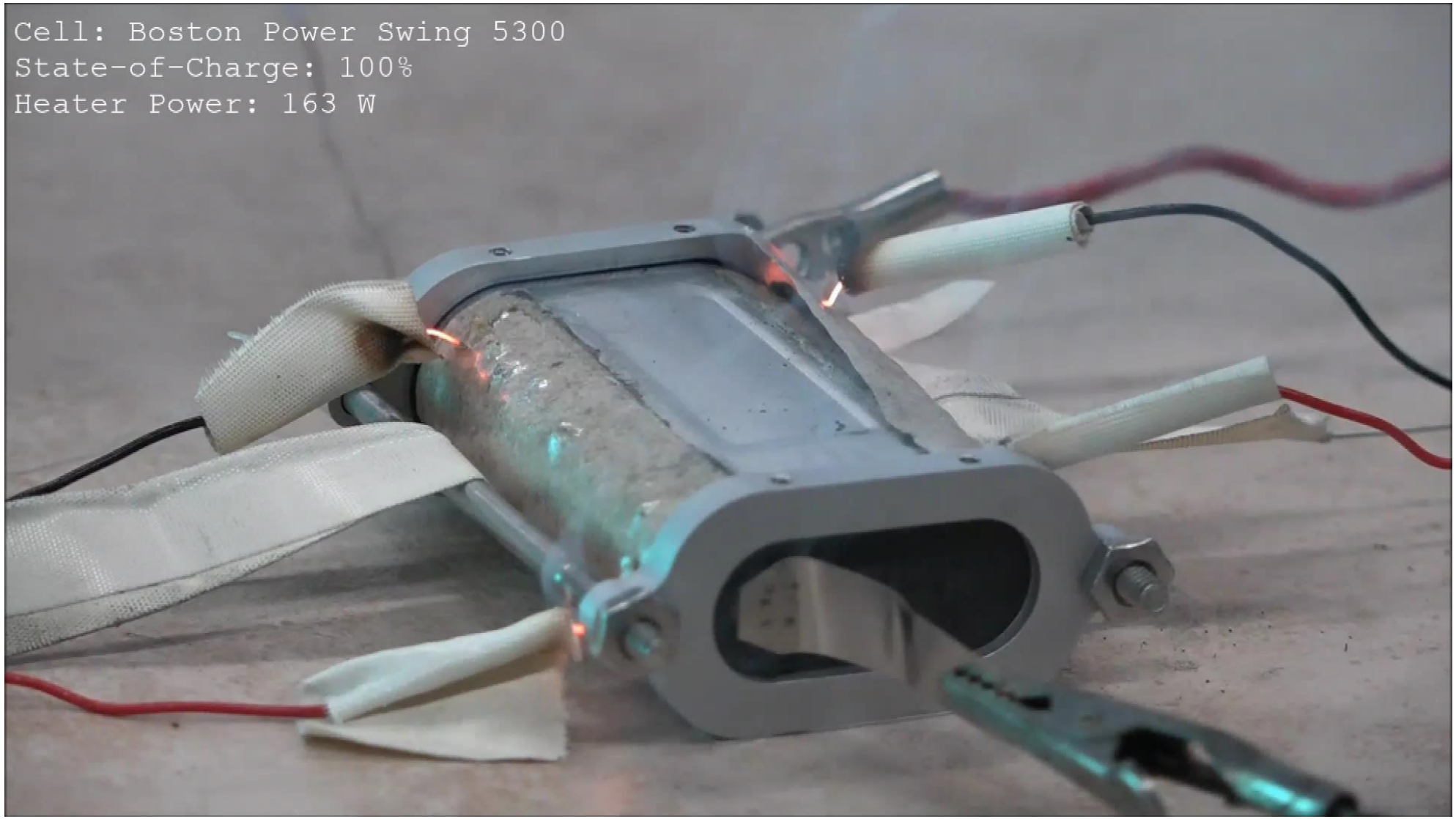

Video Credit: Yayathi et. al. [31].

27 Yayathi, et. al., J. of Power Sources, 329 (2016) 197-206.

THERMAL RUNAWAY EXAMPLE 1

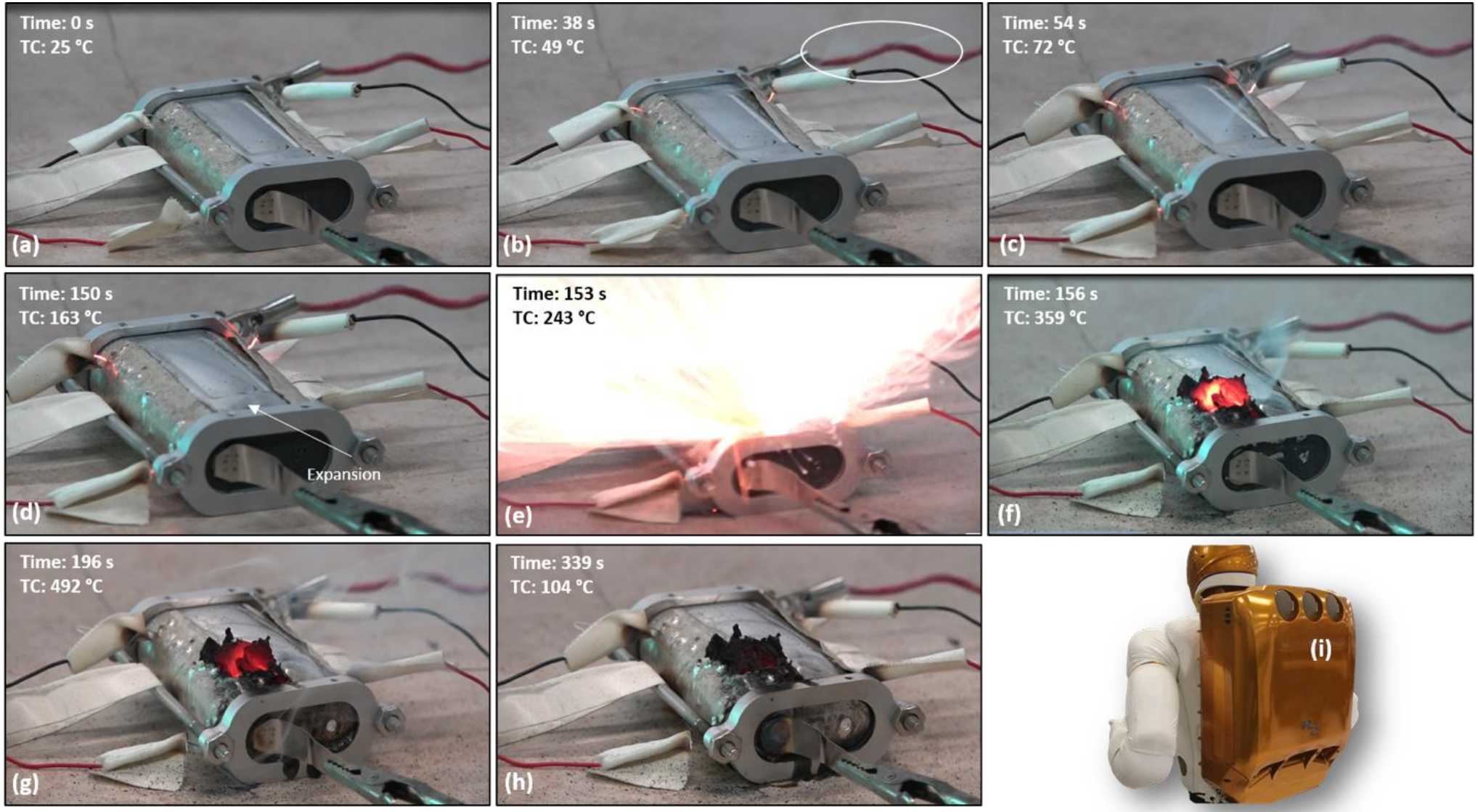

Image Credit: Yayathi et. al. [31].

27 Yayathi, et. al., J. of Power Sources, 329 (2016) 197-206.

THERMAL RUNAWAY EXAMPLE 2

[2] Rickman et. al., "Considerations for Thermal Modeling of Lithium-Ion Cells for Battery Analysis." 46th International Conference on Environmental Systems (ICES). 10-14 July 2016.

THERMAL RUNAWAY EXAMPLE 3

THERMAL RUNAWAY KINETIC RELATIONSHIPS

- **At a fundamental level, the energy released due to thermal runaway (i.e. the heat of thermal runaway) is a direct result of the following:**
  - Exothermic decomposition of the anode, SEI, cathode, and electrolyte
  - Release of remaining electrochemical energy stored in the cell
- **The temperature dependencies of the decomposition reaction rates are defined with the Arrhenius equation:**
  - The decomposition reactions are also exothermic and therefore the resulting heating profiles are directly proportional to the Arrhenius form decomposition reaction rates
  - This combination of exothermic decomposition and Arrhenius style temperature dependencies results in the cascading self-heating event known as thermal runaway
  - These associations are referred to as thermal runaway kinetic relationships
- **A series of models were published (1999 – 2015) to describe thermal runaway energy release as a function of the kinetic relationships between decomposition reaction rates and exothermic self heating rates:**
  - Richard and Dahn (1999) provided models representing the energy release due to the decomposition of the anode and the SEI layer
  - Hatchard et. al. (2001) provided models representing the energy release due to the decomposition of the cathode
  - Kim et. al. (2007) expanded the models to include the heating associated with electrolyte decomposition
  - Coman et. al. (2015) provided the most recent update which added the effects of burst pressure, the endothermic effects associated with the boiling of the electrolyte, and the release of all remaining electrochemical energy stored in the cell

23 Richard, M. Accelerating rate calorimetry study on the thermal stability of lithium intercalated graphite in electrolyte. I. experimental. *Journal of The Electrochemical Society* **146,** 2068 (1999).
24 Hatchard, T., MacNeil, D., Basu, A. & Dahn, J. Thermal model of cylindrical and prismatic lithium-ion cells. *Journal of The Electrochemical Society* **148,** A755 (2001).
25 Kim, G.-H., Pesaran, A. & Spotnitz, R. A three-dimensional thermal abuse model for lithium-ion cells. *Journal of Power Sources* **170,** 476–489 (2007).
26 Coman, P., Rayman, S. & White, R. A lumped model of venting during thermal runaway in a cylindrical Lithium Cobalt Oxide lithium-ion cell. *J Power Sources* **307,** 56–62 (2016).

THERMAL RUNAWAY KINETIC RELATIONSHIPS

$$\frac{dx_{SEI}}{dt} = -A_{SEI} x_{SEI} exp\left(\frac{-E_{SEI}}{k_b T}\right) \quad (1)$$

$$\frac{dx_a}{dt} = -A_a x_a exp\left(\frac{-z}{z_0}\right) exp\left(\frac{-E_a}{k_b T}\right) \quad (2)$$

$$\frac{dz}{dt} = A_a x_a exp\left(\frac{-z}{z_0}\right) exp\left(\frac{-E_a}{k_b T}\right) \quad (3)$$

$$\frac{dQ_{SEI}}{dt} = -m_{SEI}\, h_{SEI}\, \frac{dx_{SEI}}{dt} \quad (4)$$

$$\frac{dQ_a}{dt} = -m_a\, h_a\, \frac{dx_a}{dt} \quad (5)$$

Heating due to SEI and anode decomposition (Richard and Dahn, 1999 [23])

$$\frac{dx_c}{dt} = A_c x_c (1 - x_c) exp\left(\frac{-E_c}{k_b T}\right) \quad (6)$$

$$\frac{dQ_c}{dt} = m_c\, h_c\, \frac{dx_c}{dt} \quad (7)$$

Heating due to cathode decomposition (Hatchard et. al., 2001 [24])

$$\frac{dY_e}{dt} = -A_e Y_e exp\left(\frac{-E_e}{k_b T}\right) \quad (8)$$

$$\frac{dQ_e}{dt} = -m_e\, h_e\, \frac{dx_e}{dt} \quad (9)$$

Heating due to electrolyte decomposition (Kim et. al., 2007 [25])

$$\frac{dSoC}{dt} = -A_{ec}\,(1 - x_c) x_a \exp\left(\frac{-E_{ec}}{k_b T}\right) + \left(\frac{dx_c}{dt} - \frac{dx_a}{dt}\right) SoC \quad (10)$$

$$\frac{dQ_{ec}}{dt} = -(m_c + m_a)\, h_{ec}\, \frac{dSoC}{dt} \quad (11)$$

Heating due release of electrochemical energy (Coman et. al. 2015 [26])

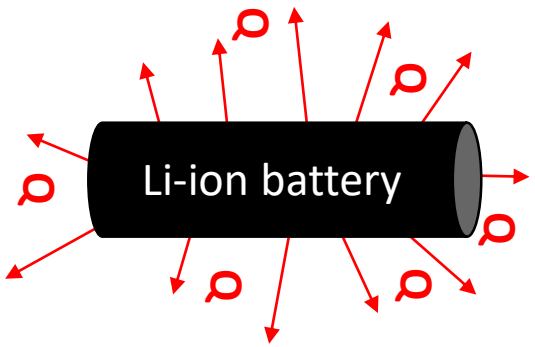

A	Frequency Factor
Y	Fraction Electrolyte
x	Fraction Remaining Lithium
E	Activation Energy
k_b	Boltzmann Constant
T	Temperature
z	Tunneling Term
m	Mass
h	Enthalpy
t	Time
Q	Heat
SOC	State-of-Charge

23 Richard, M. Accelerating rate calorimetry study on the thermal stability of lithium intercalated graphite in electrolyte. I. experimental. *Journal of The Electrochemical Society* **146,** 2068 (1999).
24 Hatchard, T., MacNeil, D., Basu, A. & Dahn, J. Thermal model of cylindrical and prismatic lithium-ion cells. *Journal of The Electrochemical Society* **148,** A755 (2001).
25 Kim, G.-H., Pesaran, A. & Spotnitz, R. A three-dimensional thermal abuse model for lithium-ion cells. *Journal of Power Sources* **170,** 476–489 (2007).
26 Coman, P., Rayman, S. & White, R. A lumped model of venting during thermal runaway in a cylindrical Lithium Cobalt Oxide lithium-ion cell. *J Power Sources* **307,** 56–62 (2016).

THERMAL RUNAWAY KINETIC RELATIONSHIPS

$$\frac{dx_{SEI}}{dt} = -A_{SEI} x_{SEI} exp\left(\frac{-E_{SEI}}{k_b T}\right) \quad (1)$$

$$\frac{dx_a}{dt} = -A_a x_a exp\left(\frac{-z}{z_0}\right) exp\left(\frac{-E_a}{k_b T}\right) \quad (2)$$

$$\frac{dz}{dt} = A_a x_a exp\left(\frac{-z}{z_0}\right) exp\left(\frac{-E_a}{k_b T}\right) \quad (3)$$

The temperature dependencies of the decomposition reaction rates are described with the Arrhenius equation

$$\frac{dQ_{SEI}}{dt} = -m_{SEI}\, h_{SEI}\, \frac{dx_{SEI}}{dt} \quad (4)$$

$$\frac{dQ_a}{dt} = -m_a\, h_a\, \frac{dx_a}{dt} \quad (5)$$

Heating due to SEI and anode decomposition (Richard and Dahn, 1999 [23])

$$\frac{dx_c}{dt} = A_c x_c (1 - x_c) exp\left(\frac{-E_c}{k_b T}\right) \quad (6)$$

$$\frac{dQ_c}{dt} = m_c\, h_c\, \frac{dx_c}{dt} \quad (7)$$

Heating due to cathode decomposition (Hatchard et. al., 2001 [24])

$$\frac{dY_e}{dt} = -A_e Y_e exp\left(\frac{-E_e}{k_b T}\right) \quad (8)$$

$$\frac{dQ_e}{dt} = -m_e\, h_e\, \frac{dx_e}{dt} \quad (9)$$

Heating due to electrolyte decomposition (Kim et. al., 2007 [25])

$$\frac{dSoC}{dt} = -A_{ec}\,(1 - x_c) x_a \exp\left(\frac{-E_{ec}}{k_b T}\right) + \left(\frac{dx_c}{dt} - \frac{dx_a}{dt}\right) SoC \quad (10)$$

$$\frac{dQ_{ec}}{dt} = -(m_c + m_a)\, h_{ec}\, \frac{dSoC}{dt} \quad (11)$$

Heating due release of electrochemical energy (Coman et. al. 2015 [26])

A	Frequency Factor
Y	Fraction Electrolyte
x	Fraction Remaining Lithium
E	Activation Energy
k_b	Boltzmann Constant
T	Temperature
z	Tunneling Term
m	Mass
h	Enthalpy
t	Time
Q	Heat
SOC	State-of-Charge

23 Richard, M. Accelerating rate calorimetry study on the thermal stability of lithium intercalated graphite in electrolyte. I. experimental. *Journal of The Electrochemical Society* **146,** 2068 (1999).
24 Hatchard, T., MacNeil, D., Basu, A. & Dahn, J. Thermal model of cylindrical and prismatic lithium-ion cells. *Journal of The Electrochemical Society* **148,** A755 (2001).
25 Kim, G.-H., Pesaran, A. & Spotnitz, R. A three-dimensional thermal abuse model for lithium-ion cells. *Journal of Power Sources* **170,** 476–489 (2007).
26 Coman, P., Rayman, S. & White, R. A lumped model of venting during thermal runaway in a cylindrical Lithium Cobalt Oxide lithium-ion cell. *J Power Sources* **307,** 56–62 (2016).

THERMAL RUNAWAY KINETIC RELATIONSHIPS

$$\frac{dx_{SEI}}{dt} = -A_{SEI} x_{SEI} exp\left(\frac{-E_{SEI}}{k_b T}\right) \quad (1)$$

$$\frac{dx_a}{dt} = -A_a x_a exp\left(\frac{-z}{z_0}\right) exp\left(\frac{-E_a}{k_b T}\right) \quad (2)$$

$$\frac{dz}{dt} = A_a x_a exp\left(\frac{-z}{z_0}\right) exp\left(\frac{-E_a}{k_b T}\right) \quad (3)$$

$$\frac{dQ_{SEI}}{dt} = -m_{SEI}\, h_{SEI} \frac{dx_{SEI}}{dt} \quad (4)$$

$$\frac{dQ_a}{dt} = -m_a\, h_a \frac{dx_a}{dt} \quad (5)$$

Heat generation rates are directly proportional to decomposition rates

Heating due to SEI and anode decomposition (Richard and Dahn, 1999 [23])

$$\frac{dx_c}{dt} = A_c x_c (1 - x_c) exp\left(\frac{-E_c}{k_b T}\right) \quad (6)$$

$$\frac{dQ_c}{dt} = m_c\, h_c \frac{dx_c}{dt} \quad (7)$$

Heating due to cathode decomposition (Hatchard et. al., 2001 [24])

$$\frac{dY_e}{dt} = -A_e Y_e exp\left(\frac{-E_e}{k_b T}\right) \quad (8)$$

$$\frac{dQ_e}{dt} = -m_e\, h_e \frac{dx_e}{dt} \quad (9)$$

Heating due to electrolyte decomposition (Kim et. al., 2007 [25])

$$\frac{dSoC}{dt} = -A_{ec} (1 - x_c) x_a exp\left(\frac{-E_{ec}}{k_b T}\right) + \left(\frac{dx_c}{dt} - \frac{dx_a}{dt}\right) SoC \quad (10)$$

$$\frac{dQ_{ec}}{dt} = -(m_c + m_a)\, h_{ec} \frac{dSoC}{dt} \quad (11)$$

Heating due release of electrochemical energy (Coman et. al. 2015 [26])

A	Frequency Factor
Y	Fraction Electrolyte
x	Fraction Remaining Lithium
E	Activation Energy
k_b	Boltzmann Constant
T	Temperature
z	Tunneling Term
m	Mass
h	Enthalpy
t	Time
Q	Heat
SOC	State-of-Charge

23 Richard, M. Accelerating rate calorimetry study on the thermal stability of lithium intercalated graphite in electrolyte. I. experimental. *Journal of The Electrochemical Society* **146,** 2068 (1999).
24 Hatchard, T., MacNeil, D., Basu, A. & Dahn, J. Thermal model of cylindrical and prismatic lithium-ion cells. *Journal of The Electrochemical Society* **148,** A755 (2001).
25 Kim, G.-H., Pesaran, A. & Spotnitz, R. A three-dimensional thermal abuse model for lithium-ion cells. *Journal of Power Sources* **170,** 476–489 (2007).
26 Coman, P., Rayman, S. & White, R. A lumped model of venting during thermal runaway in a cylindrical Lithium Cobalt Oxide lithium-ion cell. *J Power Sources* **307,** 56–62 (2016).

THERMAL RUNAWAY KINETIC RELATIONSHIPS

$$\frac{dx_{SEI}}{dt} = -A_{SEI} x_{SEI} exp(\frac{-E_{SEI}}{k_b T}) \quad (1)$$

$$\frac{dx_a}{dt} = -A_a x_a exp(\frac{-z}{z_0}) exp(\frac{-E_a}{k_b T}) \quad (2)$$

$$\frac{dz}{dt} = A_a x_a exp(\frac{-z}{z_0}) exp(\frac{-E_a}{k_b T}) \quad (3)$$

$$\frac{dQ_{SEI}}{dt} = -m_{SEI}\, h_{SEI}\, \frac{dx_{SEI}}{dt} \quad (4)$$

$$\frac{dQ_a}{dt} = -m_a\, h_a\, \frac{dx_a}{dt} \quad (5)$$

Heating due to SEI and anode decomposition (Richard and Dahn, 1999 [23])

$$\frac{dx_c}{dt} = A_c x_c (1 - x_c) exp(\frac{-E_c}{k_b T}) \quad (6)$$

$$\frac{dQ_c}{dt} = m_c\, h_c\, \frac{dx_c}{dt} \quad (7)$$

Cathode looks different because Li content is a fraction of the total

Heating due to cathode decomposition (Hatchard et. al., 2001 [24])

$$\frac{dY_e}{dt} = -A_e Y_e exp(\frac{-E_e}{k_b T}) \quad (8)$$

$$\frac{dQ_e}{dt} = -m_e\, h_e\, \frac{dx_e}{dt} \quad (9)$$

Heating due to electrolyte decomposition (Kim et. al., 2007 [25])

$$\frac{dSoC}{dt} = -A_{ec} (1 - x_c) x_a \exp\left(\frac{-E_{ec}}{k_b T}\right) + \left(\frac{dx_c}{dt} - \frac{dx_a}{dt}\right) SoC \quad (10)$$

$$\frac{dQ_{ec}}{dt} = -(m_c + m_a)\, h_{ec}\, \frac{dSoC}{dt} \quad (11)$$

Heating due release of electrochemical energy (Coman et. al. 2015 [26])

A	Frequency Factor
Y	Fraction Electrolyte
x	Fraction Remaining Lithium
E	Activation Energy
k_b	Boltzmann Constant
T	Temperature
z	Tunneling Term
m	Mass
h	Enthalpy
t	Time
Q	Heat
SOC	State-of-Charge

23 Richard, M. Accelerating rate calorimetry study on the thermal stability of lithium intercalated graphite in electrolyte. I. experimental. *Journal of The Electrochemical Society* **146,** 2068 (1999).
24 Hatchard, T., MacNeil, D., Basu, A. & Dahn, J. Thermal model of cylindrical and prismatic lithium-ion cells. *Journal of The Electrochemical Society* **148,** A755 (2001).
25 Kim, G.-H., Pesaran, A. & Spotnitz, R. A three-dimensional thermal abuse model for lithium-ion cells. *Journal of Power Sources* **170,** 476–489 (2007).
26 Coman, P., Rayman, S. & White, R. A lumped model of venting during thermal runaway in a cylindrical Lithium Cobalt Oxide lithium-ion cell. *J Power Sources* **307,** 56–62 (2016).

THERMAL RUNAWAY KINETIC RELATIONSHIPS

$$\frac{dx_{SEI}}{dt} = -A_{SEI} x_{SEI} exp(\frac{-E_{SEI}}{k_b T}) \quad (1)$$

$$\frac{dx_a}{dt} = -A_a x_a exp(\frac{-z}{z_0}) exp(\frac{-E_a}{k_b T}) \quad (2)$$

$$\frac{dz}{dt} = A_a x_a exp(\frac{-z}{z_0}) exp(\frac{-E_a}{k_b T}) \quad (3)$$

$$\frac{dQ_{SEI}}{dt} = -m_{SEI}\, h_{SEI}\, \frac{dx_{SEI}}{dt} \quad (4)$$

$$\frac{dQ_a}{dt} = -m_a\, h_a\, \frac{dx_a}{dt} \quad (5)$$

Heating due to SEI and anode decomposition (Richard and Dahn, 1999 [23])

$$\frac{dx_c}{dt} = A_c x_c (1 - x_c) exp(\frac{-E_c}{k_b T}) \quad (6)$$

$$\frac{dQ_c}{dt} = m_c\, h_c\, \frac{dx_c}{dt} \quad (7)$$

Heating due to cathode decomposition (Hatchard et. al., 2001 [24])

$$\frac{dY_e}{dt} = -A_e Y_e exp(\frac{-E_e}{k_b T}) \quad (8)$$

$$\frac{dQ_e}{dt} = -m_e\, h_e\, \frac{dx_e}{dt} \quad (9)$$

Heating due to electrolyte decomposition (Kim et. al., 2007 [25])

$$\frac{dSoC}{dt} = -A_{ec} (1 - x_c) x_a \exp\left(\frac{-E_{ec}}{k_b T}\right) + \left(\frac{dx_c}{dt} - \frac{dx_a}{dt}\right) SoC \quad (10)$$

$$\frac{dQ_{ec}}{dt} = -(m_c + m_a)\, h_{ec}\, \frac{dSoC}{dt} \quad (11)$$

Heating due release of electrochemical energy (Coman et. al. 2015 [26])

A	Frequency Factor
Y	Fraction Electrolyte
x	Fraction Remaining Lithium
E	Activation Energy
k_b	Boltzmann Constant
T	Temperature
z	Tunneling Term
m	Mass
h	Enthalpy
t	Time
Q	Heat
SOC	State-of-Charge

23 Richard, M. Accelerating rate calorimetry study on the thermal stability of lithium intercalated graphite in electrolyte. I. experimental. *Journal of The Electrochemical Society* **146,** 2068 (1999).
24 Hatchard, T., MacNeil, D., Basu, A. & Dahn, J. Thermal model of cylindrical and prismatic lithium-ion cells. *Journal of The Electrochemical Society* **148,** A755 (2001).
25 Kim, G.-H., Pesaran, A. & Spotnitz, R. A three-dimensional thermal abuse model for lithium-ion cells. *Journal of Power Sources* **170,** 476–489 (2007).
26 Coman, P., Rayman, S. & White, R. A lumped model of venting during thermal runaway in a cylindrical Lithium Cobalt Oxide lithium-ion cell. *J Power Sources* **307,** 56–62 (2016).

THERMAL RUNAWAY KINETIC RELATIONSHIPS

$$\frac{dx_{SEI}}{dt} = -A_{SEI} x_{SEI} exp\left(\frac{-E_{SEI}}{k_b T}\right) \quad (1)$$

$$\frac{dx_a}{dt} = -A_a x_a exp\left(\frac{-z}{z_0}\right) exp\left(\frac{-E_a}{k_b T}\right) \quad (2)$$

$$\frac{dz}{dt} = A_a x_a exp\left(\frac{-z}{z_0}\right) exp\left(\frac{-E_a}{k_b T}\right) \quad (3)$$

$$\frac{dQ_{SEI}}{dt} = -m_{SEI}\, h_{SEI}\, \frac{dx_{SEI}}{dt} \quad (4)$$

$$\frac{dQ_a}{dt} = -m_a\, h_a\, \frac{dx_a}{dt} \quad (5)$$

Heating due to SEI and anode decomposition (Richard and Dahn, 1999 [23])

$$\frac{dx_c}{dt} = A_c x_c (1 - x_c) exp\left(\frac{-E_c}{k_b T}\right) \quad (6)$$

$$\frac{dQ_c}{dt} = m_c\, h_c\, \frac{dx_c}{dt} \quad (7)$$

Heating due to cathode decomposition (Hatchard et. al., 2001 [24])

$$\frac{dY_e}{dt} = -A_e Y_e exp\left(\frac{-E_e}{k_b T}\right) \quad (8)$$

$$\frac{dQ_e}{dt} = -m_e\, h_e\, \frac{dx_e}{dt} \quad (9)$$

Heating due to electrolyte decomposition (Kim et. al., 2007 [25])

$$\frac{dSoC}{dt} = -A_{ec}\,(1 - x_c) x_a \exp\left(\frac{-E_{ec}}{k_b T}\right) + \left(\frac{dx_c}{dt} - \frac{dx_a}{dt}\right) SoC \quad (10)$$

$$\frac{dQ_{ec}}{dt} = -(m_c + m_a)\, h_{ec}\, \frac{dSoC}{dt} \quad (11)$$

Heating due release of electrochemical energy (Coman et. al. 2015 [26])

Release of remaining electrochemical energy is a function of SOC

A	Frequency Factor
Y	Fraction Electrolyte
x	Fraction Remaining Lithium
E	Activation Energy
k_b	Boltzmann Constant
T	Temperature
z	Tunneling Term
m	Mass
h	Enthalpy
t	Time
Q	Heat
SOC	State-of-Charge

23 Richard, M. Accelerating rate calorimetry study on the thermal stability of lithium intercalated graphite in electrolyte. I. experimental. *Journal of The Electrochemical Society* **146,** 2068 (1999).
24 Hatchard, T., MacNeil, D., Basu, A. & Dahn, J. Thermal model of cylindrical and prismatic lithium-ion cells. *Journal of The Electrochemical Society* **148,** A755 (2001).
25 Kim, G.-H., Pesaran, A. & Spotnitz, R. A three-dimensional thermal abuse model for lithium-ion cells. *Journal of Power Sources* **170,** 476–489 (2007).
26 Coman, P., Rayman, S. & White, R. A lumped model of venting during thermal runaway in a cylindrical Lithium Cobalt Oxide lithium-ion cell. *J Power Sources* **307,** 56–62 (2016).

THERMAL RUNAWAY KINETIC RELATIONSHIPS (0-D EXAMPLE)

- **Consider a 0-D example using a lump mass to represent an 18650-format Li-ion cell where the following occur:**
  - The cell is placed in an environment set to increase by 0.02 °C min^{-1}(similar to typical accelerating rate calorimeter heating rate)
  - A heat load is placed on the cell to be a function of the previously described kinetic relationships
  - The plot below displays the predicted temperature profile of the cell; observe when self-heating is first noticed vs. when the Arrhenius behavior of self-heating takes control after a certain threshold temperature is achieved
  - Similar plots can be made to describe the changes in reaction rates and self-heating rates as the temperature of the cell rises

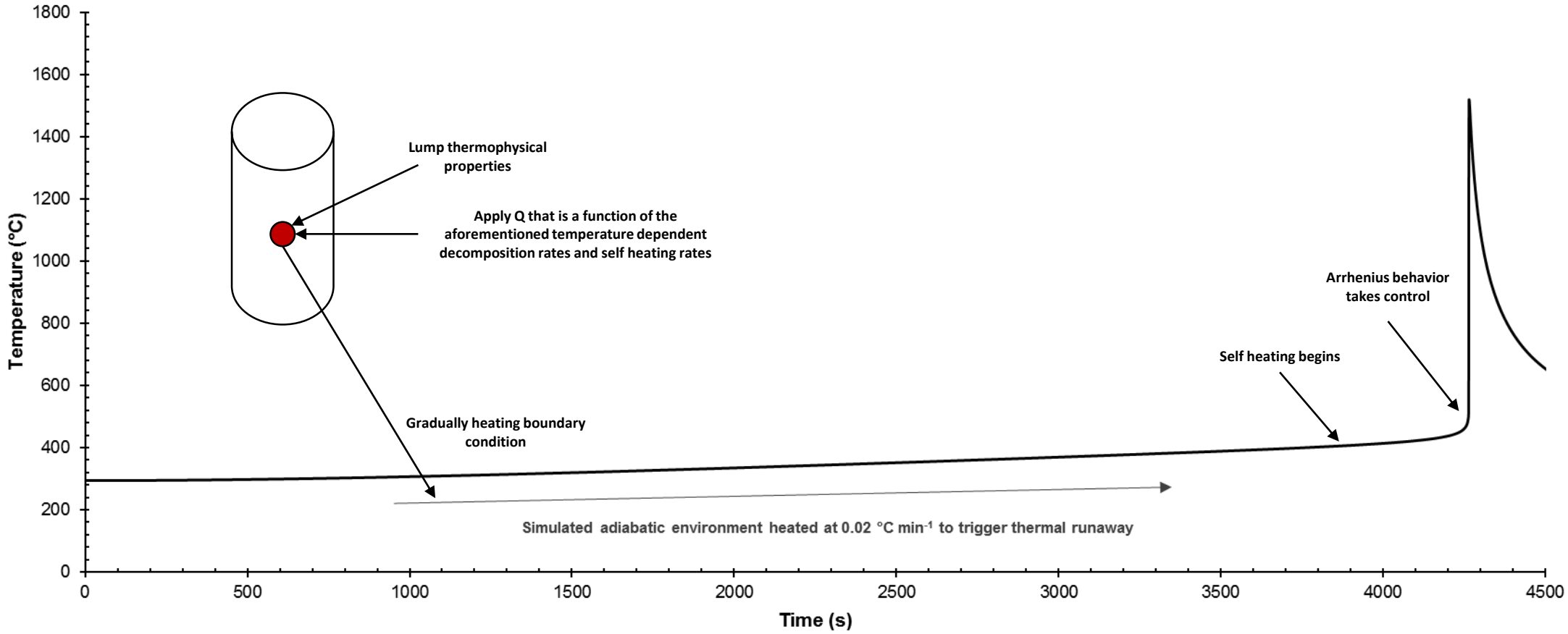

23 Richard, M. Accelerating rate calorimetry study on the thermal stability of lithium intercalated graphite in electrolyte. I. experimental. *Journal of The Electrochemical Society* **146,** 2068 (1999).
24 Hatchard, T., MacNeil, D., Basu, A. & Dahn, J. Thermal model of cylindrical and prismatic lithium-ion cells. *Journal of The Electrochemical Society* **148,** A755 (2001).
25 Kim, G.-H., Pesaran, A. & Spotnitz, R. A three-dimensional thermal abuse model for lithium-ion cells. *Journal of Power Sources* **170,** 476–489 (2007).
26 Coman, P., Rayman, S. & White, R. A lumped model of venting during thermal runaway in a cylindrical Lithium Cobalt Oxide lithium-ion cell. *J Power Sources* **307,** 56–62 (2016).

THERMAL RUNAWAY EXAMPLE 4

Cell type: Li-ion 18650
Capacity: 3 Ah
State of charge: 100 % (4.2 V)

Bottom vent: No
Wall thickness: 250 um
Orientation of cell: Upright (vent at top)
Location of ISCD radially: None
Location of ISCD longitudinally: None
Side of ISCD in image: None

Separator type: Normal
Positive current collector: Normal
Negative current collector: Normal

Location of FOV longitudinally: Top
Frame dimension (Hor x Ver): 2016 x 1111 pixels
Pixel size: 10 µm

THERMAL RUNAWAY EXAMPLE 5

Cell type: Li-ion 18650
Capacity: 3.5 Ah
State of Charge: 100 % (4.2 V)
Bottom vent: No
Wall thickness: Not known
Separator: Polymer
Orientation of cell: Positive end up
Location of ISCD radially: N/A
Location of ISCD longitudinally: N/A
Side of ISCD in image: N/A

Location of FOV longitudinally: Top
Frame rate: 2000 Hz
Frame dimension (Hor x Ver): 1280 x 800 pixels
Pixel size: 17.8 µm

THERMAL RUNAWAY EXAMPLE 6

Cell type: Li-ion 18650
Capacity: 2.1 Ah
State of charge: 100 % (4.2 V)

Bottom vent: None
Wall thickness: 250 µm
Orientation of cell: Upright (vent at top)
Location of ISCD radially: None
Location of ISCD longitudinally: None
Side of ISCD in image: None

Separator type: Normal
Positive current collector: Normal
Negative current collector: Normal

Location of FOV longitudinally: Middle
Frame dimension (Hor x Ver): 2016 x 1111 pixels
Pixel size: 10 µm

THERMAL RUNAWAY EXAMPLE 7

Cell type: Li-ion 18650
Capacity: 3 Ah
State of charge: 100 % (4.2 V)

Bottom vent: No
Wall thickness: 250 um
Orientation of cell: Upright (vent at top)
Location of ISCD radially: None
Location of ISCD longitudinally: None
Side of ISCD in image: None

Separator type: Normal
Positive current collector: Normal
Negative current collector: Normal

Location of FOV longitudinally: Top
Frame dimension (Hor x Ver): 2016 x 1111 pixels
Pixel size: 10 µm

UNDERSTANDING THERMAL RUNAWAY

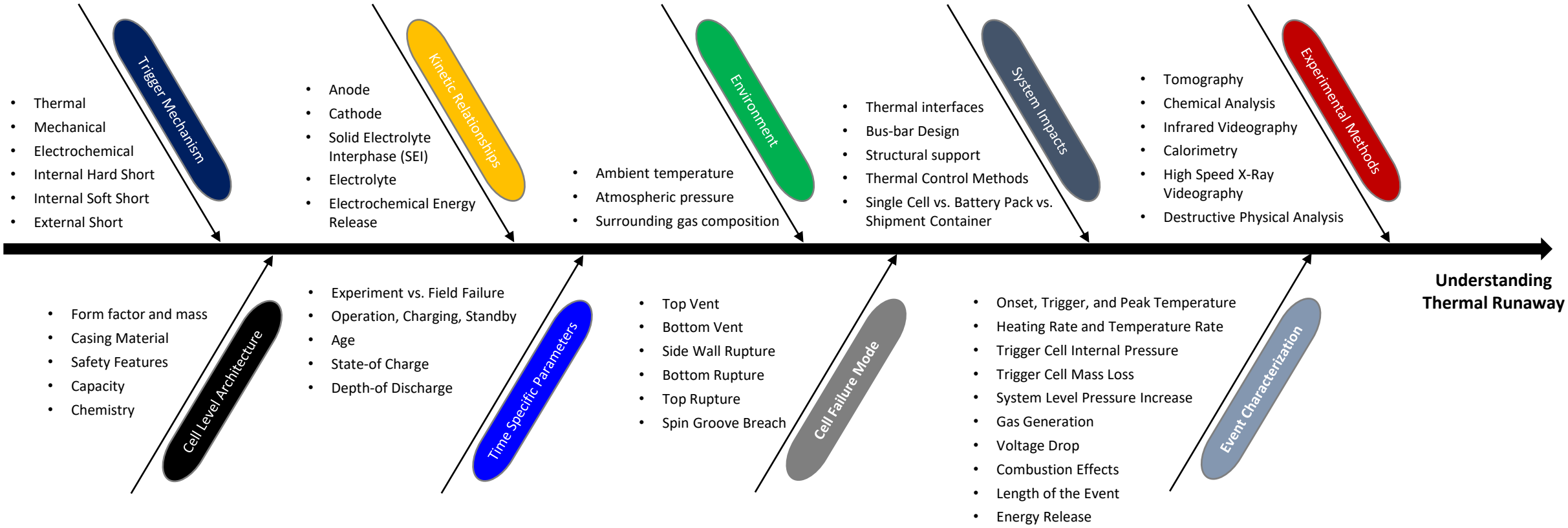

EXAMPLE FIELD FAILURES

- Boeing 787 Dreamliner: https://www.cnn.com/travel/article/boeing-787-dreamliner-investigation-report/index.html
- Tesla Supercharger: https://electrek.co/2019/06/01/tesla-fire-supercharger/
- Samsung Galaxy Note 7: https://www.androidcentral.com/samsung-galaxy-note-7
- NASA Robosimian: https://www.wired.com/2016/10/samsung-isnt-one-lithium-ion-problems-just-ask-nasa/
- Hoverboards: https://www.npr.org/sections/thetwo-way/2016/07/06/484988211/half-a-million-hoverboards-recalled-over-risk-of-fire-explosions
- Laptops: https://www.nbclosangeles.com/investigations/I-Team-Investigation-Battery-Lithium-Ion-Fire-Laptop-Computer-412459303.html








MODULE 2 SECTION 2:

THERMAL RUNAWAY TESTING TECHNIQUES

COMMERCIALLY AVAILABLE CALORIMETRIC DEVICES

- **The heat of thermal runaway is usually characterized with a variety of commercially available calorimetric techniques in which temperature rise of a known mass is measured and the energy change of the system is then calculated (i.e. $\Delta E_{Sys} = mC_p\Delta T$)**
- **Accelerating rate calorimetry (ARC) [31]:**
  - Slowly heats the environment and the contained test article at a rate of ~0.02 °C min^{-1}
  - After self heating is detected, the ARC switches modes to only add enough heat to match the environment to the surface temperature of the test article; temperatures then rise, at a rate driven by exothermic self heating, until thermal runaway occurs
  - Helpful in determining the onset temperature of decomposition
  - Effective characterization of cell body heating rates
  - Approximation of total energy release is possible, but there are some nuances…
  - Due to the slow nature of the ARC test cycle, cell venting of the electrolyte occurs hours before thermal runaway; this early venting dries out the electrolyte and can possibly degrade the total heat output
- **Bomb or steel can calorimetry [32, 33]:**
  - Test article is placed inside a sealed container and thermal runaway is triggered with heaters (usually)
  - Adequate for determining total heat output and for gas collection/analysis activities
  - Often combined with ARC (uses ARC heating environment instead of trigger heaters)
- **Copper slug calorimetry [34]:**
  - Cell is placed inside of a copper slug, where the temperature of the cell and the slug are measured
  - Effective for measuring the heat output through the cell casing
  - Estimates rate of mass ejected during thermal runaway
  - Must combine with bomb (steel can) calorimetry to calculate heat released through ejecta and gas

Image above taken from combination ARC-Bomb testing conducted for NASA by Thermal Hazard Technology. Cells characterized included the Boston Power Swing 5300, Samsung 18650-26F, and the Molicel 18650-J

Rendering for conceptual purposes only

31 Yayathi, et. al., J. of Power Sources, 329 (2016) 197-206.
32 Walters, R.N. and Lyon R.E., Report DOT/FAA/TC-15/40, March 2016.
33 Jhu, C.Y., et. al., J. of Hazardous Materials, 192 (2011) 99-107.
34 Liu, X., et. al., J. of Power Sources, 280 (2015) 516-525.

FRACTIONAL THERMAL RUNAWAY CALORIMETRY (FTRC)

- **As a NASA Engineering and Safety Center (NESC) assessment, NASA developed a new fractional thermal runaway calorimetry (FTRC) method for 18650-format Li-ion cells:**
  - Collaborators included NESC, NASA JSC, and SAIC
  - Allows discernment between (1) total heat output and (2) fraction of heat released through the cell casing vs. ejecta material
  - The energy distributions are determined by post processing temperature vs. time for each calorimeter sub-assembly (i.e. $\sum m_i C_{p_i} dT_i$)
  - Ambidextrous configuration accommodates cell designs with bottom vents (BVs) or cells that experience bottom rupture
  - Uses high flux heaters or nail penetration to initiate TR quickly (i.e. relevant to field failure)
  - Simple operation enables multiple experiments per day
  - Compatible with high speed X-ray videography [9]
  - Optional interface for measuring the gas exhaust heat

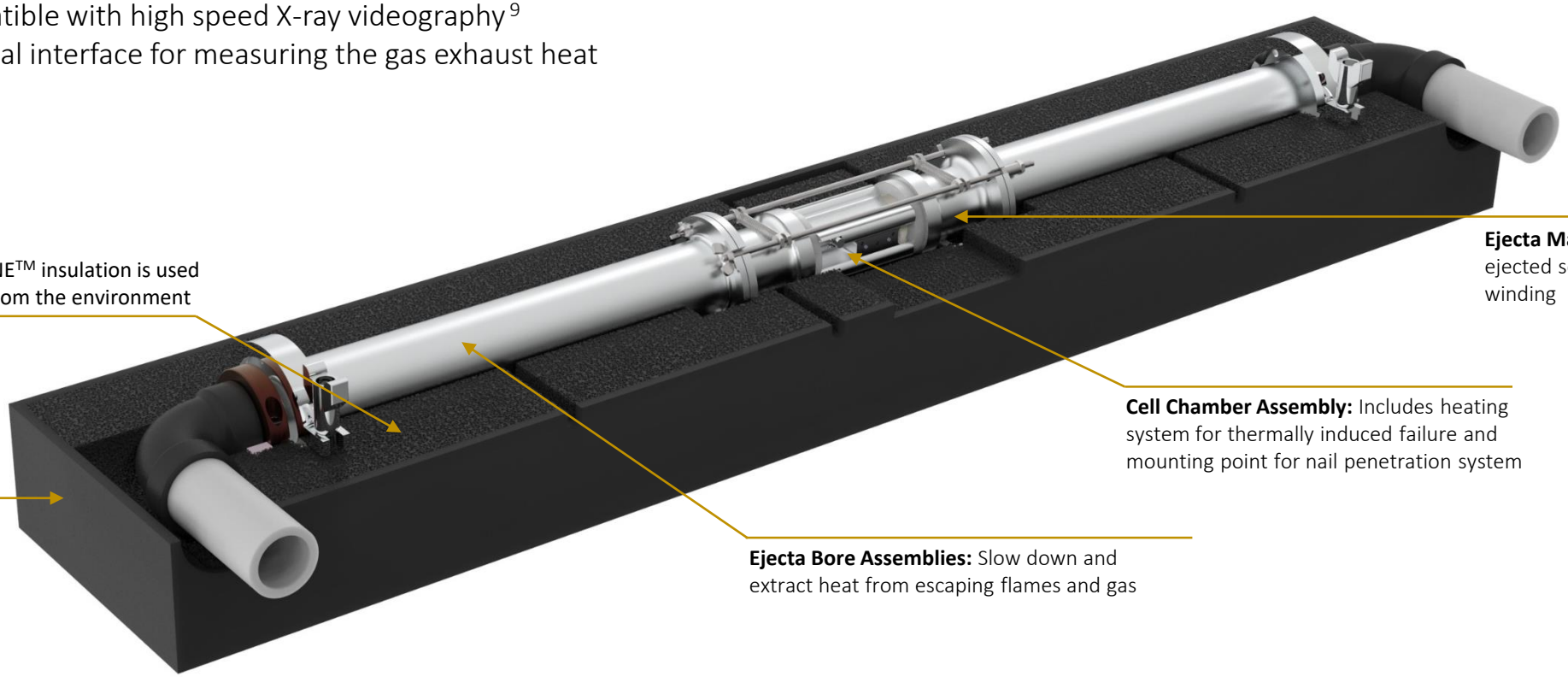

Insulation: FOAMGLAS® ONE™ insulation is used to isolate the calorimeter from the environment

Housing: Lightweight and shipping ready housing is employed to support hardware mobility

Ejecta Bore Assemblies: Slow down and extract heat from escaping flames and gas

Cell Chamber Assembly: Includes heating system for thermally induced failure and mounting point for nail penetration system

Ejecta Mating Assemblies: Captures ejected solids such as the electrode winding

FRACTIONAL THERMAL RUNAWAY CALORIMETRY (FTRC)

- **The FTRC currently supports cell chambers designed for the following cell formats: 18650, 21700, and D-Cell:**
  - Utilizes the same downstream FTRC assemblies (i.e. the only adjustment to test a new cell is to swap out the cell chamber)
  - The current architecture supports cells with >5 Ah capacities
  - Stay tuned for new capabilities to support pouch cells and larger format cells…

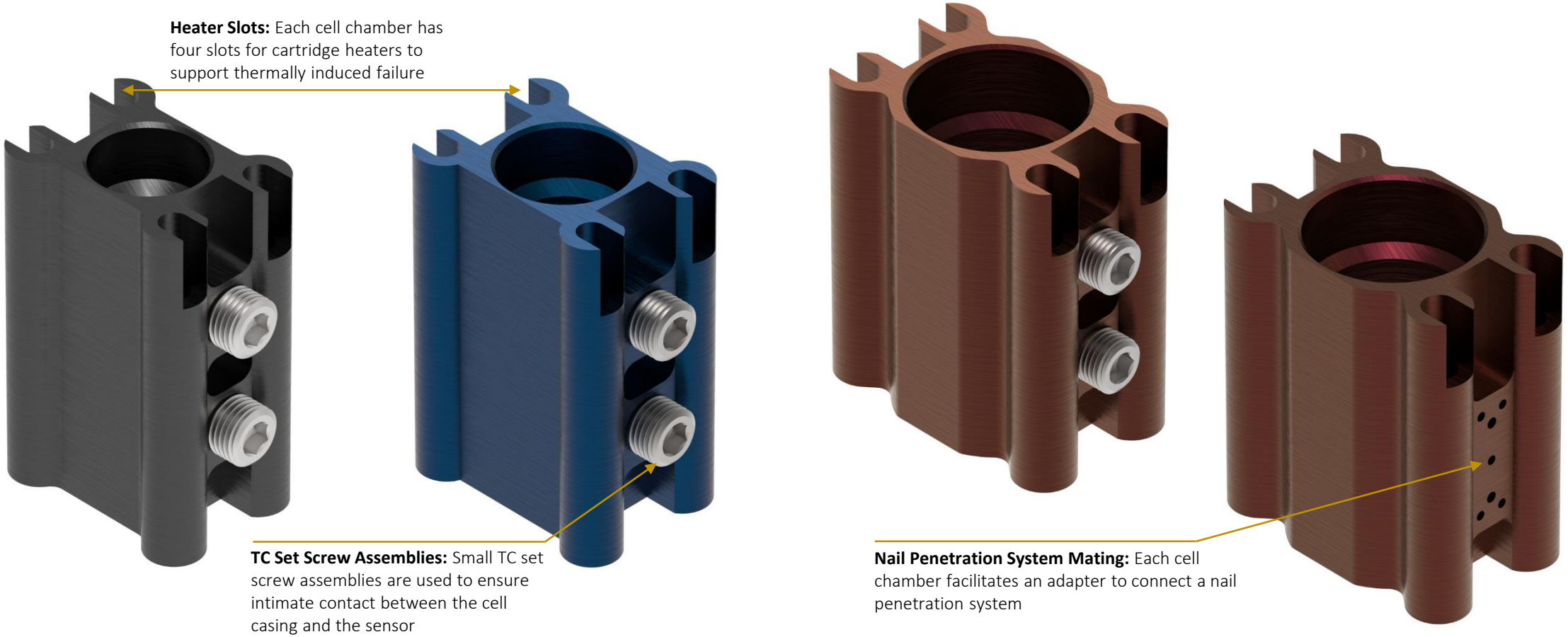

FRACTIONAL THERMAL RUNAWAY CALORIMETRY (FTRC)

- **Reliable temperature measurement from the side of the cell is critical to accurate calculation of the fraction of thermal runaway energy released through the cell casing:**
  - To support temperature measurement on the cell casing without actually installing a thermocouple, the FTRC cell chambers employ plunger like set screw assemblies that contain an imbedded thermocouple
  - When released, the spring loaded set screw assembly forces intimate contact between the embedded thermocouple and the cell casing

TC Set Screw Assemblies: Used to maintain intimate contact between the cell casing and the thermocouple

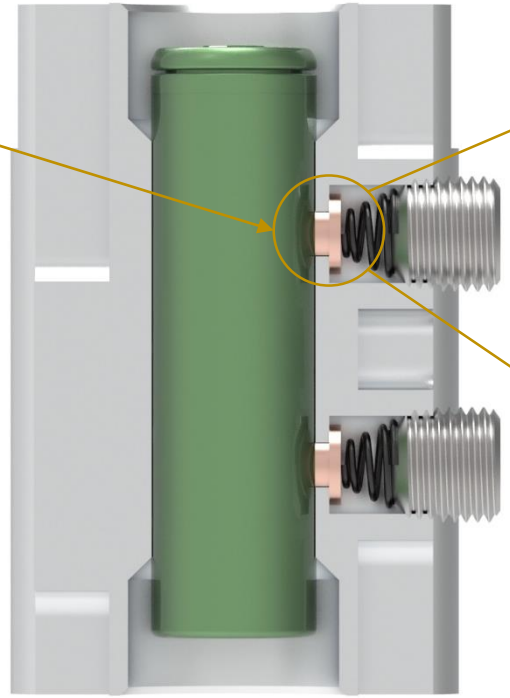

X-Ray Image: Image reveals the contact between the TC set screw assembly and an 18650 Li-ion cells installed in the FTRC during testing at Diamond Light Source in 2019.

FRACTIONAL THERMAL RUNAWAY CALORIMETRY (FTRC)

- **The FTRC is designed to not only facilitate testing of different cell types, but to also help characterize directional, or fractional, thermal runaway failure behavior (i.e. top vent, bottom vent, ruptures from any location, et…)**
- **The cell chamber assembly is isolated from the remainder of the up and down stream calorimeter components with low conductivity ceramic bushings:**
  - Maintaining this thermal isolation is critical to our team's ability to discern the fraction of energy released through the cell casing vs. through the ejecta material
  - The ejecta mating segment is designed to capture and stop complete jellyroll ejections; with this capability, we can also determine the fraction of energy associated with an ejected jellyroll

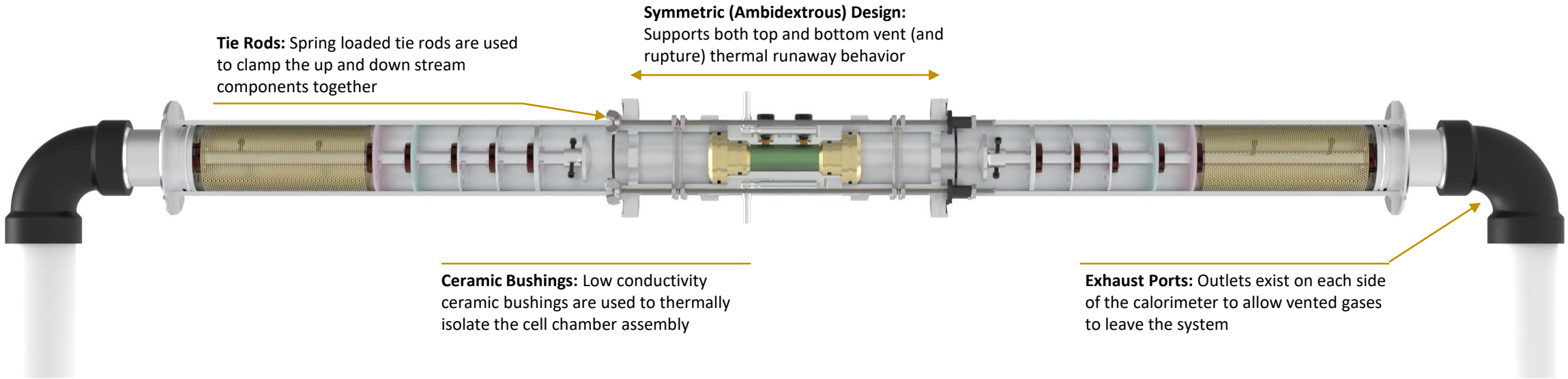

FRACTIONAL THERMAL RUNAWAY CALORIMETRY (FTRC)

- The internal baffles and copper mesh are used to create a tortuous path that effectively reduces flow velocity, captures large and fine ejected particulates, and cools down the flowing particles and gases before they exit the system (i.e. captures the energy)

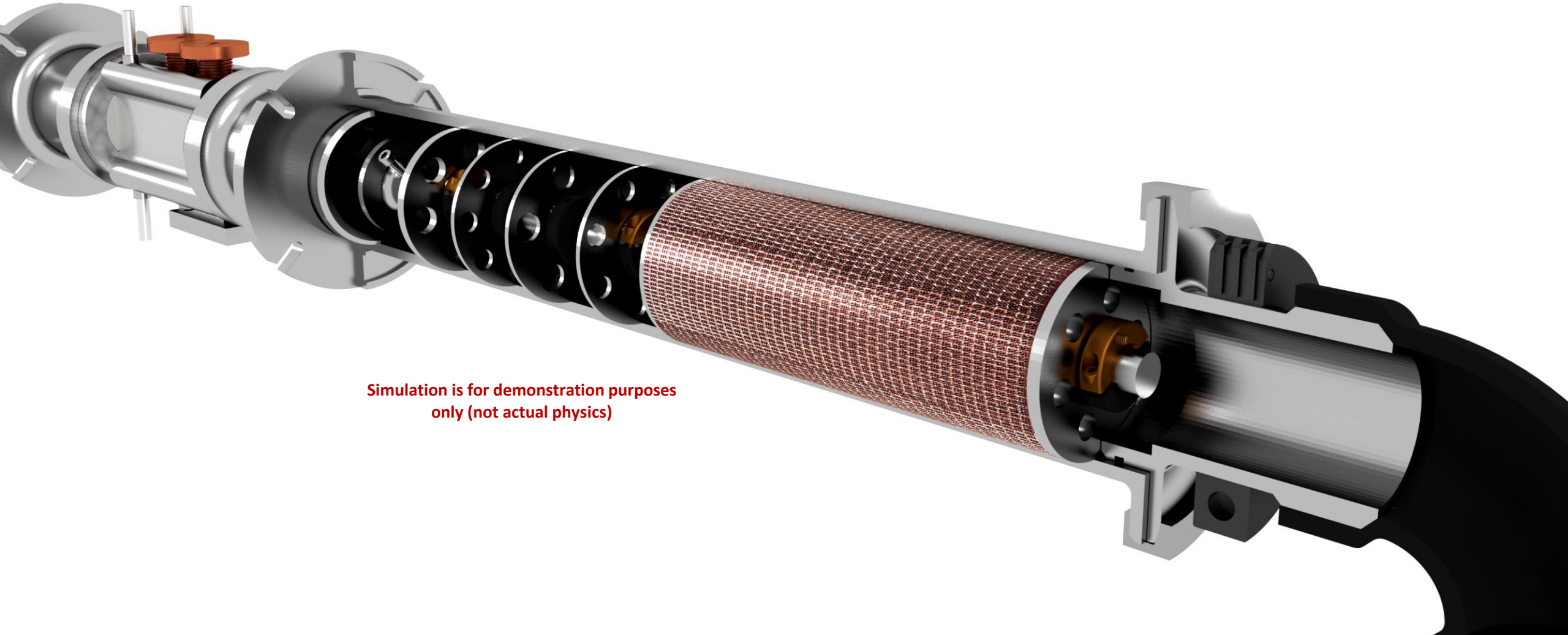

Simulation is for demonstration purposes only (not actual physics)

FRACTIONAL THERMAL RUNAWAY CALORIMETRY (FTRC)

FRACTIONAL THERMAL RUNAWAY CALORIMETRY (FTRC)

- **The calculated energy fractions are directly traceable to the calorimeter assembly as a whole (for total energy), sub-assemblies (for cell body vs. ejecta energy), and individual component (for error check)**

- **The primary assemblies used for fractional calculations are the following:**
  - Cell Chamber Assembly (Red)
  - Positive Ejecta Mating Assembly (Indigo)
  - Positive Ejecta Bore Assembly (Indigo)
  - Negative Ejecta Mating Assembly (Black)
  - Negative Ejecta Bore Assembly (Black)

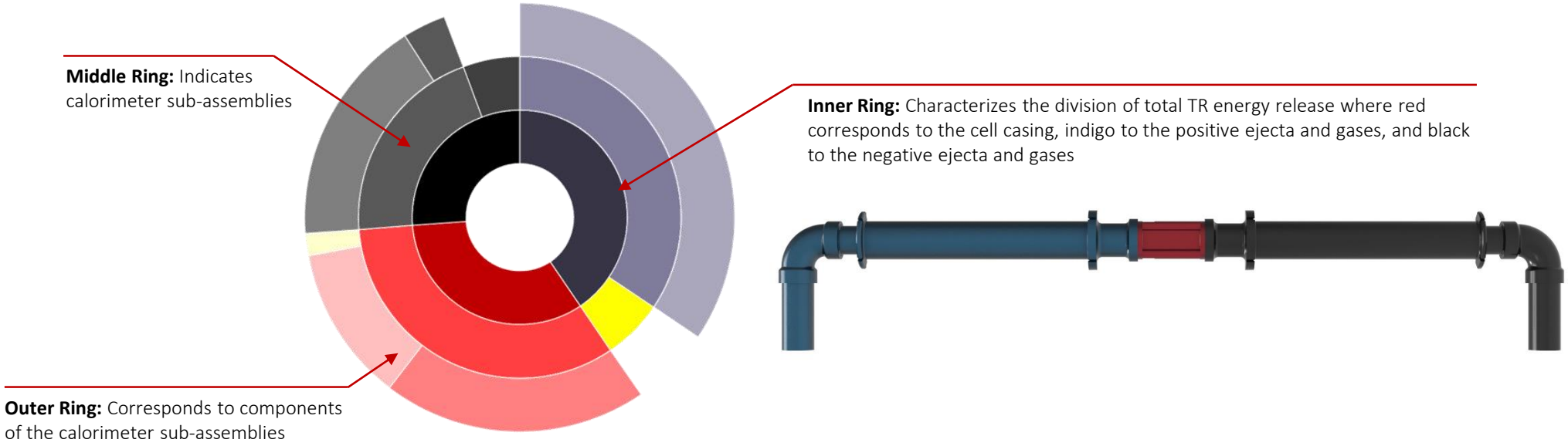

FRACTIONAL THERMAL RUNAWAY CALORIMETRY (FTRC)

Images below depict the synchrotron testing compatibility of the device:

- FTRC experiments are coupled with synchrotron light beam to support in-situ high speed x-ray videography of the Li-ion cell in the moments just prior to and during thermal runaway
- Left image depicts FTRC testing at the European Synchrotron Radiation Facility (ESRF) in France
- Right image depicts FTRC testing at the Diamond Light Source (DLS) Facility in the United Kingdom
- The FTRC has also been used extensively at the Energy Systems Test Area (ESTA) at NASA JSC for non-synchrotron thermal runaway experiments

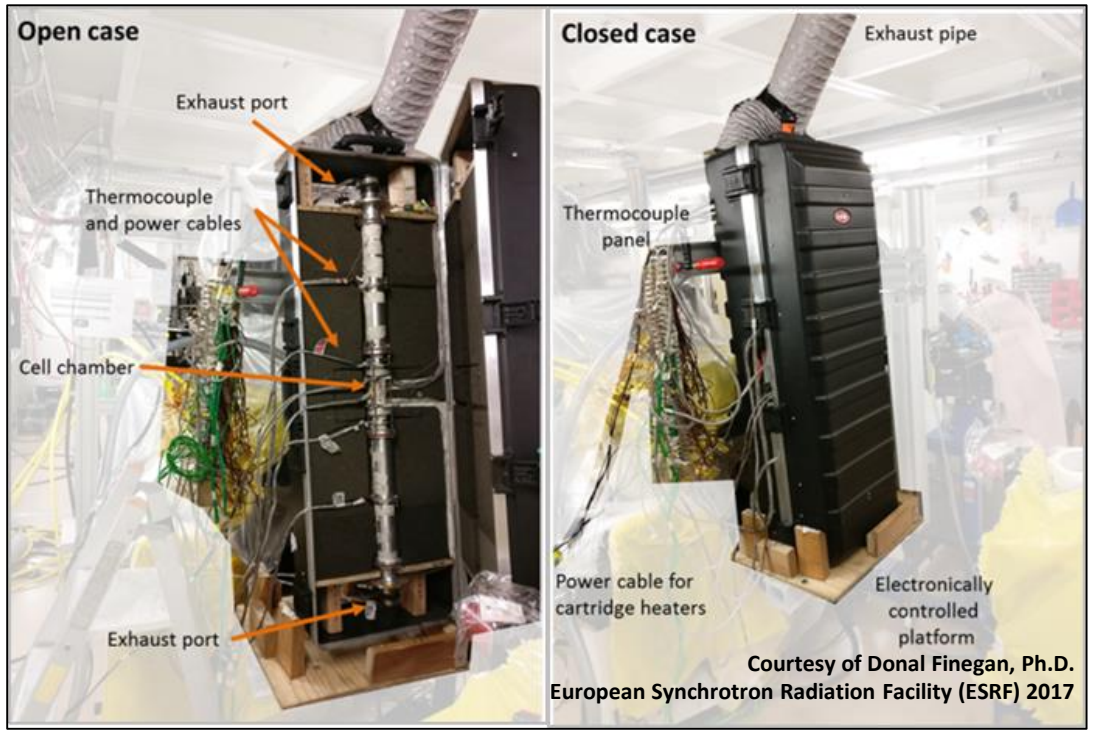

Courtesy of Donal Finegan, Ph.D.
European Synchrotron Radiation Facility (ESRF) 2017

Courtesy of William Walker, Ph.D.
Diamond Light Source (DLS) 2019






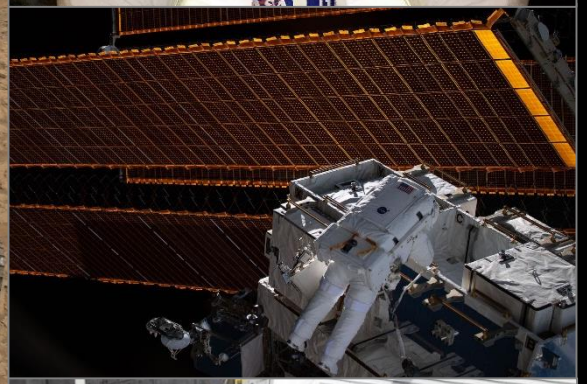

MODULE 2 SECTION 3:

ADDRESSING THE VARIANCE OF THERMAL RUNAWAY

DESCRIPTION OF CELL TYPES AND VARIABLES TESTED

- **The thermal runaway behaviors of a several cell types, with varying cell format (18650, 21700, D), chemistries, and safety features, have been characterized:**
  - Trigger mechanisms include heater, heater with embedded internal short circuiting (ISC) device, and nail penetration; the NASA/NREL developed (ISC) device is designed to allow thermal runaway to occur at lower temperatures (i.e. closer to field failure conditions)
  - All cells were tested at 100% state of charge
- **For select cell builds, control groups were established to considered the following variables:**
  - 3.35 Ah LG 18650 control groups included cells with bottom vent mechanisms (BV) vs. non-bottom vent (non-BV) mechanisms and also cells with 220 µm casing thickness vs. 250 µm casing thickness
  - 2.3 Ah MOLiCEL® 18650-J control groups included cells with standard separator and with Dreamweaver separator (both gold and silver)
  - 2.1 Ah Soteria™ (Coulometrics) 18650 control groups included cells with combinations of standard separators, Dreamweaver separators, standard current collectors, and metal-coated plastic current collectors

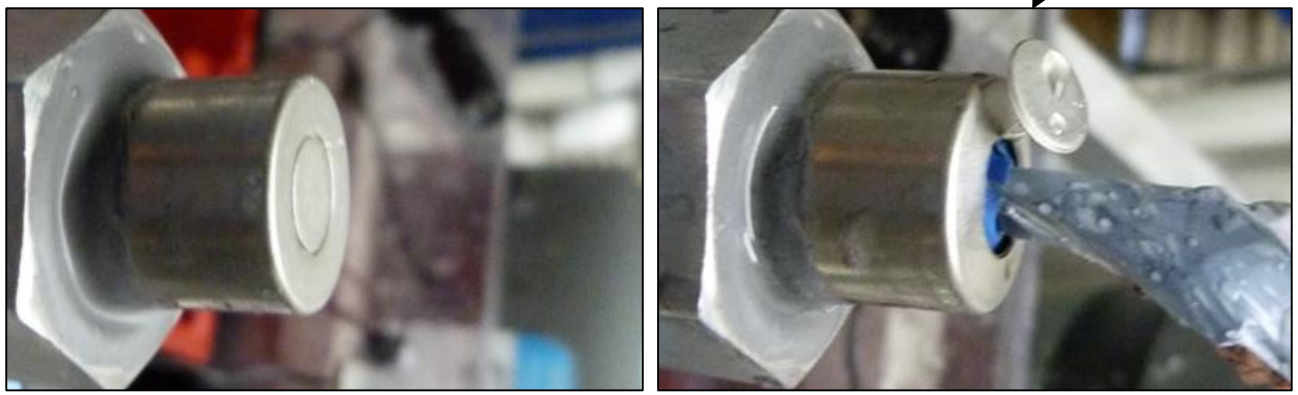

Image courtesy of Darcy, E., et. al. [10]

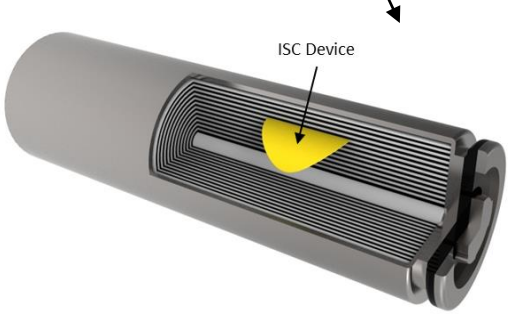

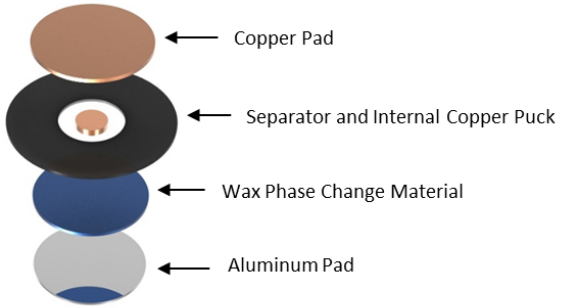

VARIABILITY OF TOTAL ENERGY RELEASE

- **Since no two thermal runaway events are the same, test-to-test variability must be considered by any scientific effort that seeks to characterize the overall range of expected thermal runaway behavior for a given cell type**

- **Assumed a normal distribution for test-to-test total thermal runaway energy release and plotted the probability density curve for each cell type based on direct post processing ($mC_p\Delta T$) of the raw data (see image on the left):**
  - The residuals shown below (right image) are based on the raw data and reflect the difference between the observed value and the average value; the even distribution about the zero line indicates that a normal distribution assumption should be appropriate
  - These plots do not break down the impacts of each the aforementioned design variables on the thermal runaway behavior; hence the significant differences in standard deviations and residual spread as seen the plots below
  - Although direct interpretation of the raw data is insightful, we recommend referring to the regression model results (next few slides) for final assessment of thermal runaway behavior

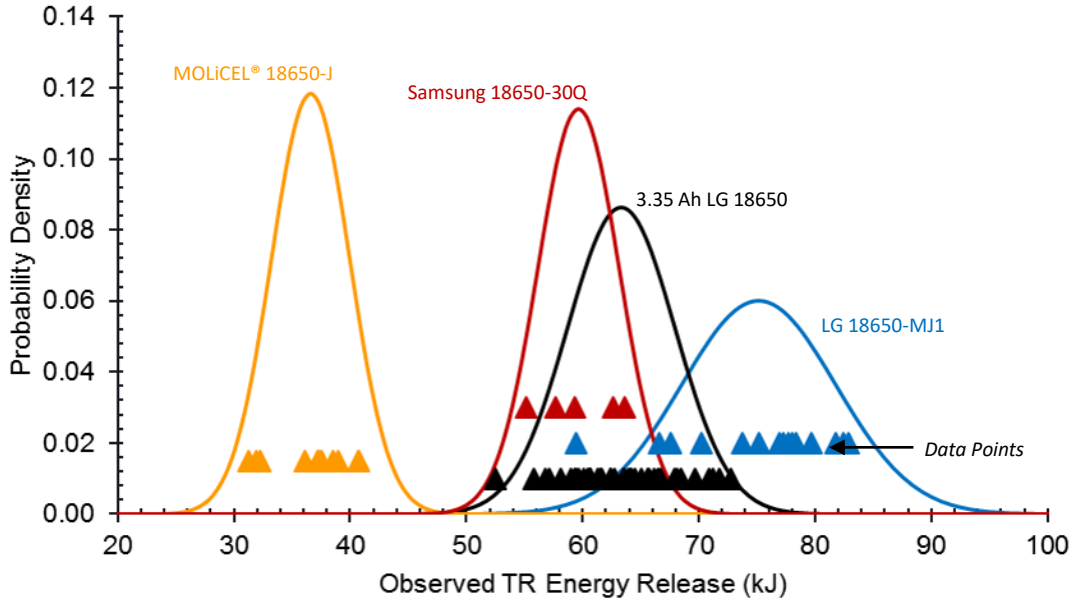

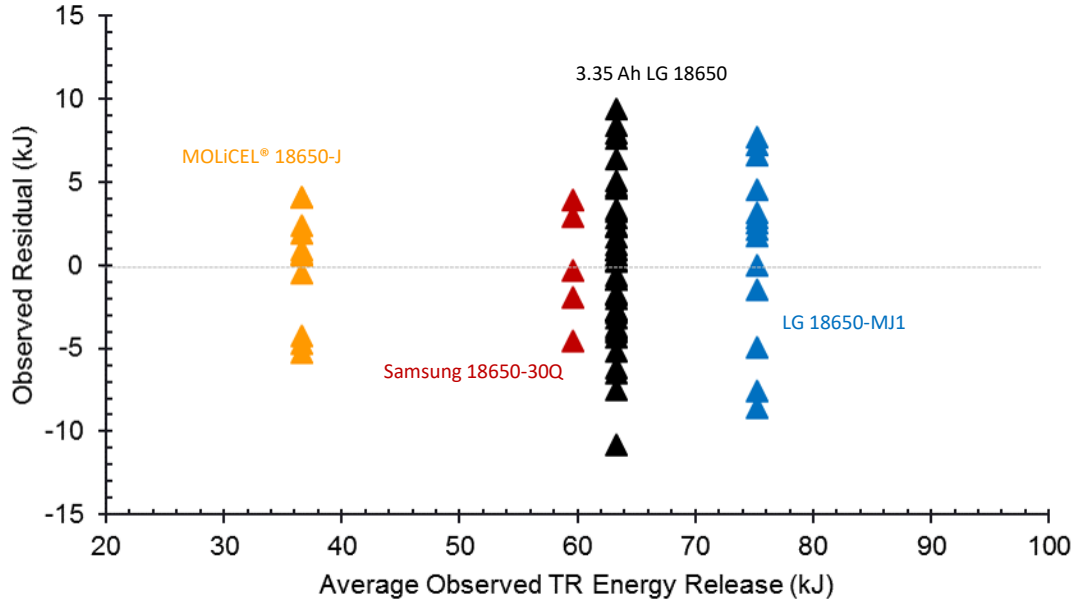

Image Credit: Walker et. al., Journal of Power Sources (2019)

VARIABILITY OF TOTAL ENERGY RELEASE

- **Building from the previous chart, this instructor recommends that battery designers consider thermal runaway energy release not just as a single value, but as a statistical distribution to help answer the following questions:**
  - What is the highest probability energy release? What is the lowest?
  - What is the absolute maximum energy release one could expect? Minimum?
  - How do different cells, of similar capacities, compare in thermal runaway heat output?
- **Ultimately, the answers to the previous series of questions will drive the design of the battery, the battery's thermal management system, and will also inform any supporting thermal analysis activities**

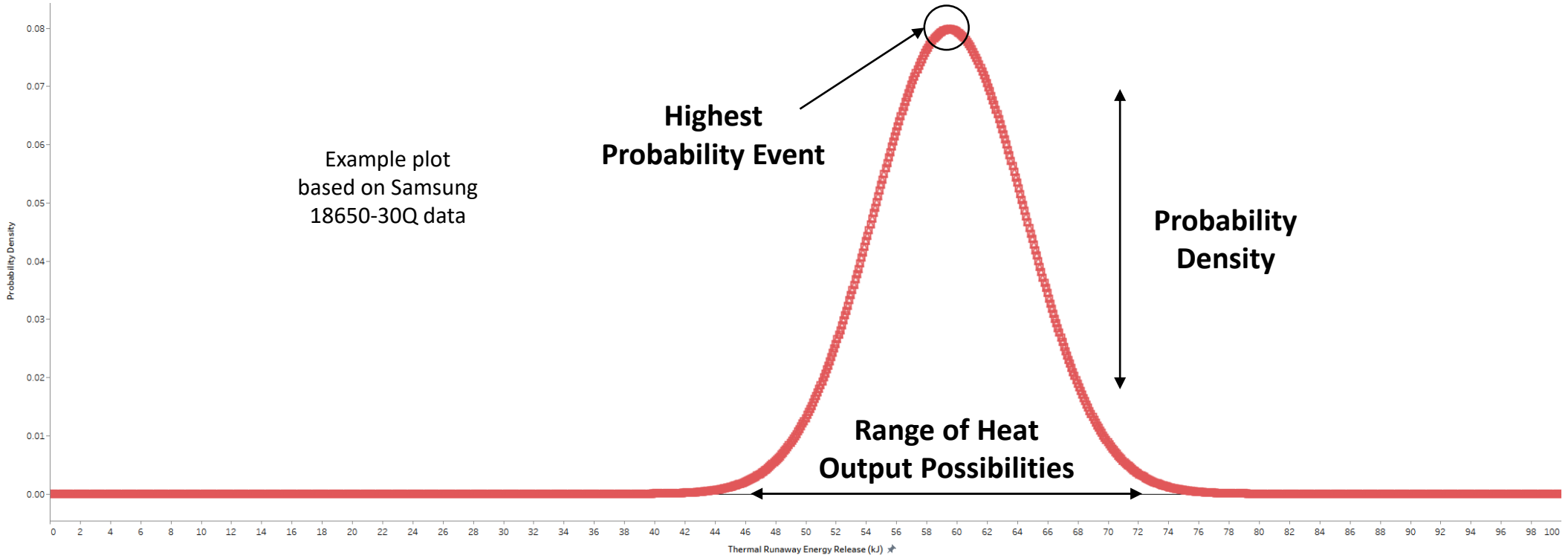

ADDRESSING VARIABILTY WITH ENGINEERING STATISTICS

- **Test-to-test variability exists for our experiments due to the various random and non-random factors associated with the experiments:**
  - Therefore we use a regression model to provide final interpretation of each experiment and to provide insight into the overall range of expected thermal runaway responses for each cell configuration
  - In this way, the calculations driving the final predictions can be based on the entire pool of data
  - Special thanks to our NESC statistician Kenneth L. Johnson who develop our regression model
- **The following "observed values" served as inputs to the regression model for each experiment:**
  - Total thermal runaway energy yield
  - Fraction of energy released through the cell casing vs. through the ejecta materials and gases
  - Remaining cell mass following TR
  - Design variables (i.e. separator, casing thickness, trigger mechanism, and cell type)
  - Cell failure mechanism (e.g. top vent, bottom vent, bottom rupture)
- **The completed regression model uses the "observed values" for each experiment and outputs a corresponding predicted total energy release:**
  - This predicted value has taken into account the effects of each design variable and the results of the entire pool of data
  - These predicted energy release values are then used to recreate distributions that characterize the range of thermal runaway energy release

ADDRESSING VARIABILTY WITH ENGINEERING STATISTICS

- **Before getting into the final results, it is first important to examine how effective the regression model is at predicting total energy release by examining the residual values**

- **A key assumption for our regression analysis was equal variability of the residuals across zero:**
  - Residual refers to the difference between predicted value and corresponding observed value
  - Initial model, based on processing total energy release in kJ, did not satisfy this assumption (left image)
  - Performed inverse-square root translation of observed total energy release ($kJ^{-0.5}$) factor to achieve a better model (right image)

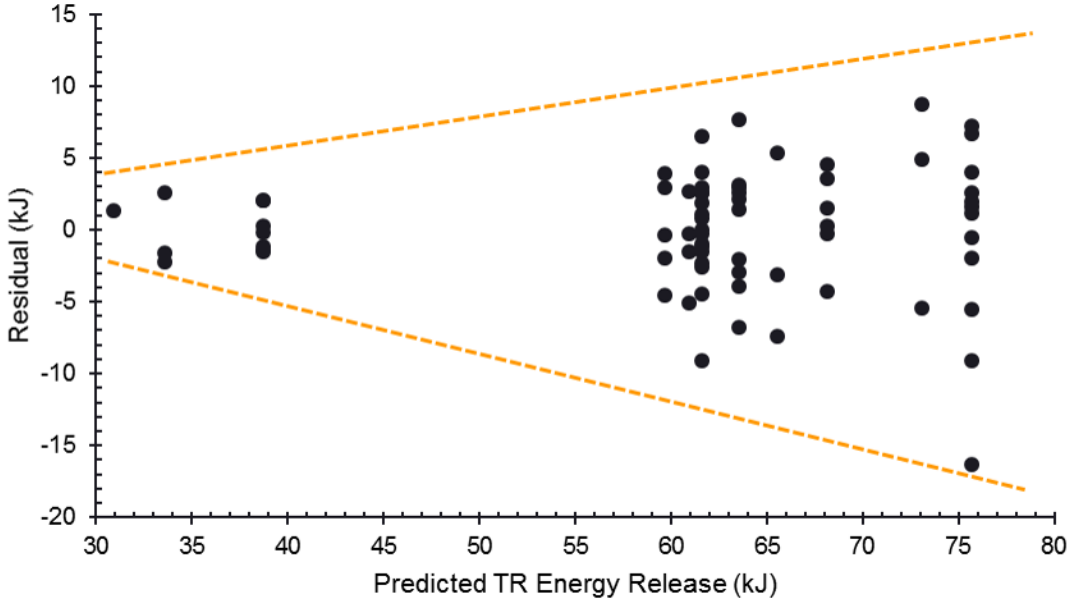

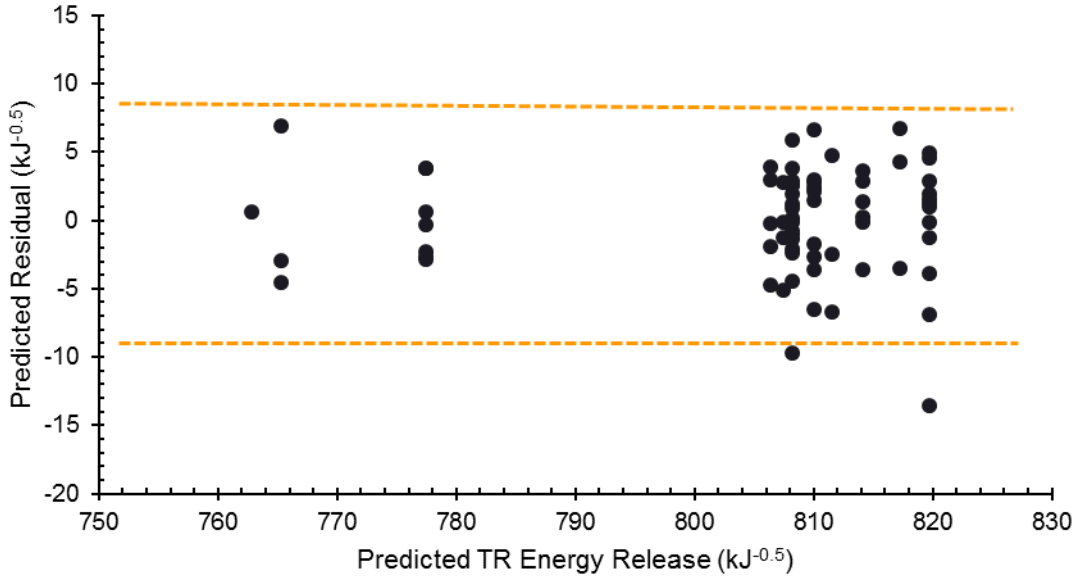

Image Credit: Walker et. al., Journal of Power Sources (2019)

ADDRESSING VARIABILTY WITH ENGINEERING STATISTICS

- **Final regression model results for total energy release were in inverse square root units (kJ $^{-0.5}$) as seen on the previous slide:**
  - These predictions were then translated back into the original units (kJ) for final interpretation
  - More details on the predicted values in inverse square root units can be found in Walker et. al., J. Power Sources (2019)
- **Distributions based on the final predicted values (in kJ) were then created:**
  - Think of the distribution curves below as the end goal for every cell, cell configuration, and cell variable that we attempt to characterize
  - The power of the regression model becomes apparent as we are now able to analyze the impacts of the random and non-random variables on thermal runaway behavior
  - The curves below only reflect the predictions 7 cell configurations for one cell format (18650); to date we've tested 20+ cell configurations ranging across three cell formats (18650, 21700, D) - there is still much work to be done

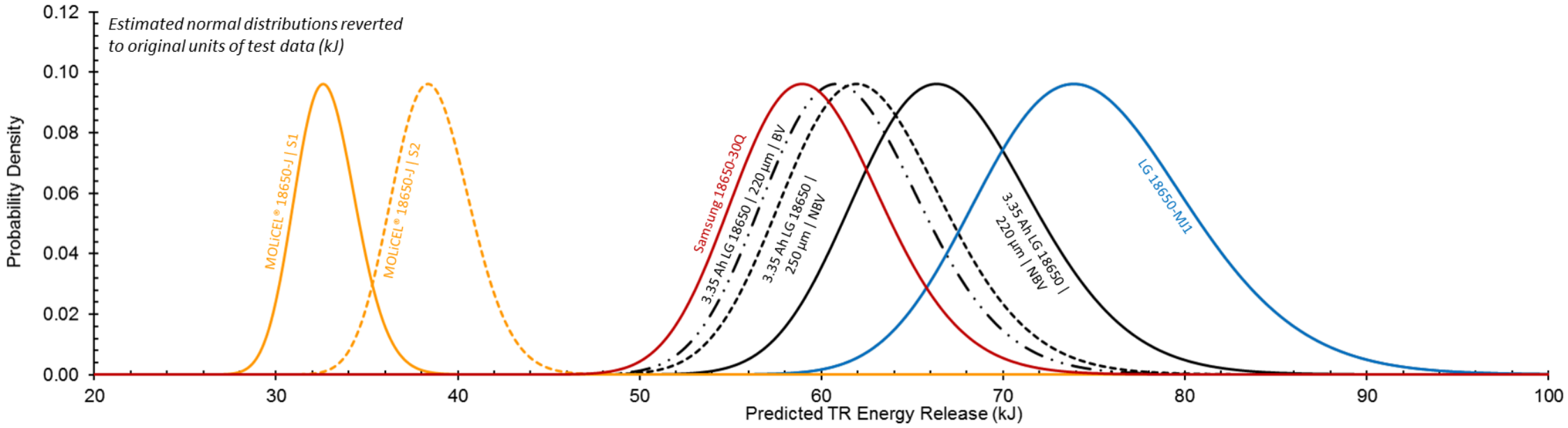

Image Credit: Walker et. al., Journal of Power Sources (2019)

KEY FINDINGS FROM STATISTICAL ANALYSIS OF FTRC DATA

- **BV cells released less TR energy (~4 kJ for 3.35 Ah LG cell) and have higher post runaway cell mass than non-BV cells:**
  - BV cells produce less and more localized heat, hence a less severe and more predictable TR event as an effect of the BV feature
  - Battery designers should be ready to accommodate and take advantage of cell designs with the BV feature in the future
- **While higher energy cells tend to produce more heat during thermal runaway, there is not a linear relationship between stored electrochemical energy and the total energy released:**
  - The two 10.8 Wh cells have significantly different thermal runaway responses with the Samsung 18650-30Q average total energy release at 59.7 kJ and the LG 18650-HG2 average total energy release at 49.7 kJ
  - The three higher energy cells (12.4 to 12.7 kJ) also have differing thermal runaway responses with the LG 18650 Test Cell average total energy release of 63.3 kJ, the Sony 18650-VC7 average total energy release of 66.5 kJ, and the LG 18650-MJ1 average total energy release of 75.2 kJ

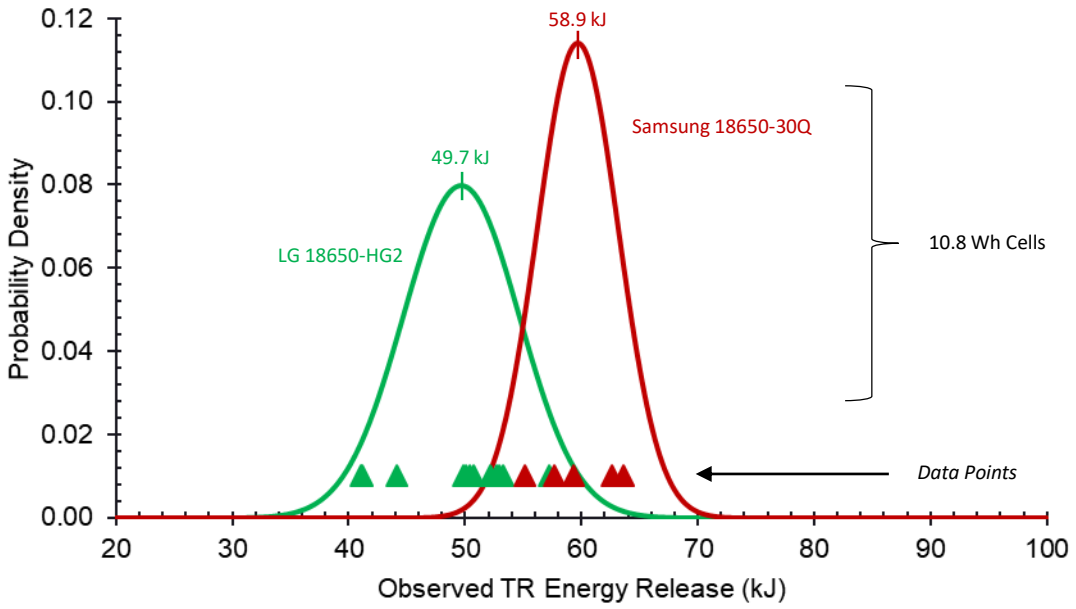

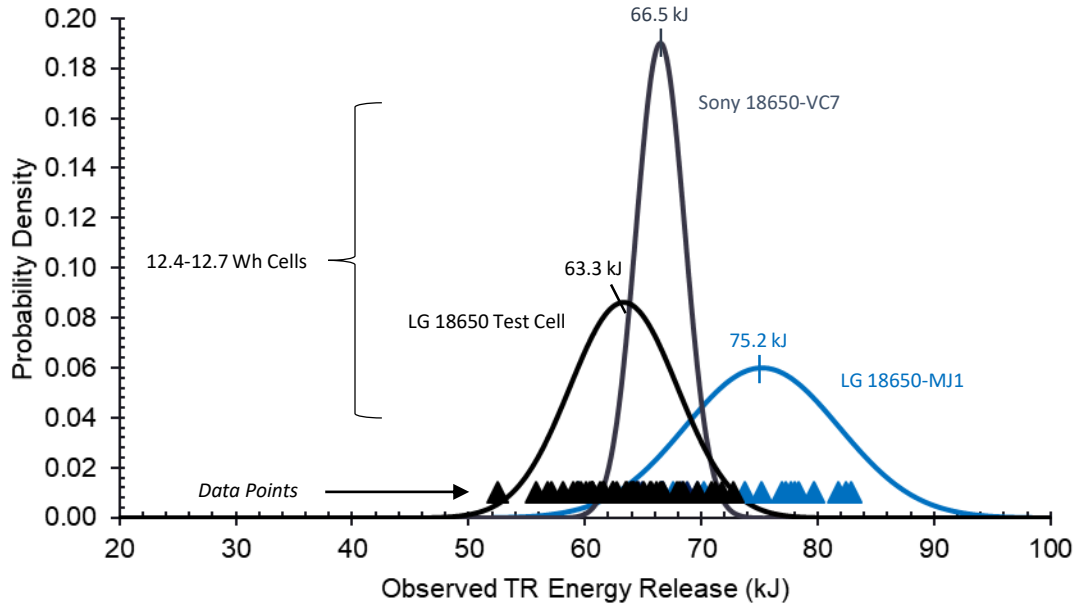

Image Credit: Walker et. al., Journal of Power Sources (2019)

KEY FINDINGS FROM STATISTICAL ANALYSIS OF FTRC DATA

- **The thermal runaway energy release fractions are determined for every cell configuration:**
  - Fractions can be determined from an average of all results for a given cell type or can be an average based on nominal vs. off nominal failure mechanism (e.g. difference between top vent vs. bottom rupture)
  - Fractional analysis is particularly helpful in comparing the distribution of standard vent cells to bottom vent cells
  - Standard cells typically release 20-30% through the cell casing and the remainder through the ejecta material
  - Bottom vent cells tend to release the energy in a three-way split between the casing and the top and bottom ejecta materials
- **The fractions quantify the direct impingement of energy on neighbor cells during runaway events**

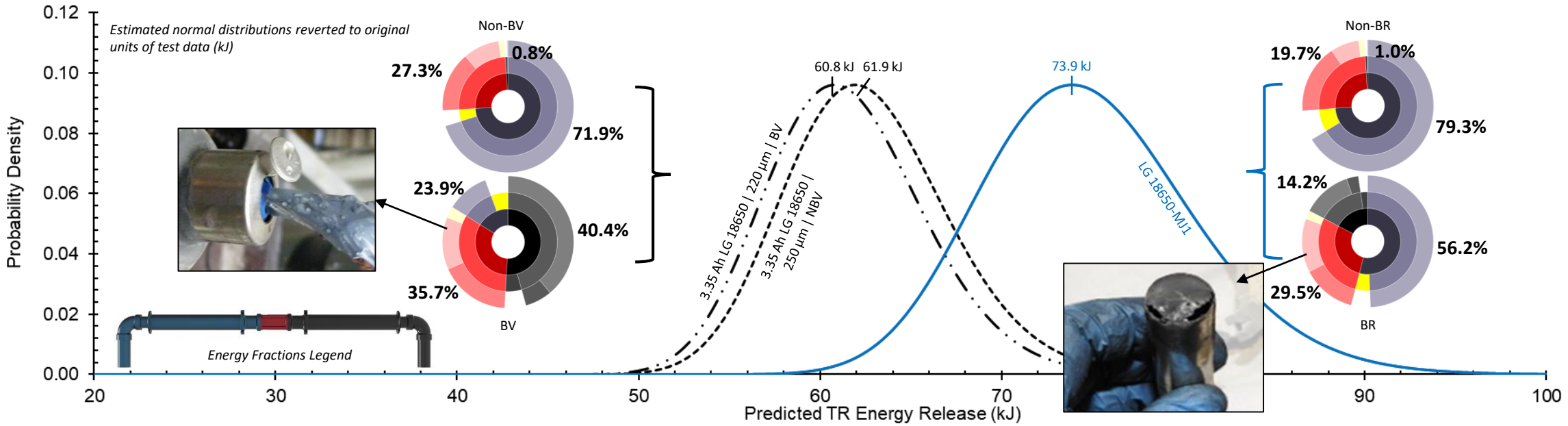

KEY FINDINGS FROM STATISTICAL ANALYSIS OF FTRC DATA

- **The Soteria™ cells with the metal coated plastic current collectors prevented thermal runaway about 50% of the time:**
  - Recall that the Soteria™ current collector model is designed to prevent internal short circuiting induced thermal runaway
  - When an short occurs, the plastic current collectors are designed to retract and break the short
- **For the experiments that did experience thermal runaway, there was a significant reduction in heat output when compared to the control cells which used standard current collectors**

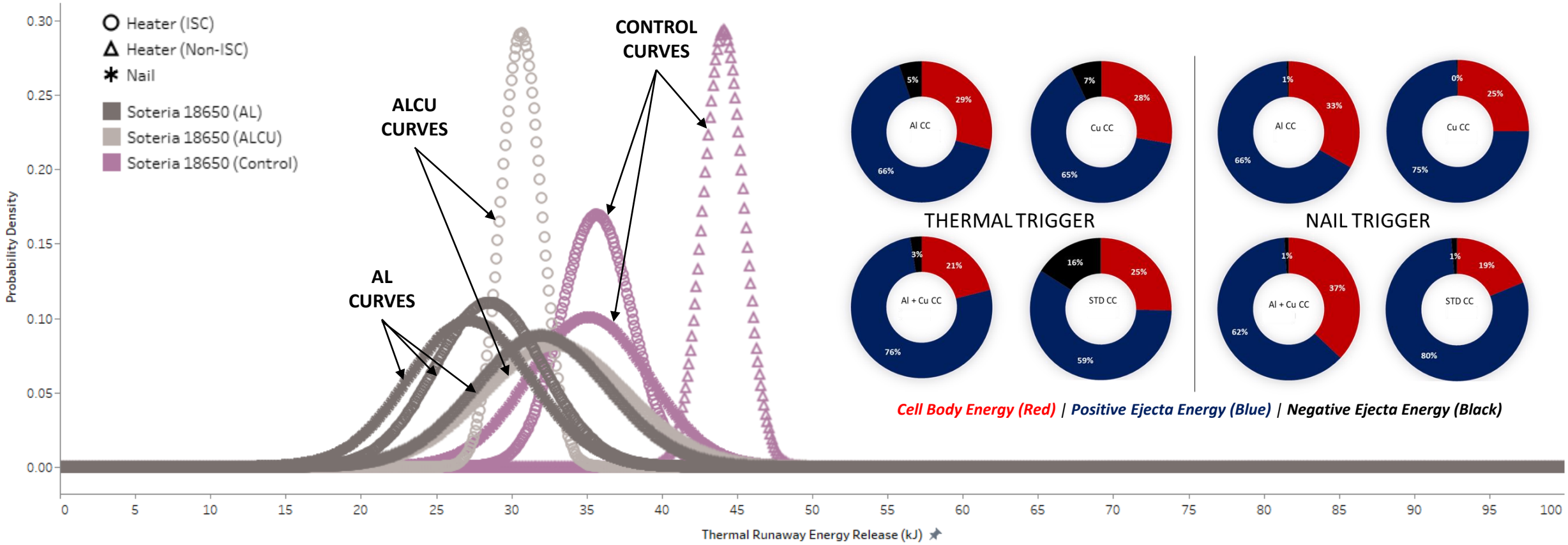

LITERATURE AVAILABLE ONLINE

Journal of Power Sources 415 (2019) 207–218

Contents lists available at ScienceDirect

Journal of Power Sources

journal homepage: www.elsevier.com/locate/jpowsour

Decoupling of heat generated from ejected and non-ejected contents of 18650-format lithium-ion cells using statistical methods

William Q. Walker[a,*], John J. Darst[a], Donal P. Finegan[b], Gary A. Bayles[c], Kenneth L. Johnson[d,e], Eric C. Darcy[a], Steven L. Rickman[a,d]

[a] National Aeronautics and Space Administration (NASA) Johnson Space Center (JSC), 2101 NASA Parkway, Houston, TX 77058, USA
[b] National Renewable Energy Laboratory (NREL), 15013 Denver West Parkway, Golden, CO 80501, USA
[c] Science Applications International Corporation (SAIC), 12010 Sunset Hills Road, Reston, VA 20190, USA
[d] NASA Engineering and Safety Center (NESC), 1 NASA Drive, Hampton, VA 23666, USA
[e] National Aeronautics and Space Administration (NASA) Marshall Space Flight Center (MSFC), 4600 Rideout Road, Huntsville, AL 35812, USA

Journal of Power Sources 417 (2019) 29–41

Contents lists available at ScienceDirect

Journal of Power Sources

journal homepage: www.elsevier.com/locate/jpowsour

Modelling and experiments to identify high-risk failure scenarios for testing the safety of lithium-ion cells

Donal P. Finegan[a,*], John Darst[b], William Walker[b], Qibo Li[a], Chuanbo Yang[a], Rhodri Jervis[c], Thomas M.M. Heenan[c], Jennifer Hack[c], James C. Thomas[b], Alexander Rack[d], Dan J.L. Brett[c], Paul R. Shearing[c], Matt Keyser[a], Eric Darcy[b]

[a] National Renewable Energy Laboratory, 15013 Denver W Parkway, Golden, CO, 80401, USA
[b] NASA Johnson Space Center, 2101 E NASA Pkwy, Houston, TX, 77058, USA
[c] Electrochemical Innovation Lab, Department of Chemical Engineering, University College London, London, WC1E 7JE, UK
[d] The European Synchrotron (ESRF), 71 Avenue des Martyrs, 38000, Grenoble, France

FUTURE OF FRACTIONAL THERMAL RUNAWAY CALORIMETRY

- FTRC currently supports 18650, 21700, and D format cells that are <5Ah; future updates will include small format pouch cells and large format prismatic cells that are >100 Ah
- Examining the effects of other design variables; e.g. cathode chemistry, cell burst pressure, speed of reaction, and level of completion of the decomposition reactions
- Developing laser triggering capability
- Improvement of regression modeling techniques
- Preparation under way for next synchrotron test series






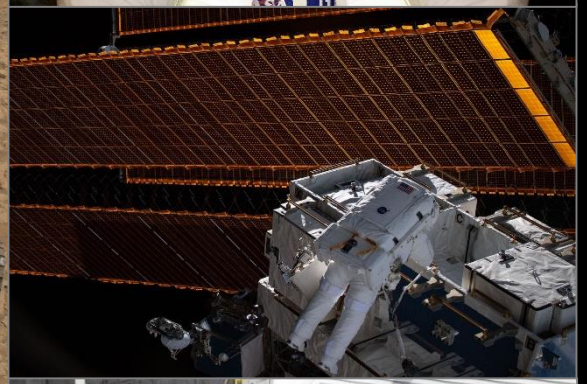

MODULE 2 SECTION 4:

NASA'S RESPONSE TO THERMAL RUNAWAY

NASA STRATEGY TO PROTECT AGAINST THERMAL RUNAWAY

- **Following the 2013 Boeing 787 Dreamliner incident, NASA teams developed new definitions for battery design success criteria for human space exploration:**
  - Always assume thermal runaway (TR) will eventually happen
  - Design should ensure that TR event is not catastrophic
  - Demonstrate that propagation to surrounding cells will not occur
- **Thermal management systems designed to mitigate the effects of thermal runaway and prevent cell-to-cell propagation should consider the following [1]:**
  - No two runaway events are the same; even for the same manufacturer and state-of-charge; there is a range of possible outcomes
  - Onset temperature, acceleration temperature, trigger temperature, trigger cell peak temperature and neighbor cell peak temperature
  - Total energy released through sides and top of the cell body
  - Cell failure type (e.g. side wall vs. top), system pressure increase, gases released and ejecta material
- **Optimization of battery assemblies that satisfy the aforementioned strategies requires knowledge of the following:**
  - Total energy output range during TR for a single Li-ion cell
  - Fraction of TR energy transferred through the cell casing
  - Fraction of TR energy ejected through cell vent/burst paths
  - The need for these data points was one of the primary drivers for the NESC assessment to develop the previously discussed FTRC

[1] *Crewed Space Vehicle Battery Safety Requirements. JSC-20793 Rev D. JSC Engineering Directorate, Power and Propulsion Division*

NASA STRATEGY TO PROTECT AGAINST THERMAL RUNAWAY

- **Also, following the 2013 Boeing 787 Dreamliner incident, the NESC was tasked to address thermal runaway related safety concerns associated with the following Li-ion batteries already being flown on the ISS:**
  - Li-ion Rechargeable Extravehicular Activity battery assembly (LREBA)
  - Li-ion Pistol Grip Tool battery assembly (LPGT)
  - Long Life Battery (LLB) for EMU

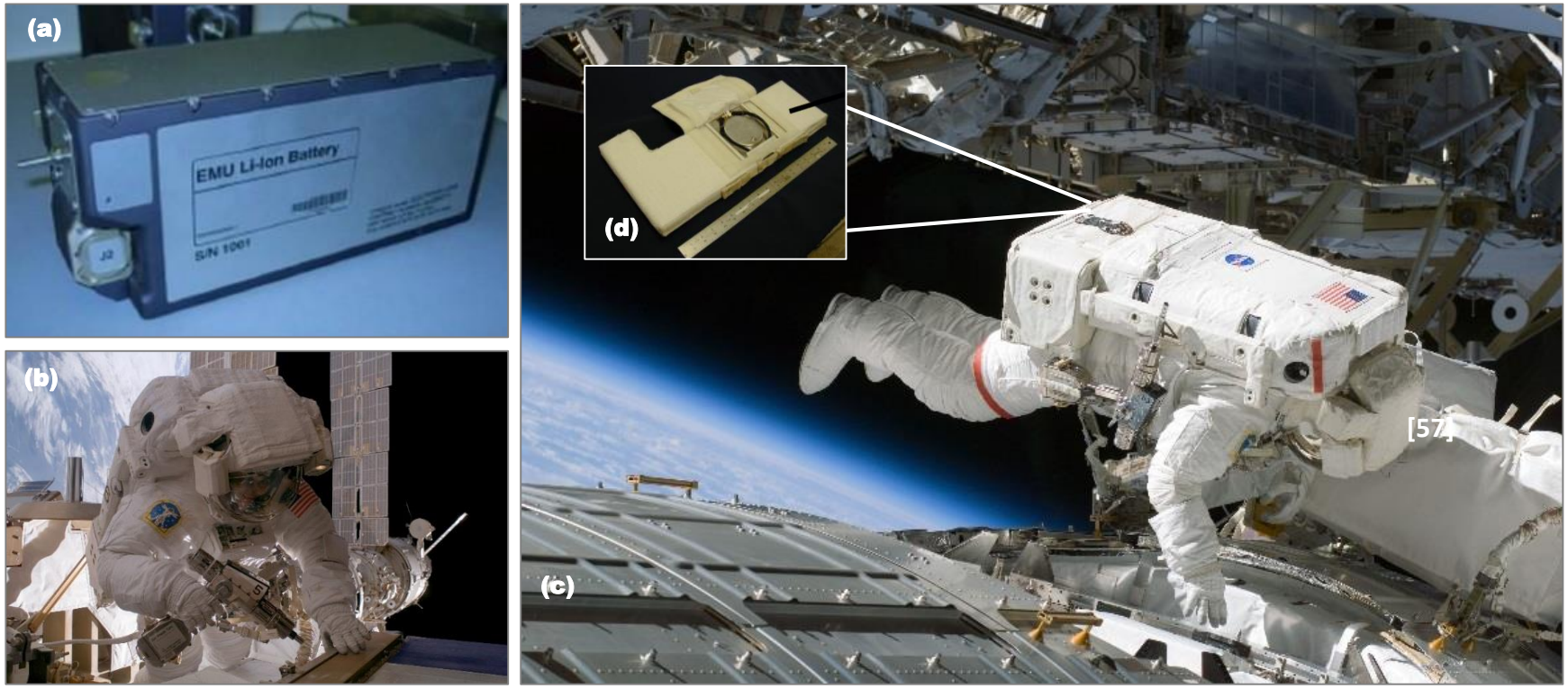

Public access images representing the EMU Li-ion batteries evaluated by the NESC: (a) LLB, (b) LPGT, (c) EMU LREBA image 1, (d) EMU LREBA image 2.

36 Darcy, E., et. al., Advanced Automotive Battery Conference (2017).

NASA STRATEGY TO PROTECT AGAINST THERMAL RUNAWAY

- **Development of optimized Li-ion battery assemblies that satisfy the previously strategies established by NASA teams to protect against thermal runaway requires knowledge of the following characteristics:**
  - Total energy output range during thermal runaway for a single Li-ion cell
  - Fraction of thermal runaway energy transferred through the cell casing
  - Fraction of thermal runaway energy ejected through cell vent/burst paths
- **The need for this data can be best understood when considering the series of design and analysis related question outlined below**
- **This data could not be gathered from standard testing mechanisms which is why FTRC was developed as part of NASA's revamped strategies for thermal runaway protection**

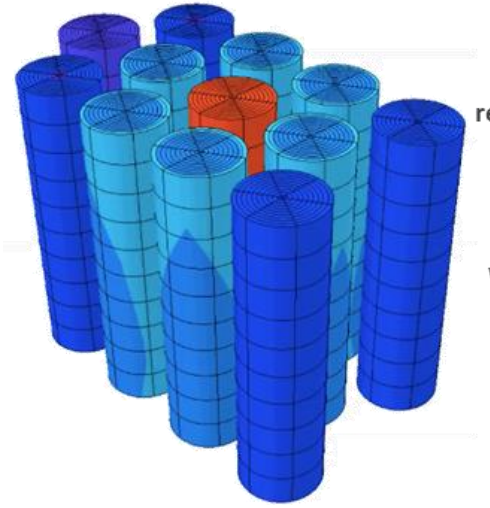

How much heat do I need to remove from the local system?

How do I support the design with thermal analysis?

What is my simulated energy distribution?

How do I best protect the adjacent cells with minimal additional mass / volume?

What works best? A heat sink, interstitial foam or a combination?

Is an interstitial material needed for thermal protection?

How far about should the individual cells be spaced?

What cell should be selected?

36 Darcy, E., et. al., Advanced Automotive Battery Conference (2017).

LESSONS LEARNED ON SAFE BATTERY DESIGNS

- Design must prevent first TR propagation from initial failed cell
- Limiting cell to cell thermal conduction appears to help prevent cell-to-cell propagation
- Maximizing heat conduction between cells and enclosure may also help prevent cell-to-cell propagation
- Parallel cell bussing can provide significant in-rush currents into failed cell, which gets them hot
- Radiative energy transfer alone is not the dominant contributor to cell-to-cell propagation
- Combustion of expelled electrolyte must directed away from adjacent cells
- Ejecta material can bridge to adjacent cells and cause cascading short circuiting
- It is imperative to control vented/ejected products

36 Darcy, E., et. al., Advanced Automotive Battery Conference (2017).

Credit: Eric Darcy

LESSONS LEARNED ON SAFE BATTERY DESIGNS

- **Compliance with the following rules can help prevent cell-to-cell propagation:**
  - Minimize side wall ruptures
  - High thermal conductivity interstitial heat sinks
  - No direct cell-cell contact; direct contact nearly assures propagation
  - 0.5mm cell spacing can work, but spacing out cells > 1mm is very beneficial
  - Individually fusing cells in parallel
  - Protect adjacent cells from ejecta materials (all solids, liquids, and gases)
- **Include flame arresting vent ports to minimize combustion effects:**
  - Create tortious path with flame arresting screens
- **Some high energy density (>600 Wh L^{-1}) are very likely to experience side wall ruptures during TR**
  - Structural syntactic foams or steel tubes work
- **Corner and edge cells are more vulnerable than interior cells towards TR propagation**
- **Ejecta is electrically conductive and can cause circulating currents**
- **Entire battery gets hotter with each subsequent cell TR event**
- **Soft goods bag and conductive absorptive material prevent exiting flames**
- **Subscale test results can be misleading and no replacement for full scale test verifications**

36 Darcy, E., et. al., Advanced Automotive Battery Conference (2017).

Credit: Eric Darcy






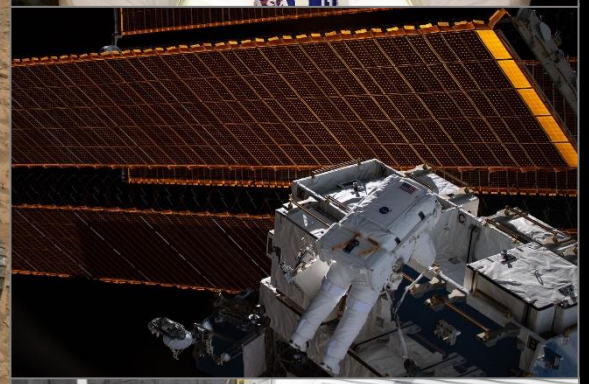

MODULE 3 SECTION 1:

PRACTICAL THERMAL MODEL CONSTRUCTION TECHNIQUES

PRACTICAL THERMAL MODEL CONSTRUCTION TECHNIQUES

- **Li-ion battery performance, efficiency, and safety are heavily influenced by the operating temperature, which is a direct function of the following:**
  - The system level architecture (i.e. the battery design, surrounding structures, and thermal management systems)
  - Battery self heating rates due to over-potential and entropy change
  - Influences of external thermal environments
  - When we talk about simulating this thermal performance, we are talking about thermo-electrochemical analysis
- **Accurate simulation of battery thermal performance during operations (i.e. charge and discharge) or during failure modes (i.e. thermal runaway) requires implementation of thermo-electrochemical models:**
  - Generally, the optimal way to perform thermo-electrochemical analysis is with a multiphysics platform, however;
  - Non-multiphysics platforms designed for thermal analysis and that support user-defined heat loads and transient variable statements can do the trick (e.g. Thermal Desktop, Logic Objects Manager, and SINDA code)
- **FYI… my original interest in using software capable of simulating thermal radiation driven space environments was driven by my goal of simulating battery heat generation rates as a function orbital environments (which is important when considering the relevant temperature dependencies)**

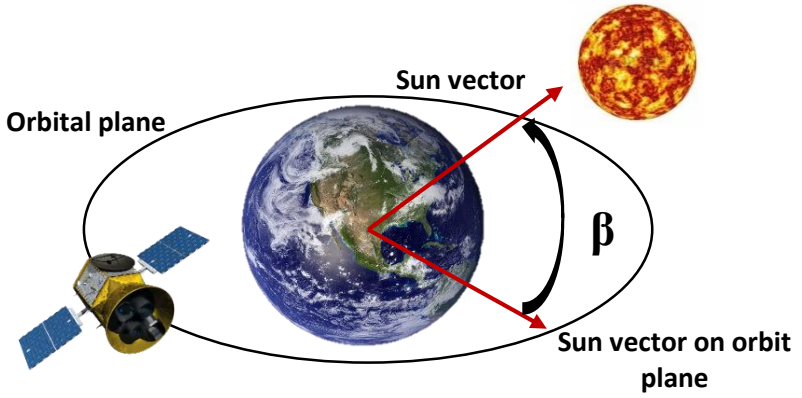

PRACTICAL THERMAL MODEL CONSTRUCTION TECHNIQUES

- **Here we use an example bank that consists of 14 Li-ion cells (18650-format)**
- **The example, shown with image (a) below, is used to demonstrate methods to quickly develop thermal models of battery assemblies via SpaceClaim, TD Direct, and Thermal Desktop:**
  - The example was chosen due to the inclusion of both an aluminum heat sink and an interstitial insulating foam
  - Users may have access to different software suites, but the principles discussed here should remain the same
  - The intent here is to not be software specific, but rather to be practical in approach

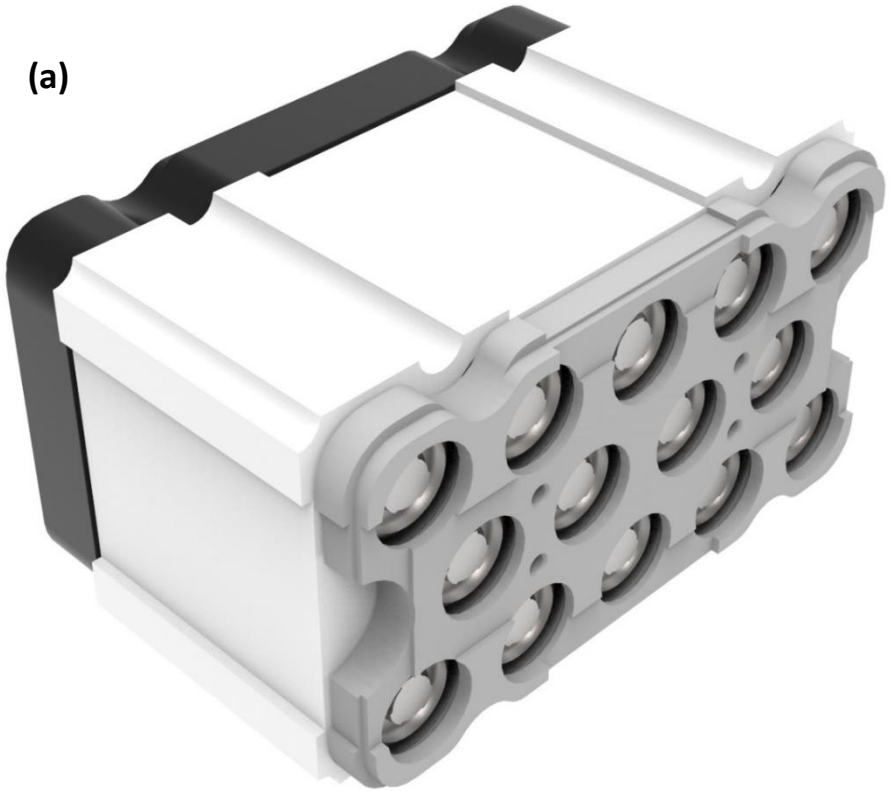

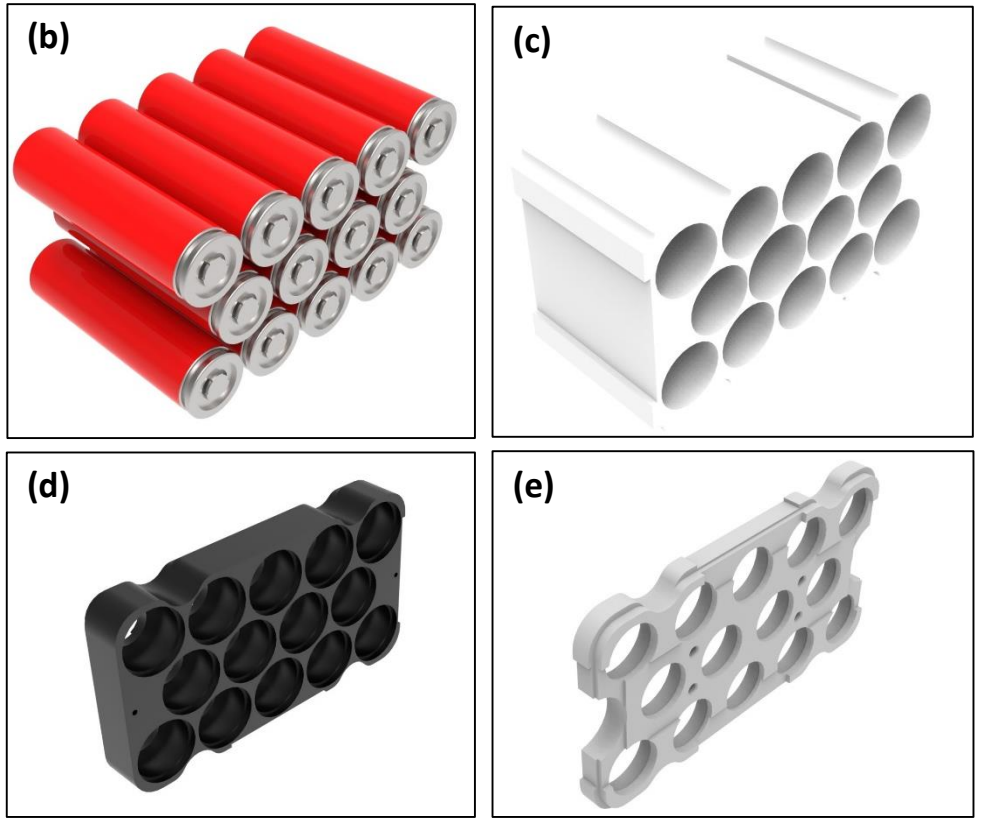

PRACTICAL THERMAL MODEL CONSTRUCTION TECHNIQUES

STEP 1: CREATE REFERENCE MODEL OF THE BANK COMPONENTS (REFERENCE MODEL 1)

Defeature CAD (Bus-bars, Endcaps, Interstitial Materials, Heat Sink)	Assign Domain Tag-sets for Each Set of Surface Interfaces	Assign Thermophysical and Optical Properties, and Radiation Analysis Groups	Mesh and Import into Thermal Desktop Reference Model 1
SpaceClaim	SpaceClaim & TD Direct	SpaceClaim & TD Direct	SpaceClaim, TD Direct, & Thermal Desktop

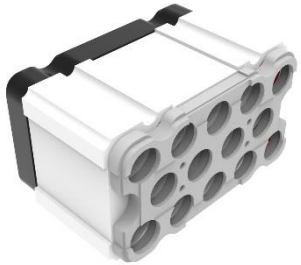

STEP 2: CREATE REFERENCE MODEL OF AN INDIVIDUAL 18650 LI-ION CELL (REFERENCE MODEL 2)

Construct Single Cell Thermal Desktop Reference Model 2 Using Native Geometries	Assign Domain Tag-Sets for Each Set of Surface Interfaces and Each Jellyroll Solid	Assign Thermophysical and Optical Properties, and Radiation Analysis Groups
Thermal Desktop	Thermal Desktop	Thermal Desktop

STEP 3: CREATE REFERENCE MODEL OF GEOMETRIES REPRESENTING CELL PLACEMENT LOCATIONS (REFERENCE MODEL 3)

Use Defeatured CAD to Create Dummy Geometry Representing Cell Placement Locations	Import Geometries into Thermal Desktop Reference Model 3
SpaceClaim	SpaceClaim

STEP 4: CREATE MASTER MODEL THAT COMBINES ALL REFERENCE MODELS VIA XREF

Use XREF Feature to Import Reference Model 1	Use XREF Feature to Import Reference Model 3	Use XREF Feature to Import Reference Model 2 at Each of the Placement Locations
Thermal Desktop	Thermal Desktop	Thermal Desktop

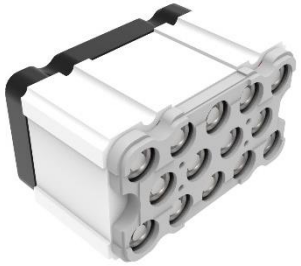

HEAT LOADS FOR CHARGE AND DISCHARGE

- **Ohmic heat generation may be applied to as a single heat load in the master file of the battery assembly**
  - In the cell reference file, create a domain tag set that contains the jellyroll
  - In the master file, create registers for each of the variables in Bernardi's equation; we will simplify here and only use current and voltage
  - In the master file, apply "heat load to solid" and select the jellyroll domain tag set; set the value as a symbol expression of Bernardi's equation
  - In the master file, create VAR0 array interpolation or bivariate array interpolation time dependent logic objects; the array value should be defined by test
- **Running a transient simulation will now update the previously defined heat load on the jellyroll before each timestep based on the change in current, open circuit voltage and working voltage**
- **For analysis purposes, this instructor recommends considering this problem with bi-variate arrays to take into account the temperature dependencies of working voltage and open circuit voltage:**

Q_{JELL} = Current x

V_{OC} Bivariate Array

	-45°C	-25°C	0°C	+25°C	+45°C
0min	#	#	#	#	#
10min	#	#	#	#	#
20min	#	#	#	#	#
30min	#	#	#	#	#
40min	#	#	#	#	#
50min	#	#	#	#	#
60min	#	#	#	#	#
70min	#	#	#	#	#

—

V_W Bivariate Array

	-45°C	-25°C	0°C	+25°C	+45°C
0min	#	#	#	#	#
10min	#	#	#	#	#
20min	#	#	#	#	#
30min	#	#	#	#	#
40min	#	#	#	#	#
50min	#	#	#	#	#
60min	#	#	#	#	#
70min	#	#	#	#	#

HEAT LOADS FOR THERMAL RUNAWAY

- **Two approaches to simulating thermal runaway heat loads:**
  - Direct simulation of the kinetic relationships between self-heating rates and decomposition rates
  - Application of distributed heat loads throughout the model that are based on calorimetric test data
- **Direct simulation of kinetic relationships is useful, but can be computationally expensive depending on the software (e.g. COMSOL can run the simulation for a 0-D example in about 10 s whereas the same model set-up in Thermal Desktop takes about 2 hrs to run)**
- **For application of distributed heat loads, recommend using the data for a given cell configuration from FTRC as a starting point:**
  - Apply the heat loads to the cell body (i.e. the jellyroll) and to the expected impingement surfaces
  - Vary the FTRC fractions and the simulated energy release time (typically 0.5 s to 1.5 s) until correlation is met with available system level abuse test data
  - If the aforementioned system level test data is not available, start with a 20% cell body energy, 80% ejecta energy, and a 1.5 s energy release time for top vent cells and a 40% cell body energy, 30% positive ejecta energy, 30% negative ejecta energy, and 1.5 s energy release time for bottom vent cells








MODULE 3 SECTION 2:

EXAMPLE THERMAL SIMULATIONS PART 1, NOMINAL OPERATIONS

EXAMPLE OF HEAT GENERATION WHEN DISCHARGING

- **Here we revisit the discharge example for a large format 185 Ah $LiCoO_2$ electric vehicle battery based on Chen et. al. [19] and Walker et. al. [20] which compared test and analysis for various discharge rates and convective cooling environment combinations:**
  - Recall that the stack of Li-ion cells was treated as a lump mass surrounded in electrolyte
  - Case study 1 considered 1-C, 2-C, and 3-C discharge rates in a 27 °C natural convection environment
  - Case study 2 considered 3-C discharge rate for a range of 27 °C forced convection environments (5 to 300 W m^{-2} $°C^{-1}$)

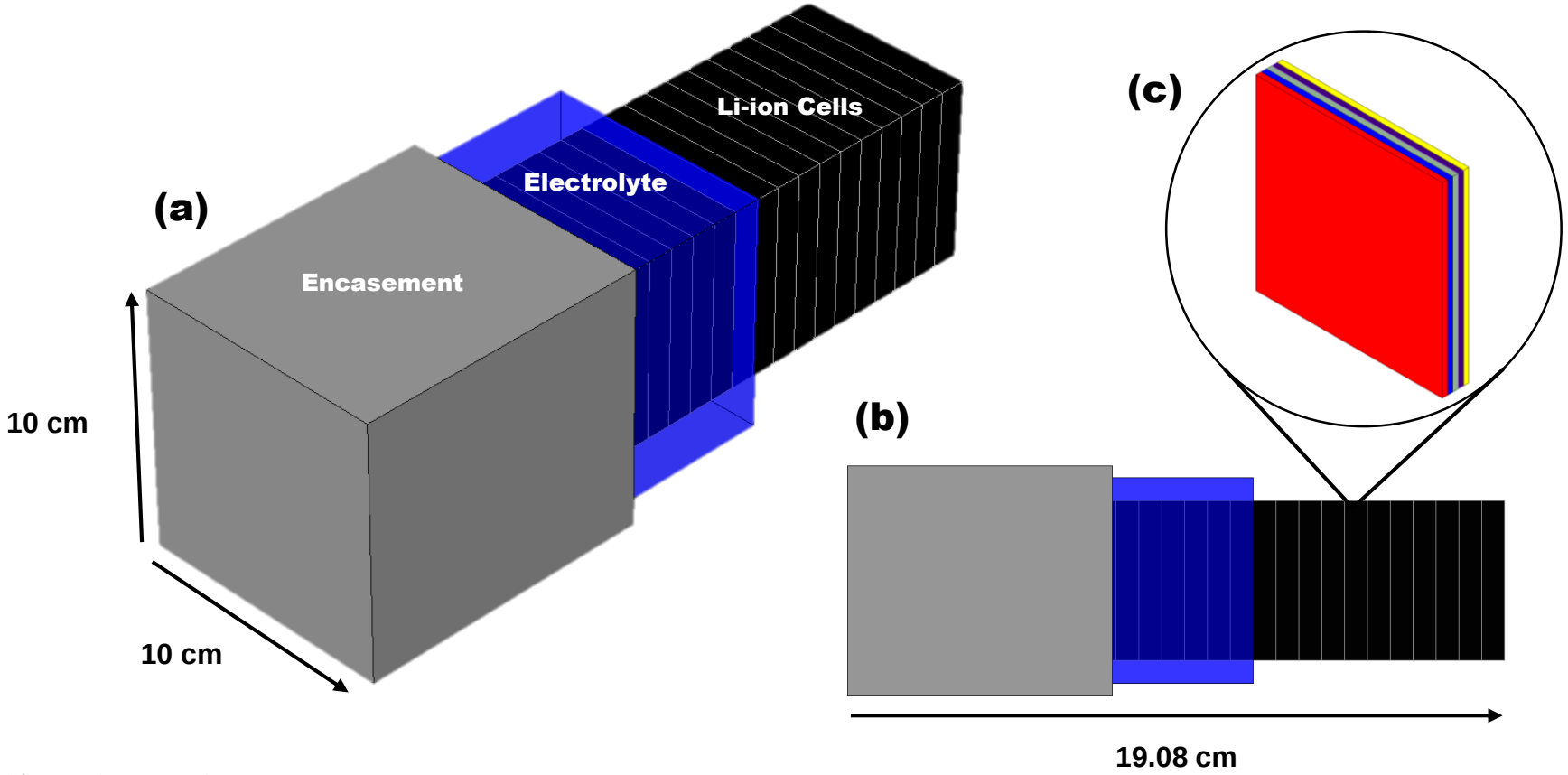

Image courtesy of Walker and Ardebili [20]

19 S. Chen, C. Wan and Y. Wang, "Thermal Analysis of Lithium-Ion Batteries," Journal of Power Sources, vol. 140, pp. 111-124, September 2005.
20 W. Walker and H. Ardebili, "Thermo-electrochemical analysis of lithium ion batteries for space applications using Thermal Desktop," Journal of Power Sources, vol. 269, pp. 486-497, 2014.

EXAMPLE OF SIMULATION FOR HEAT GENERATION WHEN DISCHARGING

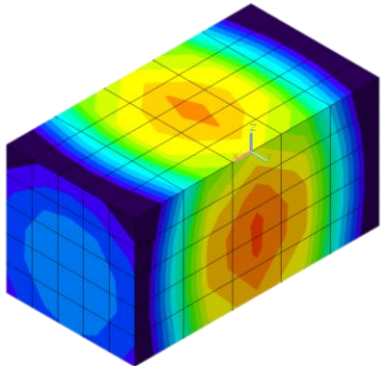

$$Q = I\left(V_{OC} - V_W - T\frac{\partial V_{OC}}{\partial T}\right)$$

EXAMPLE OF SIMULATION FOR HEAT GENERATION WHEN DISCHARGING

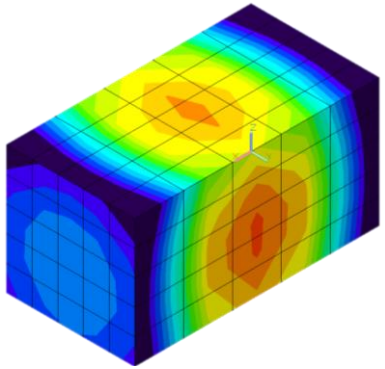

$$Q = I\left(V_{OC} - V_W - T\frac{\partial V_{OC}}{\partial T}\right)$$

EXAMPLE OF HEAT GENERATION WHEN CHARGING

- **Now we revisit the charge example based on various charging rates of a Boston Power Swing 5300® Li-ion cell [21] and Walker et. al. [22]. Please recall the following:**
  - The Boston Power 5300 cell was charged at the following three rates for this example: 0.7-C, 1-C, and 2-C
  - This example does not employ constant current like the discharge example; current (I) starts tapering when the cell reaches 80% SOC (for safety purposes to prevent overcharge)
  - The transient temperature profile observed for each of the curves is in direct relationship with the over-potential and the current taper
  - Unlike with discharge, there is not a temperature spike at the end of charging because the over-potential is nearly zero and the cell is operating under nearly entirely reversible conditions (i.e. it is operating as efficiently as possible)
  - Image Credit: Walker et. al. [22]

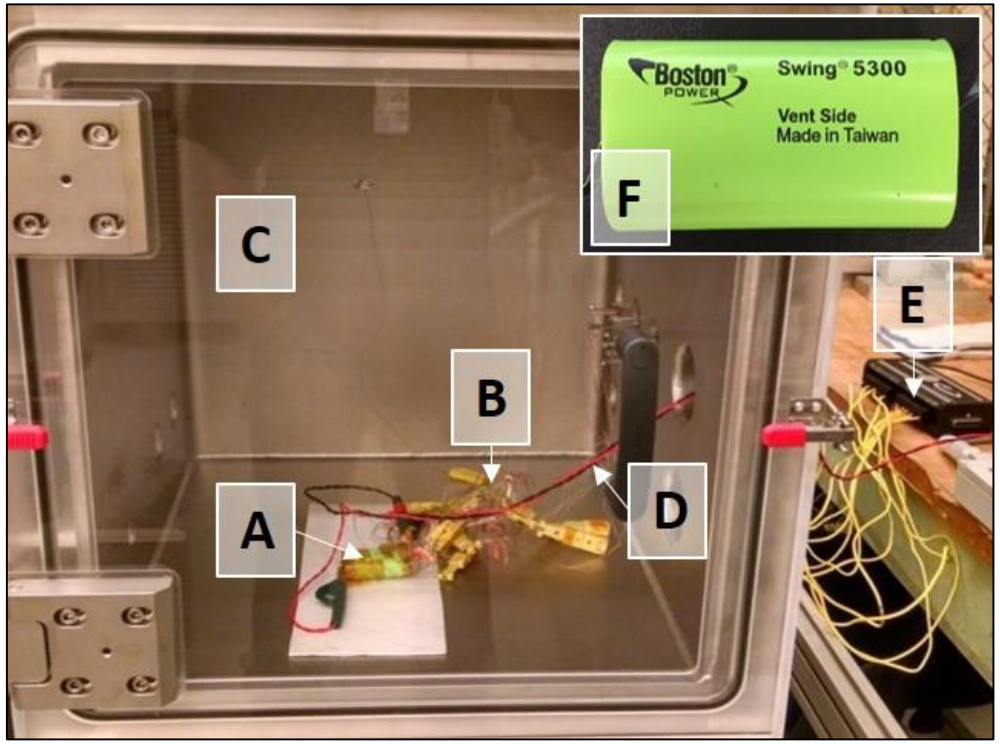

21 Boston Power, *Swing 5300 Rechargeable Lithium-ion Cell*, Westborough: Boston-Power, Incorporated, 2013.
22 W. Walker, S. Yayathi, J. Shaw and H. Ardebili, "Thermo-electrochemical evaluation of lithium-ion batteries for space applications." Submitted to Journal of Power Sources June 27th, 2015.

EXAMPLE OF SIMULATION FOR HEAT GENERATION WHEN CHARGING

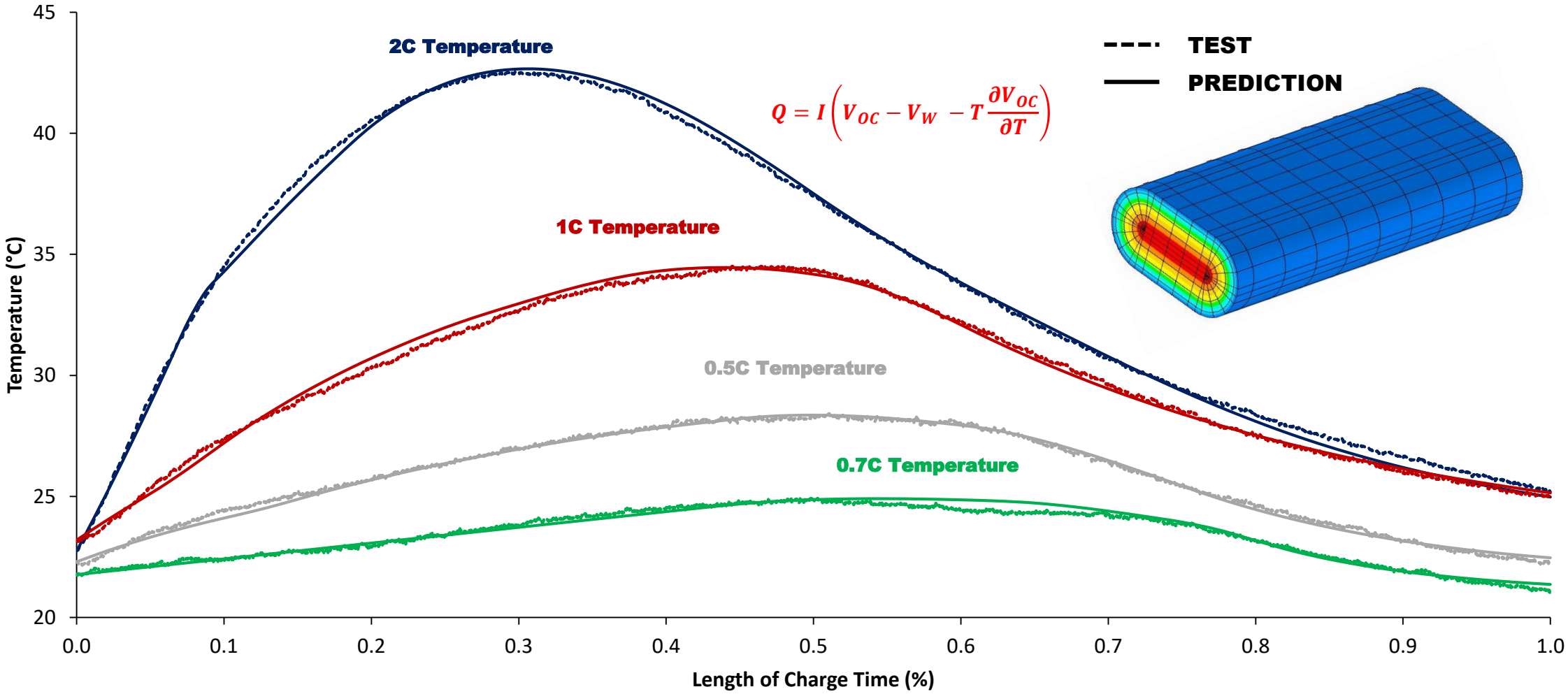






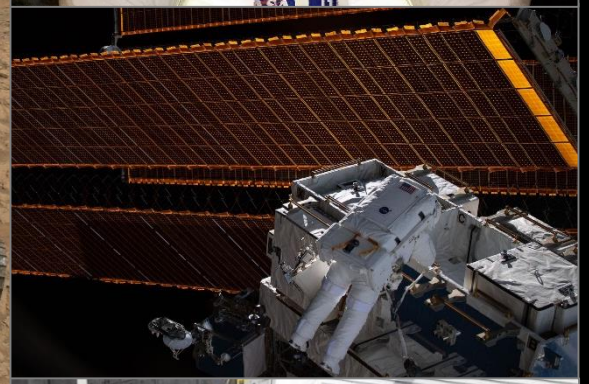

MODULE 3 SECTION 3:

EXAMPLE THERMAL SIMULATIONS PART 2, THERMAL RUNAWAY

EXAMPLE 1 FOR THERMAL RUNAWAY SIMULATION

- **Using the previously defined partial differential equations, it is possible to simulate the thermal runaway heat load as a direct function of thermal runaway kinetic relationships:**
  - Examples below compare this method using both COMSOL and SINDA
  - Primary draw-back is that this method is computationally intensive for 0-D simulation, expanding to 3-D only make it more expensive
  - Solution is heavily time-step dependent due to the Arrhenius behavior; large time steps result in inaccurate calculation, small time steps can take too much time to solve
  - Two codes using the same input parameters can result in different answers depending on solver settings (see COMSOL / SINDA comparison)
  - Although helpful in understanding thermal runaway, direct simulation of thermal runaway kinetics is not practical for assembly level simulation

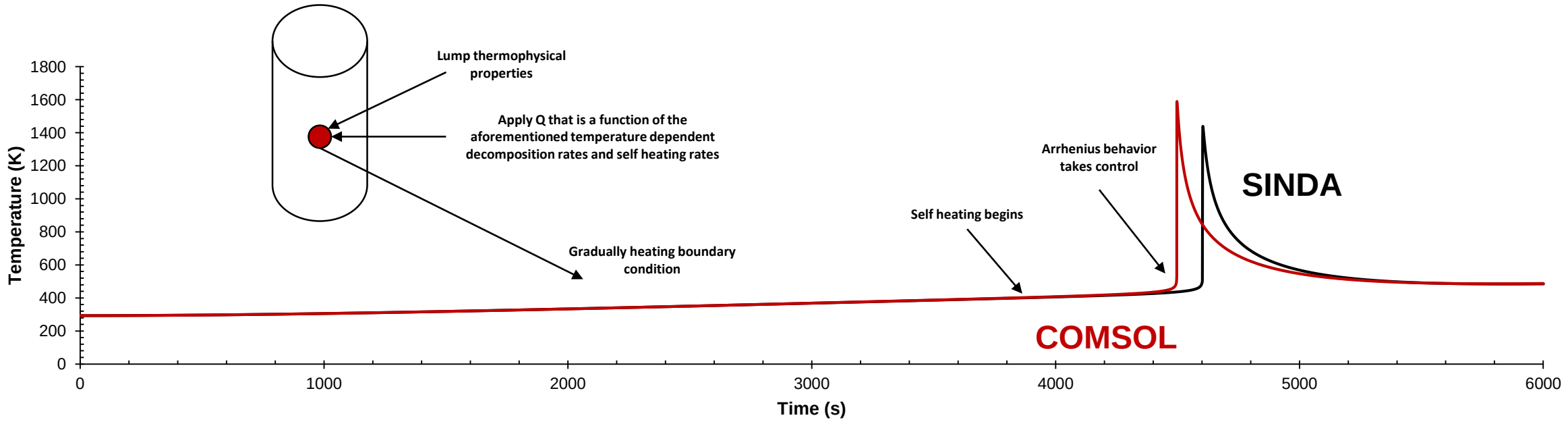

Simulations of environmentally induced thermal runaway based on mathematic models developed by Richard and Dahn, Hatchard et. al., Kim et. al. and Coman et. al. [67-70].

23 Richard, M. Accelerating rate calorimetry study on the thermal stability of lithium intercalated graphite in electrolyte. I. experimental. *Journal of The Electrochemical Society* **146,** 2068 (1999).
24 Hatchard, T., MacNeil, D., Basu, A. & Dahn, J. Thermal model of cylindrical and prismatic lithium-ion cells. *Journal of The Electrochemical Society* **148,** A755 (2001).
25 Kim, G.-H., Pesaran, A. & Spotnitz, R. A three-dimensional thermal abuse model for lithium-ion cells. *Journal of Power Sources* **170,** 476–489 (2007).
26 Coman, P., Rayman, S. & White, R. A lumped model of venting during thermal runaway in a cylindrical Lithium Cobalt Oxide lithium-ion cell. *J Power Sources* **307,** 56–62 (2016).

EXAMPLE 2 FOR THERMAL RUNAWAY SIMULATION

- **Using variable controlled heat loads based on test defined thermal runaway data (i.e. FTRC statistics), it is possible to replicate thermal runaway heating with practical simulation techniques:**
  - Establish code driven heat loads that are designed to perform the following at each time step: (1) identify temperatures, (2) observe is thermal runaway criteria is met, (3) continue if not, and (4) apply thermal runaway heat loads when criteria is met
  - Code should have mechanism to ensure that runaway heating only happens once per cell

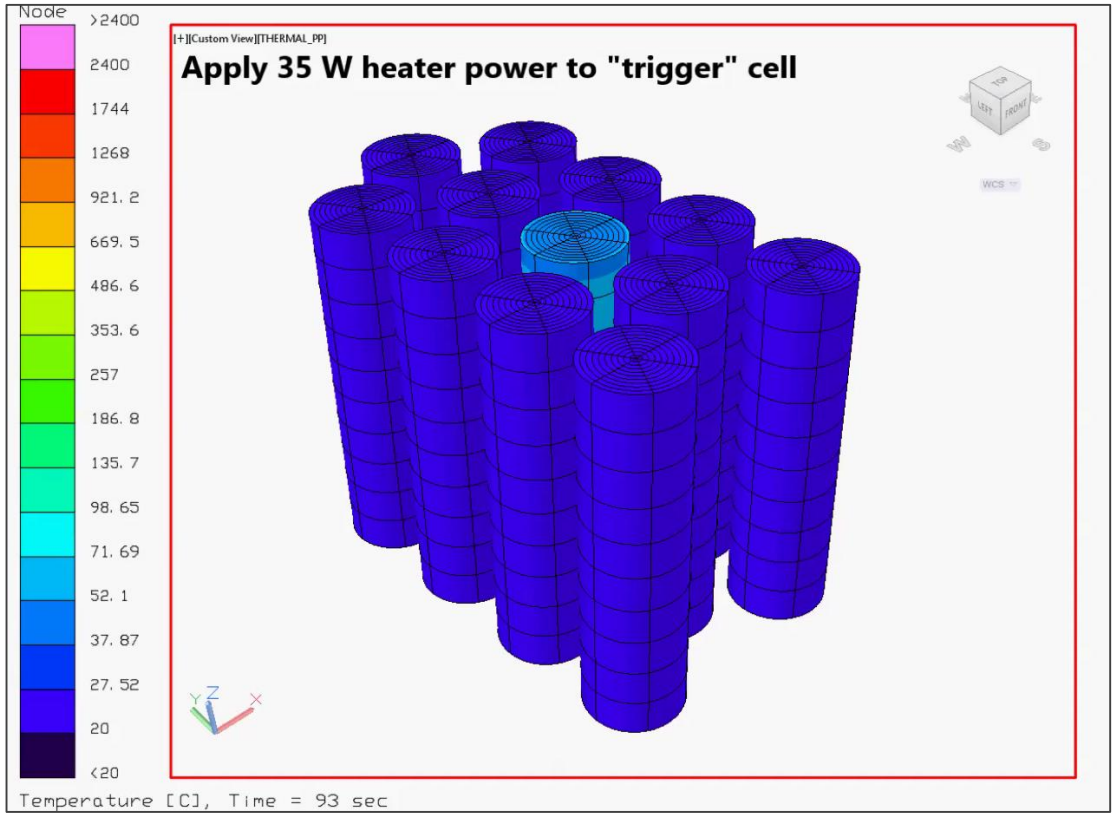

EXAMPLE 3 FOR THERMAL RUNAWAY SIMULATION

- **Example of test-correlated thermal analysis for abuse testing of a proposed battery assembly for the Advanced Portable Life Support System (PLSS):**
  - Eight 18650 cells encased in an interstitial aluminum housing
  - Challenge is to properly simulate the thermal runaway energy distribution throughout the case

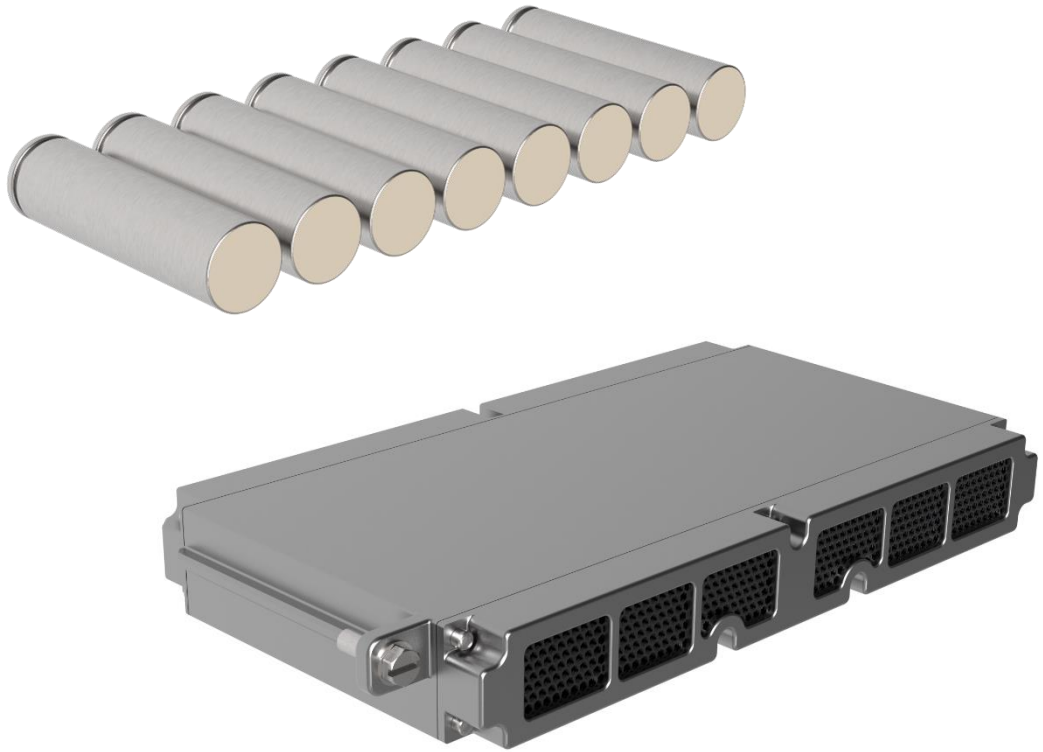

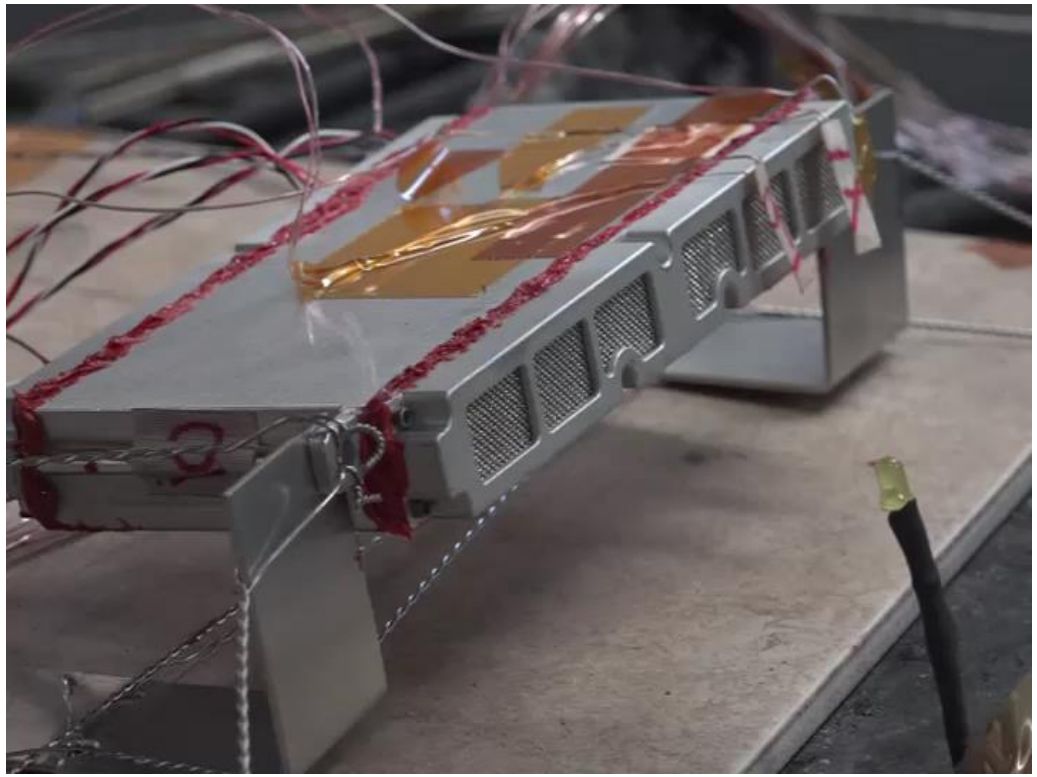

EXAMPLE 3 FOR THERMAL RUNAWAY SIMULATION

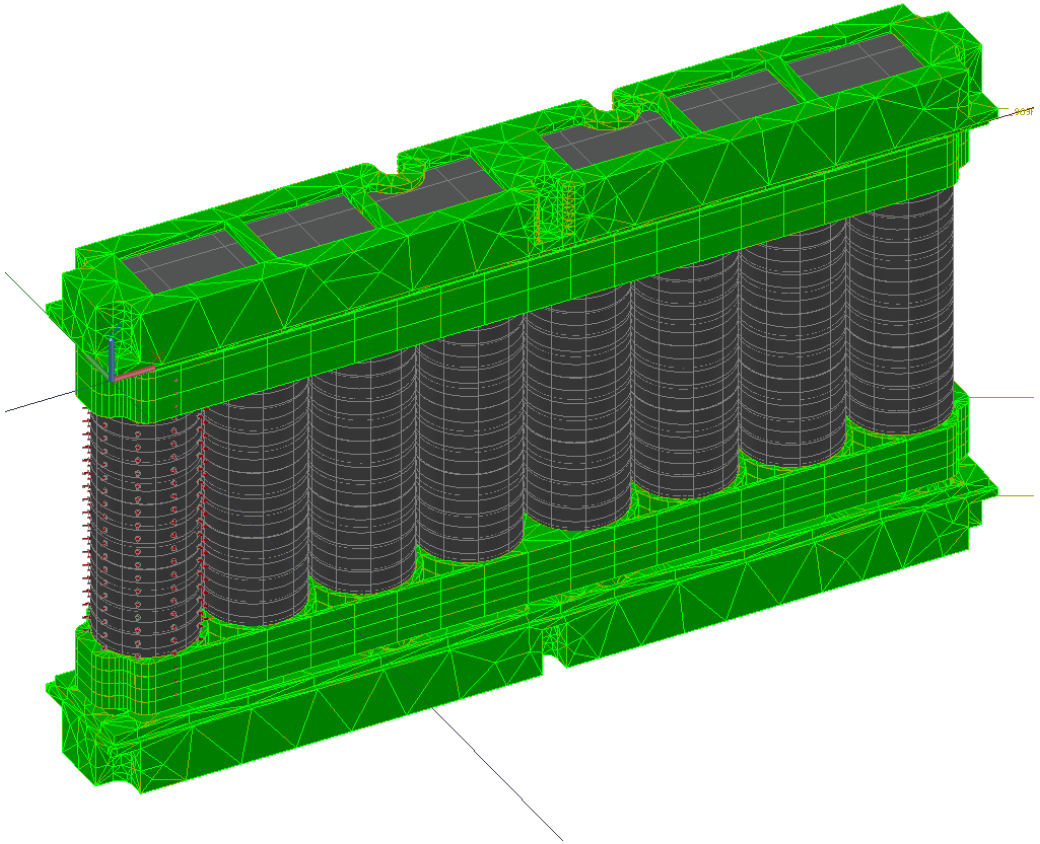

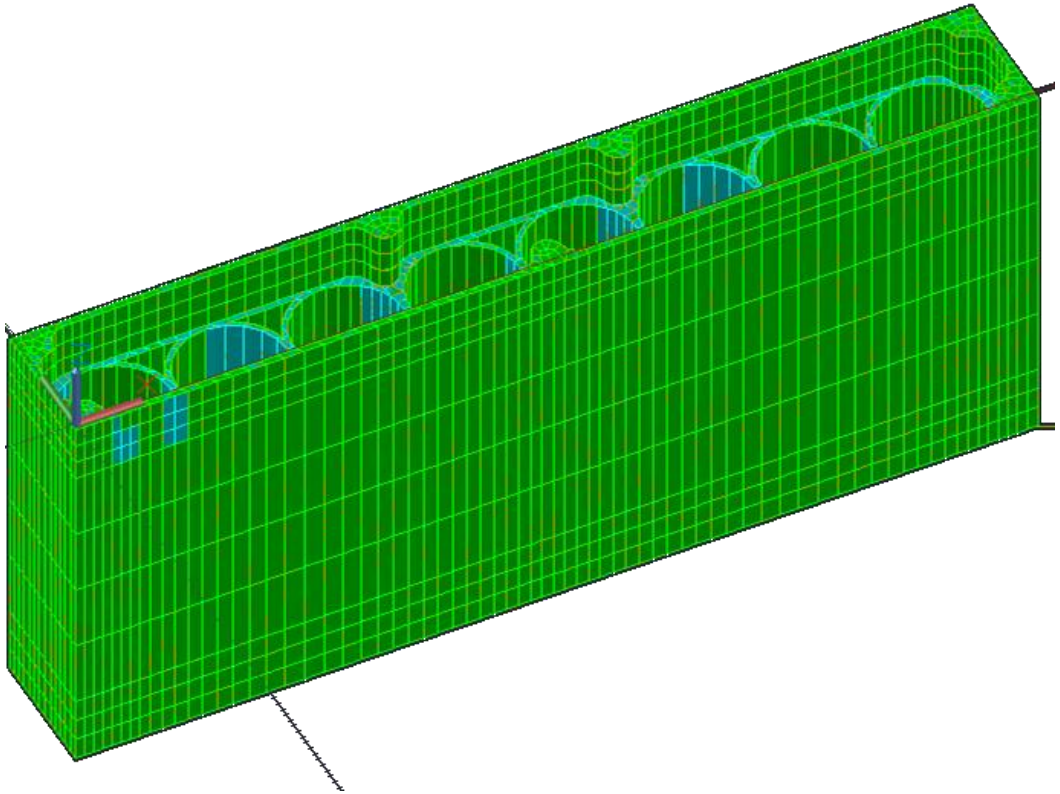

Credit: Stephania Ortega (NASA JSC)

EXAMPLE 3 FOR THERMAL RUNAWAY SIMULATION

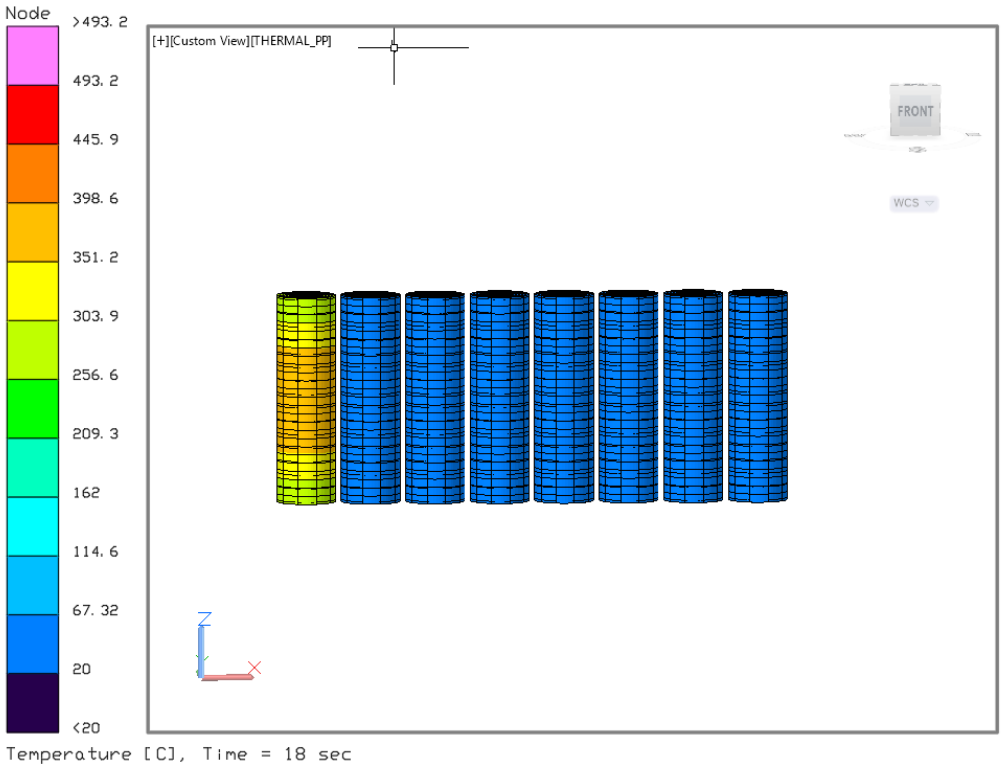

First Cell Temperature Peak

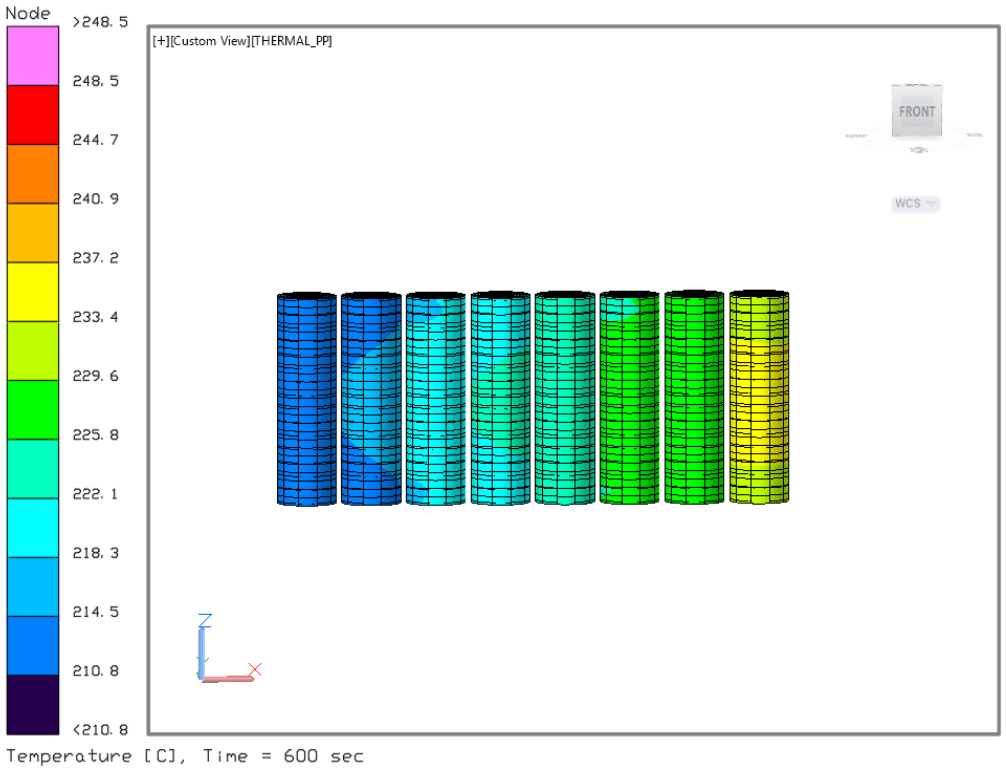

End of Transient Simulation

Credit: Stephania Ortega (NASA JSC)

EXAMPLE 3 FOR THERMAL RUNAWAY SIMULATION

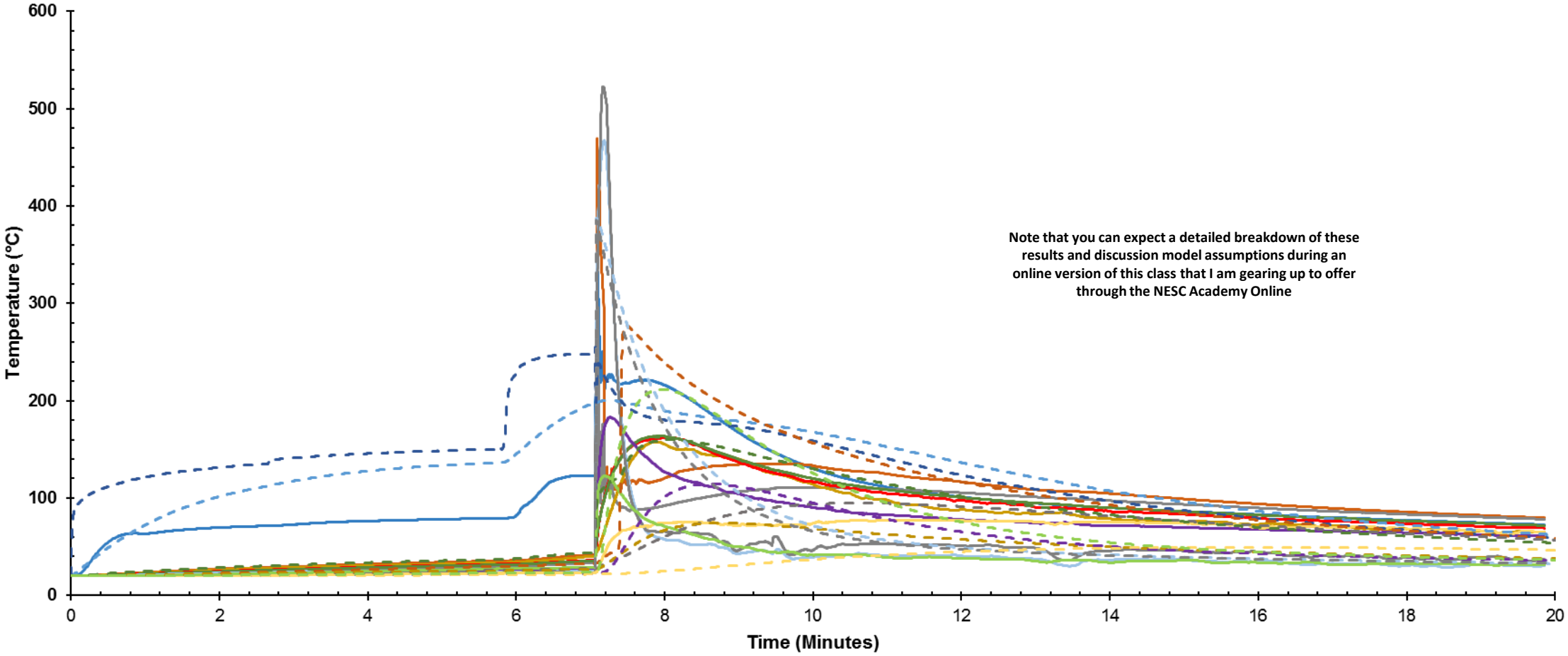

Note that you can expect a detailed breakdown of these results and discussion model assumptions during an online version of this class that I am gearing up to offer through the NESC Academy Online

Credit: Stephania Ortega (NASA JSC)






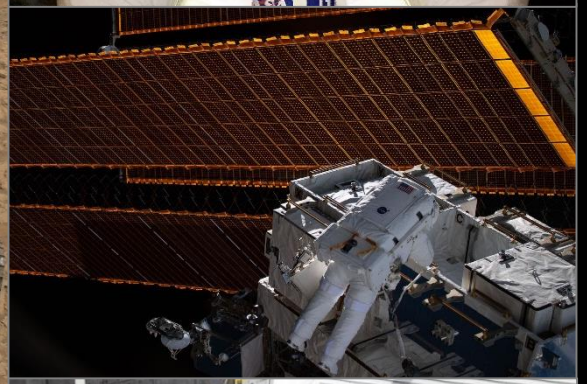

WRAP-UP AND QUESTIONS

ACKNOWLEDGEMENTS

- NASA Engineering and Safety Center
- NASA JSC Engineering Directorate (EA), Structural Engineering Division (ES) and Power and Propulsion Division (EP)
- Steve Rickman, Eric Darcy, and Christopher Iannello
- NASA JSC Energy Systems Test Area (ESTA)
- Jacob Darst, NASA JSC
- Stephania Ortega, NASA JSC
- Haleh Ardebili, University of Houston (UH)






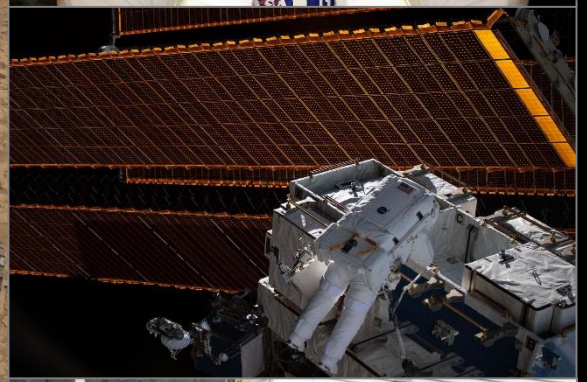

QUESTIONS?

EXAMPLE OF SIMULATION FOR HEAT GENERATION WHEN DISCHARGING

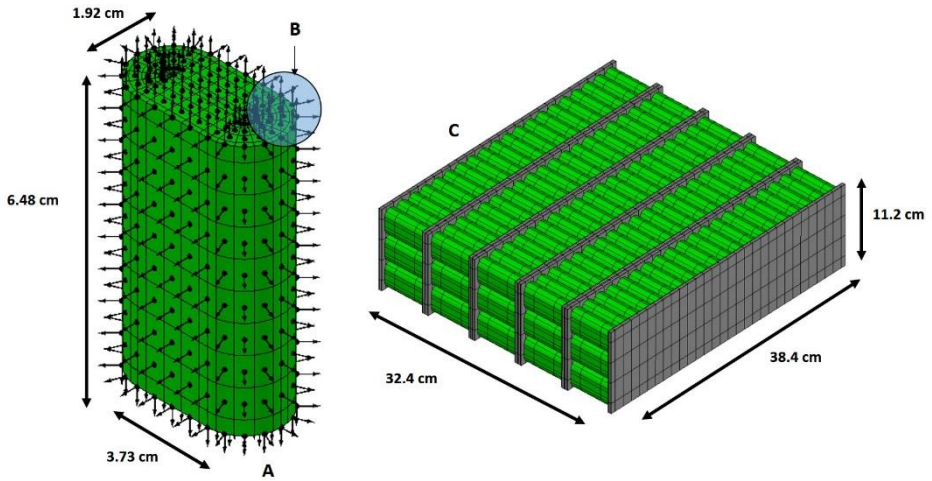

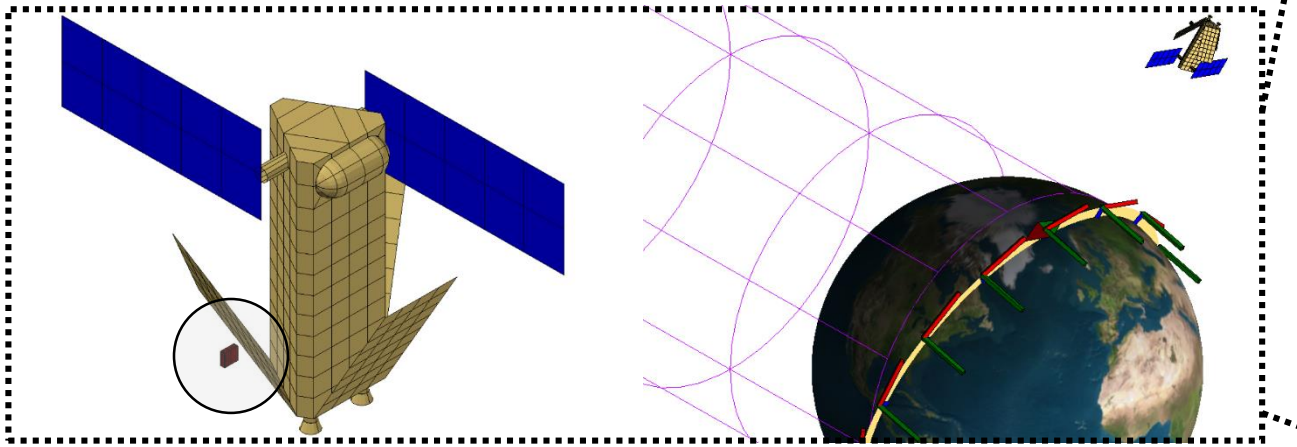

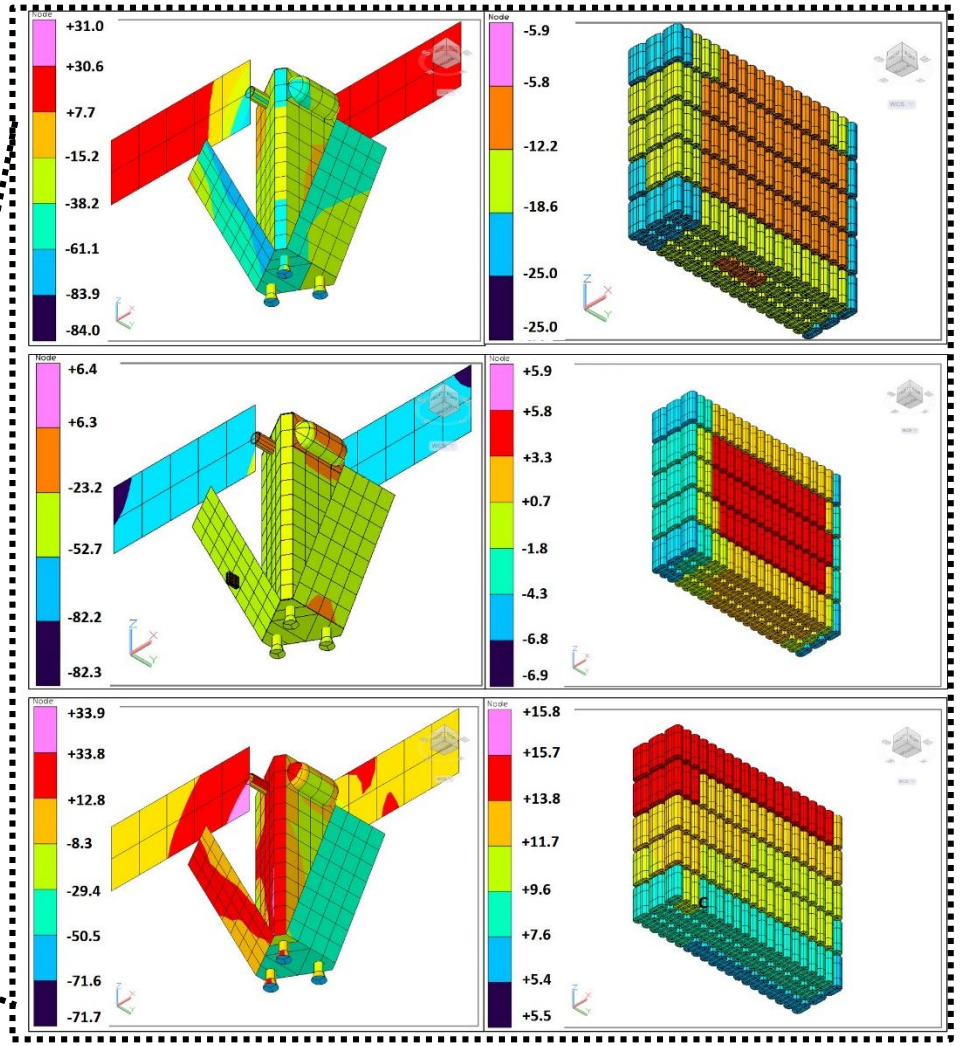

EXAMPLE 2 FOR THERMAL RUNAWAY SIMULATION

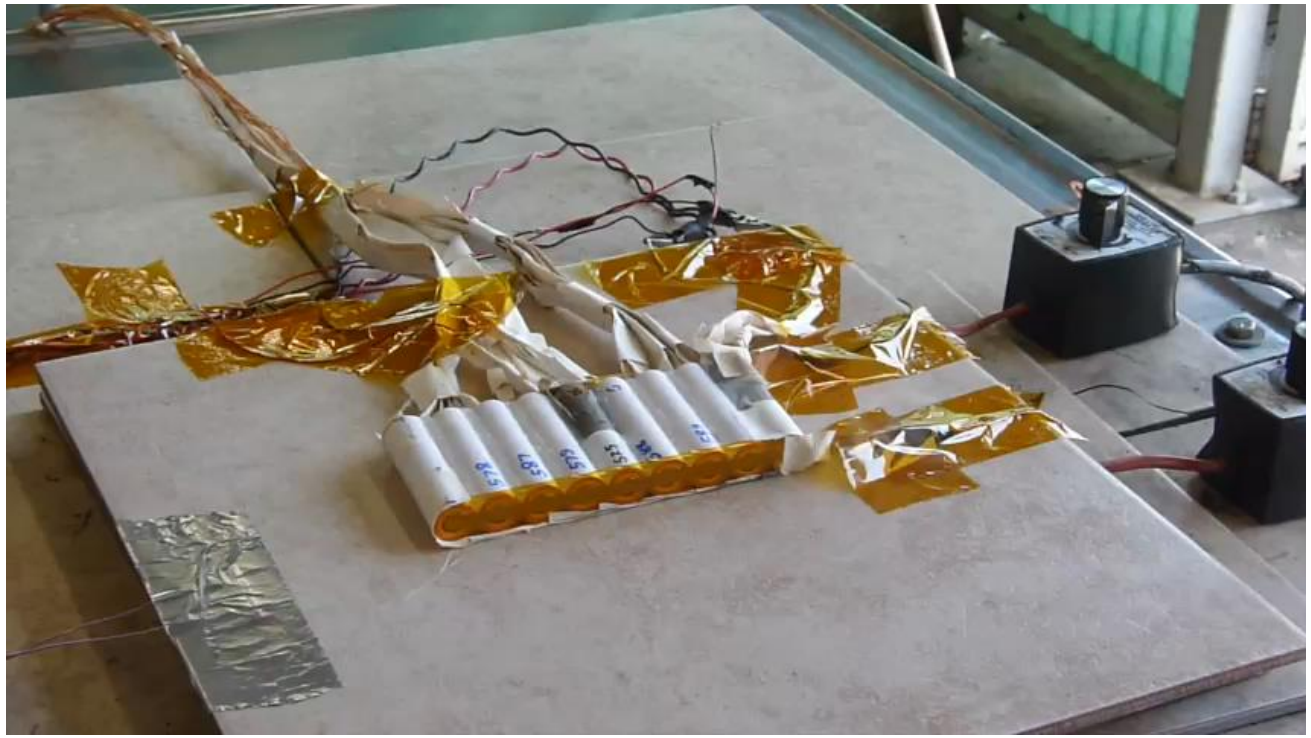

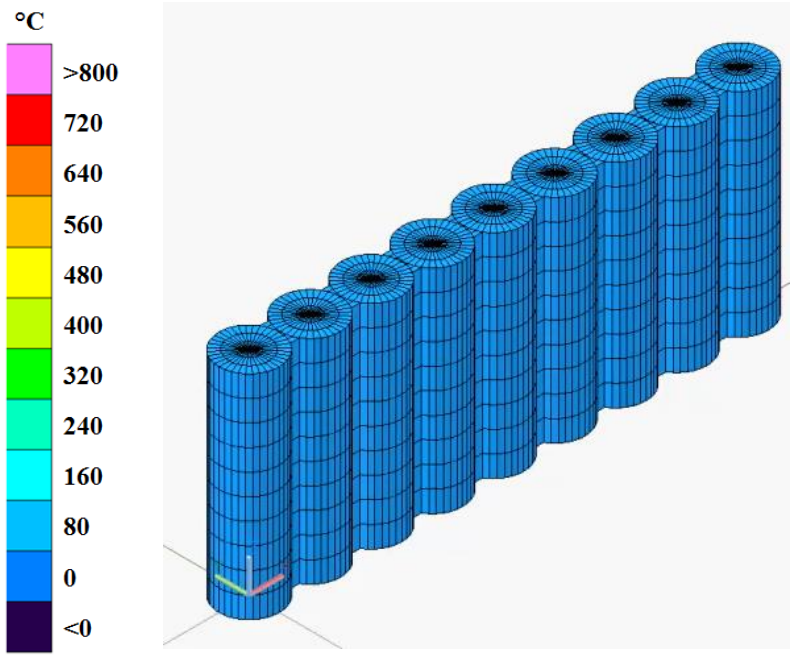

Thermal Runaway Simulation

[2] *Rickman et. al., "Considerations for Thermal Modeling of Lithium-Ion Cells for Battery Analysis." 46th International Conference on Environmental Systems (ICES). 10-14 July 2016.*

EXAMPLE 2 FOR THERMAL RUNAWAY SIMULATION

46th International Conference on Environmental Systems
10-14 July 2016, Vienna, Austria

ICES-2016-009

Considerations for the Thermal Modeling of Lithium-Ion Cells for Battery Analysis

Steven L. Rickman[1]
NASA Johnson Space Center, Houston, TX, 77058, USA

Robert J. Christie[2]
NASA Glenn Research Center, Cleveland, OH, 44135, USA

Ralph E. White, Ph. D.[3]
University of South Carolina, Columbia, SC, 29208, USA

Bruce L. Drolen, Ph. D.[4]
Boeing, Los Angeles, CA, 90009, USA

Moses Navarro[5]
NASA Johnson Space Center, Houston, TX, 77058, USA

Paul T. Coman[6]
Mads Clausen Institute, SDU, Sonderborg, Denmark

[2] *Rickman et. al., "Considerations for Thermal Modeling of Lithium-Ion Cells for Battery Analysis." 46th International Conference on Environmental Systems (ICES). 10-14 July 2016.*

STEP 5: ESTABLISH MASTER MODEL CONNECTIVITY WITH BOUNDARY CONDITIONS AND WITH REFERENCE MODEL ELEMENTS, AND APPLY HEAT LOADS